



ICESTRUCT JIP GUIDELINE

ICE ACTIONS AND ACTION EFFECTS ON
OFFSHORE STRUCTURES

DECEMBER 2013

DET NORSKE VERITAS



FOREWORD

DET NORSKE VERITAS (DNV) is an autonomous and independent foundation with the objectives of safeguarding life, property and the environment, at sea and on shore. DNV undertakes classification, certification, and other verification and consultancy services relating to quality of ships, offshore units and installations, and onshore industries worldwide. DNV also carries out research in relation to these functions.

DNV produces and maintains a large body of technical documentation, represented by the DNV Service Documents, including the DNV Rules for Classification of Ships, the DNV Service Specifications (DNV-DSS) and Standards (DNV-DS), the DNV Offshore Service Specifications (DNV-OSS) and Standards (DNV-OS), and the DNV Recommended Practices (DNV-RP).

The DNV Offshore Service Documents comprise a three level hierarchy of documents:

- *Offshore Service Specifications* (DNV-OSS), which provide principles and procedures of DNV classification, certification, verification and consultancy services;
- *Offshore Standards* (DNV-OS), which provide technical provisions and acceptance criteria for general use by the offshore industry as well as the technical basis for DNV offshore services;
- *Recommended Practices* (DNV-RP), which provide proven technology and sound engineering practice as well as guidance for the higher level Offshore Service Specifications (DNV-OSS) and Offshore Standards (DNV-OS).

The DNV Offshore Service Documents are offered within the following areas:

- | | |
|--|-------------------------|
| A) Qualification, Quality and Safety Methodology | F) Pipelines and Risers |
| B) Materials Technology | G) Asset Operation |
| C) Structures | H) Marine Operations |
| D) Systems | J) Cleaner Energy |
| E) Special Facilities | O) Subsea Systems |

ACKNOWLEDGEMENTS

The development of the present ICESTRUCT Joint Industry Project (JIP) Guideline on '*Ice Actions and Action Effects on Offshore Structures*' was sponsored and supported by the following paying JIP participants:

Statoil, Shell, Repsol, ENI, BOEMRE, Transocean, Barlindhaug, Daewoo Shipbuilding & Marine Engineering, Hyundai Heavy Industries, Dr. techn. Olav Olsen, SBM Offshore, Huisman Equipment, Marin, Granherne, and Keppel Offshore & Marine.

The JIP also benefited from contributions from the following JIP 'work in kind' participants:

Aker Arctic, Prof. Ove Gudmestad, Prof. Karl Shkhinek, NTNU, Keppel Offshore & Marine, Dalian University of Technology, and Hamburgische Schiffbau-Versuch Anstalt (HSVA).

DNV is grateful for the valuable cooperation and discussions with these partners. Their representatives are hereby acknowledged for their contributions.

The present ICESTRUCT JIP Guideline on '*Ice Actions and Action Effects on Offshore Structures*', which is publically accessible after December 2013, is based on the work documented in the ICESTRUCT JIP Background Report, '*Ice Effects on Arctic Offshore Structures*', the distribution of which is restricted indefinitely to the paying JIP participants.

Comprehensive information about DNV services, research and publications can be found at <http://www.dnv.com>, or can be obtained from DNV, Veritasveien 1, NO-1322 Høvik, Norway; Tel +47 67 57 99 00.

© Det Norske Veritas AS, 2013. All rights reserved. This publication or parts thereof may not be reproduced, modified, adapted or transmitted in any form or by any means without the prior written consent of Det Norske Veritas AS. Reference to part of this publication which may lead to misinterpretation is not permissible.



ICESTRUCT JIP:
ICE EFFECTS ON ARCTIC OFFSHORE STRUCTURES

ICESTRUCT JIP GUIDELINE

*Ice Actions and Action Effects on
Offshore Structures*

DNV RESEARCH & INNOVATION
ARCTIC TECHNOLOGY

DET NORSKE VERITAS AS, NO-1322 HØVIK, NORWAY

Rev. No.	Date: (DD.MM.YYYY)	Reason for Issue:	Prepared by:	Reviewed by:	Approved by:
A (Draft)	03.07.2011	Issued for review	CLON, FEGU, POMO	RHEL	HAR
B (Draft)	15.07.2011	Issued for review	CLON, RHEL	POMO	HAR
0 (Final Draft)	10.12.2012	Final draft	RHEL, POMO		
1 (Final version)	20.12.2013	Final version	POMO, RHEL	TOH, LINGE	RTOR

© Det Norske Veritas AS, 2013. All rights reserved. This publication or parts thereof may not be reproduced, modified, adapted or transmitted in any form or by any means without the prior written consent of Det Norske Veritas AS. Reference to part of this publication which may lead to misinterpretation is not permissible.

CONTENTS

1	INTRODUCTION.....	1	7.8	GLOBAL ICE RIDGE ACTIONS ON PLANAR SLOPING STRUCTURES	32
1.1	GENERAL.....	1	7.9	GLOBAL ICE RIDGE ACTIONS ON CONICAL STRUCTURES	33
1.2	OBJECTIVES, AND RELATION TO ISO 19906.....	1	7.10	REFERENCES	34
1.3	SCOPE AND APPLICATION	1	8	ICE INDUCED DYNAMIC STRUCTURAL RESPONSE.....	35
1.4	ABBREVIATIONS	1	8.1	GENERAL.....	35
1.5	SYMBOLS.....	2	8.2	ICE INDUCED DYNAMIC RESPONSE OF VERTICAL STRUCTURES	35
1.6	REFERENCES.....	3	8.3	ICE INDUCED DYNAMIC RESPONSE OF NARROW CONICAL STRUCTURES	39
2	DESIGN PRINCIPLES	4	8.4	FATIGUE.....	40
2.1	GENERAL.....	4	8.5	REFERENCES	41
2.2	SAFETY AND DESIGN PHILOSOPHY	4	9	FLOATING STRUCTURES IN ICE	42
2.3	REFERENCES.....	4	9.1	GENERAL.....	42
3	SEA ICE CHARACTERISTICS.....	5	9.2	REFERENCES	42
3.1	GENERAL.....	5	10	ICE ACTION EFFECTS IN FLOATING STRUCTURES	43
3.2	PHYSICAL PROPERTIES OF LEVEL ICE	6	10.1	ICE RIDGE INTERACTION	43
3.3	PHYSICAL PROPERTIES OF ICE RIDGES	7	A	APPLICATION EXAMPLES	45
3.4	MECHANICAL PROPERTIES OF LEVEL ICE.....	8	A.1	ICE INDUCED DYNAMIC STRUCTURAL RESPONSE	45
3.5	MECHANICAL PROPERTIES OF ICE RIDGES.....	9			
3.6	PROPERTIES OF ICE RUBBLE	10			
3.7	REFERENCES.....	11			
4	LOCAL ICEBERG AND MULTI-YEAR ICE ACTIONS	11			
4.1	GENERAL.....	11			
4.2	LOCAL ICEBERG AND MULTI-YEAR ICE PRESSURE.....	11			
4.3	REFERENCES.....	11			
5	REGIONAL ICE CONDITIONS.....	12			
5.1	GENERAL.....	12			
5.2	SUMMARY OF ICE CONDITIONS.....	12			
5.3	REFERENCES.....	12			
6	ICE INTERACTION SCENARIOS FOR FIXED STRUCTURES	13			
6.1	INTERACTION CONSIDERATIONS.....	13			
7	SEA ICE ACTIONS ON FIXED STRUCTURES	14			
7.1	GENERAL.....	14			
7.2	LOCAL ACTIONS	14			
7.3	GLOBAL LEVEL ICE ACTIONS ON VERTICAL STRUCTURES	14			
7.4	GLOBAL LEVEL ICE ACTIONS ON PLANAR SLOPING STRUCTURES.....	17			
7.5	GLOBAL LEVEL ICE ACTIONS ON CONICAL STRUCTURES	24			
7.6	FIRST-YEAR ICE RIDGE ACTIONS.....	30			
7.7	GLOBAL ICE RIDGE ACTIONS ON VERTICAL STRUCTURES	30			



1 INTRODUCTION

1.1 GENERAL

1.1.1 BACKGROUND

1.1.1.1 For Arctic offshore structures, the most severe actions are often caused by ice-structure interaction, and it is of great importance that ice actions and ice action effects are addressed appropriately.

1.1.1.2 Although there have been offshore activities in the Arctic since the late 1960s, the industry is continuously working to increase knowledge and to improve engineering practice. The development of ISO 19906 represents an attempt at such an improvement.

1.1.1.3 The activity of determining characteristic ice actions and therefrom associated design actions and action effects is not trivial. There are large epistemic uncertainties involved which must be considered in the analyses: it is often the case that detailed site specific ice conditions are not known during preliminary design assessments; also, there is additional uncertainty associated with the generally incomplete understanding of ice mechanics and of the accuracy of conventional ice action equations, which are only partly based on full scale field measurements. The assessment of ice actions therefore often relies on expert judgement.

1.1.1.4 Despite the uncertainties involved, it is important that ice actions and ice action effects are addressed *consistently* within the context of offshore design philosophies. The present Guideline aims to assist the designer in consistently addressing ice actions during preliminary design assessments, in compliance with ISO 19906.

1.2 OBJECTIVES, AND RELATION TO ISO 19906

1.2.1 OBJECTIVES, AND RELATION TO ISO 19906

1.2.1.1 The present Guideline, resulting from the ICESTRUCT Joint Industry Project (JIP), aims to assist the non-specialist Arctic offshore structure designer in determining representative ice actions in a consistent manner. The Guideline is intended to conform to and supplement the new ISO Standard 19906, '*Petrochemical and Natural Gas Industries: Arctic Offshore Structures*'.

1.2.1.2 A non-specialist Arctic offshore structure designer is here defined as a designer who has considerable experience with structural design in general but who has limited or no experience in Arctic technology and ice mechanics.

1.2.1.3 The objective also addresses the need to assist the non-specialist Arctic offshore structure designer in following the normative and informative provisions of ISO 19906 for the safe design of Arctic offshore structures.

1.2.1.4 With ISO 19906 as basis, the present Guideline aims to present instructions on possible methodologies for determining representative ice actions, taking into account uncertainty.

1.3 SCOPE AND APPLICATION

1.3.1 SCOPE

1.3.1.1 The Guideline is intended as a self-contained document, presenting the relevant material in a form readily understood by non-specialist Arctic offshore structure designers.

1.3.2 APPLICATION

1.3.2.1 It is intended that the information provided by the present Guideline will be useful for Arctic offshore structure design purposes, not only in accordance with ISO 19906 but also within the context of other offshore structure design codes.

1.3.2.2 The present Guideline does not represent an attempt to completely cover all preliminary design aspects of Arctic offshore structures; the application of the methods presented in the Guideline should not in any way be interpreted as approved by DNV (as, for instance, objects, units or projects, which are certified, classified or verified by DNV). The publication of this Guideline carries no future guarantee that DNV will approve the described methodology when applied to a specific object in a certification, classification or verification project.

1.3.2.3 The focus in this present Guideline is on determining characteristic actions and characteristic action effects.

1.3.2.4 Design values involve the use of action factors, and these are specified by ISO 19906 as well as by ISO 19901-5, ISO 19902 and ISO 19903.

1.4 ABBREVIATIONS

1.4.1 ABBREVIATIONS

FE	Finite Element
FEA	Finite Element Analysis
FY	First year
IIV	Ice induced vibrations
ISO	International Organization for Standardization
JIP	Joint Industry Project
MY	Multi-year
MDoF	Multiple Degrees of Freedom
ppt	parts per thousand
SDoF	Single Degree of Freedom

1.5 SYMBOLS

1.5.1 LATIN SYMBOLS

A_T	Dimensionless factor	H_T	Horizontal top component
$B_{r,n}$	parameter relating the global pressure to the number of annual events and return period	I	Crushing intensity
B_T	Dimensionless factor	L_{tot}	Length of ice passing the site
c_k	Cohesion of the ice ridge keel	L_{event}	Reference event length
C_A	Local shape coefficients	M_n	Modal mass
C_P	Ice strength coefficient	$m(z)$	Mass distribution along the structure
C_{FDD}	Cumulative freezing degree days	p_G	global pressure
C_R	Strength parameter	p_L	local pressure
D_A	Local shape coefficients	r	return period in terms of years
D_P	Pressure coefficient	$R_{cohesive}$	Reference resistance
D_T	Diameter at the top of the cone	S	Salinity
e	Keel macro-porosity	S	Dimensionless strength parameters
E	Young's modulus of sea ice	T	Ice action period
E_0	Young's modulus of freshwater ice	\bar{T}_f	Average freezing temperature
E_K	Impact energy	$\bar{T}_{a,d}$	Average daily air temperature
f_{comp}	Ice sheet compression factor	T_m	The m-th natural period
$f_{B,\sigma}$	Breaking strength factor	V_B	Vertical breaking component
f_{BS}	Dimensionless factor	v_b	Relative brine volume
F_E	Maximum impact action	v_i	Velocity of ice
F_E	Maximum global level ice action	v_T	Total porosity
f_{HB}	Dimensionless factor	V_{ice}	Volume of ice in rubble pile
$f_{HB,\mu}$	Horizontal breaking friction factor	V_L	Vertical lift component
$f_{HR,\mu}$	Horizontal ride-up friction factor	V_P	Vertical push component
F_{max}	Maximum value of stochastic ice action	V_R	Vertical ride-up component
F_{mean}	Mean value of stochastic ice action	V_T	Vertical top component
f_{max}	Peak value in the action function	w	Width at the waterline
f_{min}	Minimum value in the action function	w_d	Distance between frames
f_n	Natural frequency of the eigenmode	w_R	Width at the top of the rubble pile
f_{nom}	Nominal action	W_B	Reference action
f_r	Characteristic action	W_{ref}	Reference weight
F_{std}	Standard deviation of stochastic ice action	$W_{rubble,front}$	Reference action
$f_{R,h}$	Ride-up thickness factor	$W_{rubble,slope}$	Reference action
$f_{R,\alpha}$	Ride-up slope factor	$W_{sheet,slope}$	Reference action
$f_{VB,\mu}$	Vertical breaking friction factor	W_{slab}	Reference action
$f_{VR,\mu}$	Vertical ride-up friction factor	a_d	Distance between stringers
h	Sheet ice thickness		
h_c	Consolidated layer thickness		
h_{end}	Average annual end of season ice thickness		
h_r	Effective ride-up thickness		
H_B	Horizontal breaking action		
H_k	Ice ridge keel draught		
H_L	Horizontal lift component		
H_P	Horizontal push component		
H_r	Effective ride-up height		
H_R	Horizontal rubble component		



1.5.2 GREEK SYMBOLS

α	Slope angle, measured against the horizontal
α	Average cone angle
α_{delta}	Ratio between fluctuating and maximum action
α_{mean}	Ratio between mean and maximum action
ζ_m	The m -th damping ratio
θ	Stability coefficient
θ	Cone angle
θ_r	Angle of repose
μ	Ice-structure friction coefficient
μ_i	Ice-ice friction coefficient
μ	Annual number of impacts
v_m	The m -th mass-normalized mode shape vector
$v_{m,p}$	The m -th mass-normalized mode shape evaluated at the point of ice loading on the structure
ξ_n	Modal damping of the n -th mode of vibration
ρ_i	Bulk density of sea ice
ρ_w	Density of sea water
σ_c	Compressive strength of level sea ice
$\sigma_{c,index}$	compressive strength
$\sigma_{c,index,ref}$	reference strength index
σ_f	Flexural strength of level sea ice
τ_c	Loading ratio
ϕ_k	internal friction angle
ϕ_{nc}	The m -th mode shape, not necessarily mass normalized, evaluated at the ice action point
$\phi_n(\bar{z})$	The n -th mode shape, not necessarily mass normalized.

1.6 REFERENCES

- ISO 19901-5:2012(E), *Petroleum and natural gas industries – Site-specific assessment of mobile offshore units*.
- ISO 19902:2007(E), *Petroleum and natural gas industries – Fixed steel offshore structures*.
- ISO 19903:2006(E), *Petroleum and natural gas industries – Fixed concrete offshore structures*.
- ISO 19906:2010(E), *Petroleum and natural gas industries – Arctic Offshore Structures*.

2 DESIGN PRINCIPLES

2.1 GENERAL

2.1.1 UNCERTAINTY: LIMITED DATA AND INSUFFICIENT KNOWLEDGE

2.1.1.1 The ice actions imposed on Arctic offshore structures and the resulting ice action effects, due to ice-structure interaction and associated ice deformation and failure, usually represent the governing design actions and design action effects, but the availability of reliable data for ice characteristics is limited.

2.1.1.2 The philosophy for determining the characteristic actions and action effects must then take into account uncertainty associated with lack of knowledge, and at the same time it must provide the designer with means to assess the safety of the design within a systematic framework.

2.2 SAFETY AND DESIGN PHILOSOPHY

2.2.1 RELIABILITY LEVELS

2.2.1.1 The key principle in design based on *reliability differentiation* (see, for example, ISO 2394, on which ISO 19900 is based; alternatively, see DNV CN 30.6), is that the design shall satisfy a predetermined reliability level, given a particular design situation that reflects a particular mode of operation under a given set of environmental conditions.

2.2.1.2 Although a target reliability level is not to be interpreted as the 'actual' frequency of non-failure of a given structure (for example, human factors are not taken into account, and these clearly affect the probability of failure), the structural reliability level is considered sufficiently approximate such that the degree to which a given design can be classified as 'safe' may be quantified.

2.2.1.3 The target structural reliability level also provides a measure of the safety associated with one particular design as compared with another.

2.2.1.4 Once established within the context of a regulatory framework or a framework of agreed normative requirements, different designs based on the same requirements should exhibit similar (but not necessarily exactly identical) degrees of safety.

2.2.1.5 The starting point of the reliability-based design procedure is the choice of agreed reliability targets.

2.2.2 EXPOSURE LEVELS

2.2.2.1 ISO 19906 adopts the philosophy whereby the 'required reliability depends on the exposure level, which is determined by the life-safety category and the environmental and economic consequence category of the structure or component'.

2.2.2.2 There are three different exposure levels L1, L2 and L3, where a structure associated with L1 requires the highest level of reliability; L2 and L3 are associated with a structure for which the safety requirements can be relaxed as compared with L1.

2.2.3 DESIGN PHILOSOPHY

2.2.3.1 The design philosophy adopted in ISO 19906 is the 'limit state'-based partial action factor design method.

2.2.3.2 The key principle is that satisfactory performance of the design, for any specified mode of operation, shall be verified through the evaluation of a limit state function, involving design values of the governing environmental and structural variables.

2.2.3.3 The design values are obtained by multiplying characteristic values by action factors, whose numerical values have been calibrated such that they correspond to a given target reliability level corresponding to a given exposure level.

2.3 REFERENCES

DNV CN 30.6, *Structural reliability analysis of marine structures*. Classification Note, July 1992.

ISO 19900:2010, *Petroleum and natural gas industries – General requirements for offshore structures*.

ISO 19906:2010(E), *Petroleum and natural gas industries – Arctic Offshore Structures*.

ISO 2394:1998, *General principles on reliability of structures*.



3 SEA ICE CHARACTERISTICS

3.1 GENERAL

3.1.1 SEA ICE, AND THE CHALLENGE OF PREDICTING ICE ACTIONS

3.1.1.1 Sea ice is frozen sea water and generally grows steadily in thickness during the winter months and melts during summer. During interaction with an offshore structure, considerable loads (or actions) may occur during the season, whenever the ice is cold and has reached a thickness sufficiently large to resist the strains occurring inside the ice structure without immediately failing. This imposes pressure on the structure, and the resulting environmental action experienced by the structure will increase until the failure load of the ice is reached, and ice failure occurs by crushing, splitting, breaking, etc.

3.1.1.2 Ice mechanics is at present an immature field of science, and the level of understanding is presently insufficient for providing engineers with accurate and theoretically satisfactory prediction tools for design purposes, comparable with the tools provided from the established theories of hydrodynamics, wave mechanics, structural mechanics, etc.

3.1.1.3 In engineering applications of ice mechanics, including offshore engineering applications, it is presently usual to use equations for ice failure loads adopted from *conventional theory of strength of materials*. These are familiar and convenient equations attractive for use in engineering analysis and design due to their simplicity, but they are also based on theory which typically treats the material as homogeneous, isotropic and elasto-plastic. Thus, the analyses involve assumptions that are generally *not valid* for sea ice.

3.1.1.4 Ice is an inhomogeneous and anisotropic natural ceramic; it is a natural ceramic by definition, because it is a naturally occurring non-metallic, inorganic and crystalline material. As such, it exhibits a complicated visco-elastic, quasi-brittle and brittle behaviour, depending on scale, strain rate and loading conditions. Therefore its mechanical properties, as required in the context of engineering analyses, depend very much on the testing conditions; and when reported in the literature, '*widely varying or even contradictory results of nominally similar tests*' appear (Schwarz, et al., 1981).

3.1.1.5 The conventional ice action prediction equations require knowledge of the *effective* mechanical properties of the sea ice. A consistent approach then requires standardized methods for determining the effective mechanical properties of ice. The present Guideline does not offer recommendations on standard methods for *measuring* properties, but the Guidelines does provide recommendations on nominal values of different properties.

3.1.1.6 ISO 19906 (ISO, 2010) offers equations for determining the ice actions on fixed structures, where the ice actions arise due to flexural failure of the ice or due to

compressive failure (or crushing) of the ice. These equations require as input several familiar variables representing the mechanical properties of ice: compressive strength, flexural strength, elastic modulus and Poisson's ratio. Other equations require also an internal friction angle and an apparent cohesion associated with the keel of a ridge. The present Guideline provides recommendations on the use of these variables.

3.1.2 LEVEL ICE

3.1.2.1 For design purposes, sea ice can be classified as either level ice or ice ridges. In reality there is of course much greater diversity; however, the generalization is required and useful for action calculations.

3.1.2.2 Level ice (or sheet ice) is formed from frazil crystals. Once formed, it grows throughout the winter. Its rate of growth depends on environmental conditions of snow, air temperature, oceanic flux of warm water, and on cloud cover.

3.1.2.3 As sea water freezes, salt is captured inside the ice structure in brine pockets. This weakens the ice compared to freshwater ice.

3.1.2.4 First year sea ice is formed during the early part of the winter season, every year, and melts completely by the end of the winter season. Second year sea ice has survived (i.e. not melted entirely during) the summer season, and multi-year sea ice has survived at least two consecutive summer seasons.

3.1.3 ICE RIDGES

3.1.3.1 Ice ridges are formed by compression or shear in the plane of the sea ice cover. This is caused by waves, current and wind.

3.1.3.2 An ice ridge consists of a sail, a consolidated layer and a keel. The action contribution from the sail is usually neglected in action calculation. The consolidated layer is a solid layer of ice blocks that have frozen together, while the keel consists of ice blocks that have only partially frozen together.

3.1.4 NOMINAL VALUES FOR ICE PROPERTIES

3.1.4.1 The nominal values recommended for preliminary assessments are summarized in Table 3.1. The nominal values should not be used if other more accurate values are available.

3.1.4.2 For properties not found in Table 3.1 further information is found below in this Section.

Table 3.1: Nominal values of relevant ice properties.

Ice property	Recommended nominal value
Relative brine volume	0.05
Relative air volume	0.02
Ice density	900 kg/m ³
Consolidated layer thickness	1.5 × <i>h</i> ^(c)
Keel macro porosity	0.3
Flexural strength	0.5 MPa
Uniaxial compressive strength	2.8 MPa
Young's modulus	3 GPa
Friction coefficient (ice-steel)	0.15
Friction coefficient (ice-concrete)	0.20
Angle of internal friction	35°
Keel cohesion	10 kPa

^(c) Here, *h* is level ice thickness.

3.2 PHYSICAL PROPERTIES OF LEVEL ICE

3.2.1 DETERMINING LEVEL ICE THICKNESS

3.2.1.1 The average end-of-season level ice thickness should be determined based on the following order of preference:

- At least five years of site-specific measurements of level ice thickness (see for instance SP 11-114-2004).
- At least twenty years of air temperature measurements for the determination of annual average cumulative freezing degree-days and annual average end-of-season ice thickness according to Section 3.2.2.
- The approximate annual average cumulative freezing degree-days for the appropriate geographical area as given in Table 5.1. The annual average end-of-season ice thickness can then be estimated according to Eq. (3.2).

3.2.1.2 If the ice data at a given geographical location are missing, but the ice is considered to originate from a different location, the basis for finding the appropriate level ice thickness should be the location from which the ice drifts.

3.2.2 DETERMINING LEVEL ICE THICKNESS FROM AIR TEMPERATURE RECORDS

3.2.2.1 Daily air temperature data can be used to determine the annual cumulative freezing degree days by:

$$C_{\text{FDD}} = \sum_{\substack{d, \text{ days of freezing} \\ \bar{T}_f < \bar{T}_{a,d}}} (\bar{T}_f - \bar{T}_{a,d}) \geq 0, \quad (3.1)$$

where:

\bar{T}_f is the average freezing temperature (°C) at the location;

$\bar{T}_{a,d}$ is the average daily air temperature (°C) at the location.

3.2.2.2 Typical values for the freezing temperature of sea water with about 35 ppt salinity are around -1.8°C, while brackish water with a lower salinity of 6 to 8 ppt has a freezing temperature of around -0.5°C.

3.2.2.3 The average end-of-season ice thickness, h_{end} , can be estimated from:

$$h_{\text{end}} = 2.6 \times 10^{-2} \sqrt{C_{\text{FDD}}}. \quad (3.2)$$

3.2.3 BULK ICE TEMPERATURE

3.2.3.1 The temperature of the ice can be considered to represent a reference proxy for strength, since the brine volume in sea ice is largely related to ice temperature.

3.2.3.2 A nominal value for the average ice temperature can be obtained from the cumulative freezing degree-days by using the following procedure (valid for areas with sea water salinity of approximately 35 ppt):

- 1) Determine the nominal average air temperature, $T_{\text{air, nom}}$, as given by Eq. (3.3);
- 2) Determine the nominal average ice surface temperature, $T_{\text{surf, nom}}$, as given by Eq. (3.4);
- 3) Determine the nominal average ice temperature, $T_{\text{ice, nom}}$, as given by Eq. (3.5).

3.2.3.3 A nominal air temperature can be obtained from:

$$T_{\text{air, nom}} = - \left(\frac{0.223 \times C_{\text{FDD}}}{30.4} + 1.8 \right). \quad (3.3)$$

3.2.3.4 A nominal ice surface temperature can be obtained from:

$$T_{\text{surf, nom}} = \max \{ T_{\text{air, nom}}, 0.6 \times T_{\text{air, nom}} - 4.0 \}. \quad (3.4)$$

3.2.3.5 The nominal ice temperature (in the spatial average sense) is given by:

$$T_{\text{ice, nom}} = 0.5 \times (T_{\text{surf, nom}} - 1.8). \quad (3.5)$$

3.2.4 BULK ICE SALINITY

3.2.4.1 Salt is trapped in brine pockets in the sea ice as it freezes and grows in thickness. The amount of brine in the sea ice is related to the salinity of the water and the growth rate of the ice.

3.2.4.2 For first year Arctic sea ice, a nominal value of the average bulk salinity (given in parts per thousand, ppt) can be determined from:

$$S_{\text{nom}} = 4.61 + \frac{0.916}{h}, \quad (3.6)$$

where *h* is the level ice thickness, measured in metres.



3.2.4.3 Typical values of salinity of first year sea ice at the end of the freezing season range from 4 to 6 ppt.

3.2.5 BULK ICE POROSITY

3.2.5.1 Sea ice is a porous material, where the pores may be filled by brine and air (and solid salts). The total porosity, v_T , is approximately the sum of the relative brine volume, v_b , and the relative air volume, v_a .

Guidance note:

Determining uniaxial compressive strength requires knowledge about porosity, whereas the equations for the effective elastic modulus and the flexural strength given in terms of the relative brine volume.

---e-n-d---o-f---G-u-i-d-a-n-c-e---n-o-t-e---

3.2.5.2 The relative brine volume v_b can be obtained from:

$$v_b = 45 \frac{S_{\text{nom}}}{T_{\text{ice,nom}}} \quad (3.7)$$

3.2.5.3 Since the ice strength is sensitive to the brine volume, the average ice temperature should be determined as accurately as possible. A nominal value for the relative brine volume higher than 0.10 (10%) is not recommended for preliminary action calculations in Arctic areas, and in most cases a nominal value of 0.05 (5%) might be appropriate.

3.2.5.4 Relative air volume is dependent largely on the oceanic conditions during the formation and growth of the ice and can be estimated from the ice density ρ_i as given by:

$$v_{a,\text{nom}} = 1 - \left(\frac{\rho_i}{922} \right) \quad (3.8)$$

3.2.5.5 Unless accurate site-specific information is made available to the designer, a nominal value of the relative air volume can be taken as 0.02 (2%).

3.2.6 BULK ICE DENSITY

3.2.6.1 The density of sea ice varies greatly and is difficult to measure with great precision. A nominal value can be taken as 900 kg/m^3 .

3.3 PHYSICAL PROPERTIES OF ICE RIDGES

3.3.1 ICE RIDGE KEEL DRAUGHT

3.3.1.1 The keel draught is the vertical distance between the mean water level and the bottom of the ridge keel.

3.3.1.2 The keel draught is here considered different from the keel depth, which is here considered to be the vertical distance between the bottom of the consolidated layer and the bottom of the keel; i.e. by this definition (which differs

from the definition conventionally used) the keel depth is the vertical length of the keel *only*.

3.3.1.3 Keel draught should be determined by rigorous statistical treatment of measurement data.

3.3.1.4 Preferably, the characteristic keel draught sought should be the average, taken over several years, annual maximum keel draught.

3.3.1.5 In the case where available data are insufficient, two options are presented here, in order of preference, to be *used for preliminary assessments only*:

- 1) The annual maximum keel draught is estimated by Eq. (3.9), which is based on measurements of keel draught, sail height and block thicknesses:

$$H_{k,\text{av}} \approx 12.5 \times \sqrt{h_{\text{end}}} \quad (3.9)$$

- 2) Estimates of annual maximum keel draughts for specific geographical regions are found in Table 5.1 (denoted as 'average annual' by ISO 19906).

3.3.2 CONSOLIDATED LAYER THICKNESS

3.3.2.1 The thickness of the consolidated layer is varying both spatially and temporally and is generally varying between 1.5 and 2 times the thickness of the surrounding level ice.

3.3.2.2 Unless a different value is specified, a nominal value of 1.5 times the level ice thickness is recommended. This nominal value should be seen in relation to the mechanical properties described in Section 3.4.

3.3.2.3 The density of the consolidated layer can be assumed to be equal to the ice density value reported in Table 3.1.

3.3.3 RIDGE KEEL MACRO-POROSITY

3.3.3.1 As the ridge keel consists of ice blocks partly frozen together, the macro-porosity of the ridge keel is the ratio of the volume of pores to the total volume of the keel, which is $1 -$ relative volume of ice in the keel.

3.3.3.2 Unless a different value is specified, the ridge keel macro-porosity may be assigned a nominal value of 0.3 (30%) *for preliminary assessments*.

3.3.4 OTHER PHYSICAL PROPERTIES OF ICE RIDGES

3.3.4.1 Any properties not described in Section 3.3 can be conservatively assigned nominal values identical to those for the associated properties of first year level ice (Section 3.2).

3.4 MECHANICAL PROPERTIES OF LEVEL ICE

3.4.1 FLEXURAL STRENGTH

3.4.1.1 For the purpose of predicting global ice actions on sloping structures in arctic conditions, where the actions (or loads) are associated with flexural failure of the surrounding ice, it is usual to represent the mechanical behaviour of the ice by conventional beam and plate bending models. The load at failure is then associated with a maximum bending moment capacity, and hence a flexural strength may be defined from simple beam (or plate) bending models in terms of the bending moment at failure. The flexural strength of sea ice should therefore be interpreted as a measure of the bending moment capacity rather than a direct measure of flexural strength.

Guidance note:

In the case of a beam (see ISO 19906 clause A.16.5.4.2) with a rectangular cross section of breadth b and height h , where a bending moment M acts over the cross section, the largest magnitude of longitudinal stress σ in the beam occurs at the top and bottom of the cross section and is given as $\sigma = 6 \times M / bh^2$ (as obtained from simple beam-theory, assuming a linearly elastic, homogeneous and isotropic material). When applied to ice, the flexural strength σ_f is simply defined as the value of the product $6 \times M_f / bh^2$, where M_f is the value of the bending moment at flexural failure of the ice. This can be measured for carefully prepared test specimens. Hence, for ice, flexural strength must be interpreted as a measure of the bending moment capacity, such that the product $(\sigma_f bh^2 / 6)$ equals the bending moment capacity of the ice sheet.

---e-n-d---o-f---G-u-i-d-a-n-c-e---n-o-t-e---

3.4.1.2 The flexural strength σ_f of sea ice (interpreted in the sense described in 3.4.1.1 above) can be estimated from (Timco and O'Brien, 1994):

$$\sigma_f = 1.76 \times \exp(-5.88 \times \sqrt{v_b}) \quad (\text{MPa}), \quad (3.10)$$

where v_b is the average relative brine volume (see section 3.2.5.2), where the average is taken over the depth of the specimen. Here, σ_f is given in units of MPa.

3.4.1.3 Equation (3.10) is valid only for growing ice during the freezing season, and it conforms to the intuitive expectation that strength in general decreases with increasing porosity, which in this case is represented by the relative brine volume v_b .

3.4.1.4 Unless a site-specific value is given, a nominal value of flexural strength can be taken as 0.5 MPa.

3.4.2 EFFECTIVE ELASTIC MODULUS

3.4.2.1 In addition to requiring a flexural strength (section 3.4.1.1), conventional beam and plate bending models

used for predicting global ice loads on sloping structures also require the effective elastic modulus as an input variable. Its role is to represent the flexural stiffness of the ice under quasi-static loading.

3.4.2.2 The effective elastic modulus, measured via quasi-static load-response techniques, is not identical to Young's modulus, measured via ultrasonic (i.e. high frequency) techniques: the modulus measured via quasi-static load-response techniques represents an *effective 'modulus'*, taking into account not only the time independent elastic strain but also the time dependent but reversible strain, or reversible creep. Thus, the modulus required for ice action predictions based on simple quasi-static load-response models is the *effective* modulus of ice, which is expected to be smaller than the true elastic modulus, due to the reduced 'stiffness' associated with the creep.

3.4.2.3 The effective elastic modulus can be estimated from:

$$E = E_0 - 27.9 \sqrt{v_b}, \quad (3.11)$$

in which E_0 is the effective elastic modulus of fresh water ice, which can be taken as 10 GPa.

3.4.2.4 Unless a different value is given, a nominal value of Young's modulus can be taken as 3 GPa.

3.4.3 EFFECTIVE POISSON RATIO

3.4.3.1 In addition to requiring the flexural strength and the effective elastic modulus, the conventional beam and plate bending models adopted for predicting global ice loads on sloping structures also require the effective Poisson ratio ν_p as an input variable.

3.4.3.2 The effective Poisson ratio is different from the true Poisson ratio: the latter is obtained for ice from high frequency measurements (which aim to ensure elastic behaviour), while the effective Poisson ratio takes into account creep deformations associated with the relatively low strain rates comparable to those associated with ice-structure interaction (here, 'relatively low' refers to strain rates much lower than those associated with ultrasonic measurements of Poisson's ratio).

3.4.3.3 Poisson's ratio is about 0.3, but the effective Poisson ratio is greater, and it increases with increasing temperature and increases with decreasing strain rate. Unless a different value is given, a nominal value of the effective Poisson ratio can be taken as 0.4.

3.4.4 ICE-STRUCTURE FRICTION COEFFICIENT

3.4.4.1 In addition to requiring the flexural strength, the effective elastic modulus and the effective Poisson ratio, the conventional beam and plate bending models adopted for predicting global ice loads on sloping structures also require the coefficient of kinetic ice-structure friction μ as an input variable.



3.4.4.2 Generally, the kinetic friction coefficient of sea ice associated with its interaction with different materials is dependent on the relative interaction velocity, on temperature, on contact pressure and on the roughness of the interaction surface.

3.4.4.3 For interaction with steel (conservatively assumed to be corroded steel), a nominal value of the kinetic friction coefficient can be taken as 0.15.

3.4.4.4 For interaction with concrete, a nominal value of the kinetic friction coefficient can be taken as 0.20.

3.4.5 UNIAXIAL COMPRESSIVE STRENGTH

3.4.5.1 The compressive strength of sea ice is often estimated based on results from uniaxial compression tests of small scale specimens.

3.4.5.2 The average compressive strength of horizontally loaded columnar level year ice may be estimated in terms of the porosity v_T as:

$$\sigma_c = 7.6 \times \left(1 - \sqrt{v_T / 0.45}\right)^2. \quad (3.12)$$

3.4.5.3 As an alternative to Eq. (3.12), one of the following equations may be used, depending on the cumulative freezing degree-days, C_{FDD} , to determine a nominal value of the sheet ice compressive strength:

$$\begin{aligned} 250 \text{ }^\circ\text{C-days} \leq C_{FDD} < 500 \text{ }^\circ\text{C-days:} \\ \sigma_{c, \text{nom}} = 1.78 \times \log_{10} C_{FDD} - 3.35, \end{aligned} \quad (3.13)$$

$$\begin{aligned} 500 \text{ }^\circ\text{C-days} \leq C_{FDD} < 2000 \text{ }^\circ\text{C-days:} \\ \sigma_{c, \text{nom}} = 2.24 \times \log C_{FDD} - 4.59, \end{aligned} \quad (3.14)$$

$$\begin{aligned} 2000 \text{ }^\circ\text{C-days} \leq C_{FDD} < 5000 \text{ }^\circ\text{C-days:} \\ \sigma_{c, \text{nom}} = 1.69 \times \log C_{FDD} - 2.75, \end{aligned} \quad (3.15)$$

$$\begin{aligned} 5000 \text{ }^\circ\text{C-days} \leq C_{FDD} < 8000 \text{ }^\circ\text{C-days:} \\ \sigma_{c, \text{nom}} = 1.86 \times \log C_{FDD} - 3.39, \end{aligned} \quad (3.16)$$

3.4.5.4 In the lack of information about either porosity or cumulative freezing degree-days, a nominal value of compressive strength of 2.8 MPa can be used unless a different value is specified.

3.5 MECHANICAL PROPERTIES OF ICE RIDGES

3.5.1 PROPERTIES REQUIRED BY CONVENTIONAL RIDGE ACTION EQUATIONS

3.5.1.1 The equation recommended in ISO 19906 for the contribution to the ice ridge load from the ridge keel is based on Mohr-Coulomb theory: the equation thus requires both a keel material cohesion, c_k , and a keel internal

friction angle, ϕ_k , both associated with the assumed simultaneous failure along an assumed planar failure surface in the keel. These properties are by convention *assumed* to exist, not because of physical reasons but because they are required in the equations originally taken from soil mechanics. They may or may not be appropriate descriptions of the mechanical properties of a ridge keel.

3.5.1.2 In the present guideline, the keel cohesion c_k is referred to as the *effective keel cohesion*, and the internal friction angle is referred to as the *effective internal friction angle* ϕ_k of the keel. They are both considered as spatial average quantities.

3.5.2 THE EFFECTIVE INTERNAL FRICTION ANGLE

3.5.2.1 The effective internal friction angle ϕ_k of the ice ridge keel cannot be measured directly and has to be estimated by post-processing results from small scale laboratory tests and from medium scale field measurements. The range of reported values of ϕ_k is large.

3.5.2.2 Unless a different value of ϕ_k is given, a nominal value can be taken as 35°.

3.5.3 THE EFFECTIVE KEEL COHESION

3.5.3.1 The effective ridge keel cohesion c_k of the ice ridge keel cannot be measured directly and has to be estimated by post-processing results from small scale laboratory tests and from medium scale field measurements. The range of reported values of c_k is also large.

3.5.3.2 The cohesion is generally considered to vary linearly through the depth of the keel, from a maximum at the bottom of the consolidated layer, reducing to zero at the base of the keel. Thus, an average value for the keel volume should be used.

3.5.3.3 The effective keel cohesion c_k and the effective angle of internal friction ϕ_k appear (from results of limited field measurements and of numerical modelling) to be correlated, and a nominal value of the effective keel cohesion can be obtained from:

$$c_k = 27 - 4.9 \times \ln(\phi_k), \quad (\text{kPa}), \quad (3.17)$$

where ϕ_k is measured in degrees (for example, 35°), and c_k is measured in kPa (for example, $c_k = 9.6$ kPa for $\phi_k = 35^\circ$).

3.5.3.4 Unless a site-specific characteristic value has been specified, a nominal value c_k can be taken as 10 kPa.

3.5.4 OTHER MECHANICAL PROPERTIES OF ICE RIDGES

3.5.4.1 Any properties not described in the present section (Section 3.5) can be conservatively assigned nominal values equal to those of the corresponding properties of first year level ice (Section 3.4).

3.6 PROPERTIES OF ICE RUBBLE

3.6.1 RUBBLE ACCUMULATION

3.6.1.1 When estimating ice actions on conical and planar sloping structures, the effects of ice rubble accumulation over the face of the structure must be taken into account.

3.6.1.2 Ice rubble is essentially a pile of ice blocks, where partial or full consolidation (i.e. re-freezing) has taken place between some or all of the ice blocks.

3.6.1.3 Although ice rubble piles appear in different shapes, the typical shape assumed for ice action calculation purposes is illustrated in Figure 3.1 below: the figure shows a vertical cross section of the idealized rubble pile over the face of a wide planar sloping structure, with slope angle α .

3.6.1.4 The ice action equations given in ISO 19906 require the use of **either** (see sections 3.6.1.5 and 3.6.1.6): (i) a rubble pile height, H_r , and an effective angle of repose, θ_r ; or (ii) a rubble ride-up thickness, h_r .

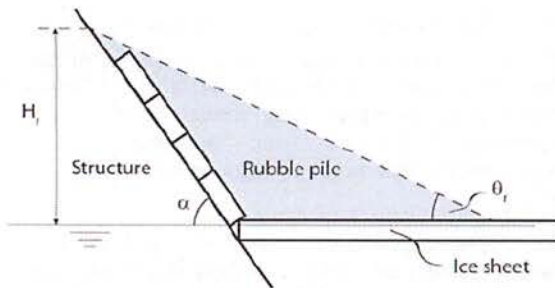


Figure 3.1: Ice rubble pile-up over the face of a planar sloping structure (see section 3.6.1.4 for notation).

3.6.1.5 In the Croasdale equations (for wide sloping but planar structures), the rubble pile height, H_r , and the angle of repose, θ_r , are used directly as input variables. Sometimes the model is used for narrow structures, but then it should be noted that the model may not be valid.

3.6.1.6 In the Ralston equations (for conical structures), the rubble pile is represented by level ice distributed over the front surface of the cone but with a generally different thickness than that of the incoming level ice. The thickness of the ice distributed over the curved surface and transported upwards along the surface is referred to as the ride-up thickness. In the present guideline, this ride-up thickness is obtained from considering the volume of the rubble, and the relevant equation (Section 7.5.14) depends on the rubble pile height, H_r , and on the angle of repose, θ_r .

3.6.2 RUBBLE PILE HEIGHT

3.6.2.1 The average rubble pile height can be approximated as:

$$H_r = 5.24 \times h^{0.18}, \quad (3.18)$$

where h is either: (i) the surrounding level ice thickness, in the case of level ice interactions; or (ii) the consolidated layer thickness, in the case of ice ridge interactions.

3.6.2.2 Eq. (3.18) is based on full-scale data on conical structures with a waterline diameter of 10-14 m.

3.6.2.3 The structural configuration, potentially involving a cone angle and the angle of the neck section, may limit the rubble pile height, in which case Eq. (3.18) is expected to yield conservative results.

3.6.2.4 The rubble pile height estimated from Eq. (3.18) is sometimes referred to herein as the *nominal* rubble pile height (when necessary, to distinguish it from the *effective* rubble pile height, as considered in Sect. 7.5.14).

3.6.3 ANGLE OF REPOSE

3.6.3.1 By definition, the angle of repose θ_r must be less than the slope angle of the structure.

3.6.3.2 There is normally substantial ice rubble accumulation below the ice sheet. However, the effect of this is not considered in the equations recommended in ISO 19906.

3.6.3.3 A nominal value of θ_r over planar sloping structures can be taken as:

$$\theta_{r, \text{planar}} = \alpha - 10^\circ, \quad (3.19)$$

in which α is the slope angle of the structure (measured in degrees).

3.6.3.4 In the case of rubble over conical sloping structures, a nominal value of θ_r can be taken as:

$$\theta_{r, \text{conical}} = \alpha - 16^\circ. \quad (3.20)$$

3.6.4 RUBBLE MACRO POROSITY

3.6.4.1 It is assumed here that the consolidation between individual ice blocks is not considerable. Ice rubble is considered here as a pile of ice blocks where the individual ice blocks have frozen together only to a small extent. In reality, ice rubble may also consolidate further, however this is not treated here.

3.6.4.2 Unless a different value is specified, a nominal value of 0.2 (20%) may be used for preliminary assessments.

3.6.5 EFFECTIVE KEEL COHESION

3.6.5.1 Unless specific information is available, a nominal value of 1 kPa can be used for the effective cohesion of ice rubble.



3.6.6 ICE-ICE FRICTION COEFFICIENT

3.6.6.1 For interaction between two pieces of sea ice, a nominal value of the kinetic friction coefficient can be taken as 0.1.

3.6.7 OTHER MECHANICAL PROPERTIES OF ICE RUBBLE

3.6.7.1 Any properties not described in Section 3.6 can be conservatively assigned nominal values equal to those of similar properties of first year level ice (Section 3.4) or of ice ridges (Section 3.5), as relevant.

3.7 REFERENCES

DNV, 2013, *ICESTRUCT JIP*, DNV Research & Innovation.

SP 11-114-2004, *Site investigation on the continental shelf for offshore oil and gas facilities construction*, Russian code of practice for construction engineering surveys.

Timco, G. W., O'Brien, S., 1994, 'Flexural strength equation for sea ice', *Cold Regions Science and Technology*, 22, 285-298.

4 LOCAL ICEBERG AND MULTI-YEAR ICE ACTIONS

4.1 GENERAL

4.1.1 GENERAL DESCRIPTION OF ICEBERGS AND ICE ISLANDS

4.1.1.1 Icebergs and ice islands consist of freshwater ice. They calve from glaciers and ice shelves in the Arctic and Antarctic.

4.1.1.2 In this context, the term iceberg refers to all freshwater glacial ice including relatively small growlers (mass ~1000 tonnes) up to very large icebergs (mass > 10 million tonnes).

4.1.1.3 Most of the icebergs found in the North Atlantic have calved from glaciers West coast of Greenland. Some icebergs also calve from glaciers in the Canadian Arctic and East Greenland. The icebergs calved on the East coast are often carried by ocean currents south along the coast of Greenland. In the Barents Sea most icebergs originate from the glaciers of Svalbard, Franz Josef Land and Novaya Zemlya.

4.1.1.4 Ice islands calve from floating ice shelves, mostly in Antarctica, but ice islands have also been observed calving from the ice shelves at Ellesmere Island in Canada and from both the East and the West coast of Greenland.

4.1.1.5 Icebergs and ice islands drift under the influence of the prevailing winds and ocean currents.

4.2 LOCAL ICEBERG AND MULTI-YEAR ICE PRESSURE

4.2.1 NOMINAL LOCAL PRESSURE FROM ICEBERGS AND MULTI-YEAR ICE

4.2.1.1 Deterministic calculation of local iceberg actions is covered by Clause A.8.2.5.3 in ISO 19906, while probabilistic calculation is covered in Clause A.8.2.5.4 therein.

4.2.1.2 As an initial estimate for the local pressure from icebergs and impact with multi-year ice, the nominal local pressure can be estimated by:

$$P_{\text{nominal}} = \begin{cases} 7.4 \times A^{-0.70}, & A \leq 10 \text{ m}^2, \\ 1.5, & A > 10 \text{ m}^2, \end{cases} \quad (4.1)$$

where A is the design area.

4.2.1.3 Eq. (4.1) is recommended for thick ice ($h > 1.5$ m).

4.2.2 CHARACTERISTIC LOCAL PRESSURE FROM IMPACTS WITH MULTI-YEAR ICE

4.2.2.1 In the case where the annual number of impacts is known, or if a specific return period is required, the characteristic local pressure can be determined by:

$$P_r = \{\ln(\mu \times r)\} \times A^{-0.7}, \quad (4.2)$$

where

μ is the annual number of impacts,

r is the return period measured in years.

4.2.2.2 The local pressure calculated by Eq. (4.2) should not be lower than the limiting value of 1.5 MPa for areas larger than 10 m².

4.3 REFERENCES

ISO 19906:2010(E), *Petroleum and natural gas industries — Arctic offshore structures*, International Organization for Standardization, Switzerland.

5 REGIONAL ICE CONDITIONS

5.1 GENERAL

5.1.1 VARIATION AND QUALITY OF DATA

5.1.1.1 Ice conditions vary to a great extent across different geographical regions, and there are also local variations within each region. Ice conditions also change throughout the ice season, and the values given in this Section are nominal 'average annual' values (term taken from ISO 19906; see bottom of Table 5.1 for interpretations).

5.1.1.2 The accuracy of calculated ice actions and action effects depends on the quality and quantity of data available for analysis of metocean and ice conditions.

5.1.1.3 ISO 19901-1 identifies the owner of the offshore installation as responsible for specifying appropriate environmental conditions for the design, while an alternative but common understanding is that the responsibility lies with the operator.

5.2 SUMMARY OF ICE CONDITIONS

5.2.1 NOMINAL VALUES OF RELEVANT QUANTITIES

5.2.1.1 Table 5.1 lists nominal values of relevant quantities. The information has been taken from Annex B in ISO 19906 and represents 'average annual' freezing degree days, level ice thickness, ice ridge keel draught as well as maximum ice ridge keel draught.

5.2.2 DATA USED FOR DESIGN

Experts shall be consulted when selecting load calculation input variables during detail design. The values listed in Table 5.1 are not to be used for detail design; however, in lack of any other data, the values can be used to obtain a first estimate for *preliminary design assessments*. See also Section 3.2.1.

5.3 REFERENCES

ISO 19901-1:2005, *Petroleum and natural gas industries – Specific requirements for offshore structures – Part 1: Metocean design and operating considerations*.

ISO 19906:2010(E), *Petroleum and natural gas industries – Arctic Offshore Structures*.

Table 5.1: Summary of cumulative freezing degree-days, C_{FDD} , and sea ice conditions for different geographical regions.

Geographical Region	'Average annual' C_{FDD} (°C-days)	'Average annual' thickness h (m), FY level floe ice ^(a)	'Average annual' keel draught H_k (m), FY ridge ^(b)	Indicated 'maximum' keel draught H_k (m), FY ridge ^(c)
Baffin Bay & Davis Strait	5000	1.60	6.5	20.0
Labrador	1600	1.50	8.0	15.0
Newfoundland	500	1.00	5.0	8.0
Canadian Archipelago	7000	2.20	20.0	25.0
Beaufort Sea	4500	1.80	25.0	28.0
Chuckchi Sea, SE	3300	0.85	10.0	15.0
Chuckchi Sea, NE	4000	1.05	10.0	15.0
Bering Sea, offshore Alaska, N	2300	1.00	10.0	20.0
Bering Sea, offshore Alaska, W	200	1.00	15.0	25.0
Bering Sea, offshore Alaska, SE	1500	0.50	12.5	20.0
Bering Sea, offshore Russia	<i>not given</i>	1.00	10.0	20.0
Cook Inlet	1168	0.80	5.0	10.0
Okhotsk Sea, Magadan	3000	1.30	16.0	20.0
Okhotsk Sea, Sakhalin NE	2400	0.90	21.0	23.0
Okhotsk Sea, Sakhalin SE	1950	0.90	17.0	20.0
Tatar Strait, offshore Russia	2370	0.85	7.0	12.0
Tatar Strait, Sakhalin W	2485	0.70	7.0	11.0
Bohai Sea	<i>not given</i>	0.40	7.8	<i>not given</i>
Gulf of Bothnia (Baltic)	1200	0.60	12.0	25.0
Gulfs of Finland/Riga (Baltic)	800	0.50	12.0	15.0
Baltic Sea	700	0.40	10.0	12.0
Danish Belts (Baltic)	600	0.40	10.0	15.0
Barents Sea, W	2000	1.30	17.5	20.0
Barents Sea, NE	3500	1.40	15.0	16.0
Barents Sea, SE	2500	0.80	16.0	18.0
Sea of Azov	390	0.33	3.6	<i>not given</i>

(a): This is interpreted as being the average, over several years, of the spatially averaged thickness observed at the end of the freezing season.

(b): This is interpreted as being an estimate of the average, over several years, of the annual 'maximum' keel depth.

(c): This is interpreted as being an indication of the largest keel depth observed in the specified region.

6 ICE INTERACTION SCENARIOS FOR FIXED STRUCTURES

6.1 INTERACTION CONSIDERATIONS

6.1.1 INTERACTION SCENARIOS

6.1.1.1 Table 6.1 lists relevant interaction scenarios and associated ice actions that should be considered during design of different types of fixed Arctic offshore structures.

6.1.1.2 The interaction scenarios are mainly divided into local and global scenarios. The listed scenarios are not specific to any particular geographic area, however, during design the final selection of relevant interaction scenarios has to be based on site-specific knowledge.

6.1.2 VERTICAL SINGLE-LEG STRUCTURES

6.1.2.1 The global interaction scenarios should consider limit states that involve overturning moment and base shear force. The type of foundation need to be considered.

6.1.2.2 The structure should be assessed with respect to susceptibility to ice-induced vibrations.

6.1.3 VERTICAL MULTI-LEG STRUCTURES

6.1.3.1 The global interaction scenarios should consider limit states that involve overturning moment and base shear force. The type of foundation need to be considered.

6.1.3.2 The global ice action on a multi-leg structure is a sum of contributions from individual ice actions on each leg. Depending on leg diameter and configuration, one or several legs may be fully or partly sheltered if they are located in the wake of other legs. The sheltering effect should be taken into account in relevant global scenarios.

6.1.3.3 The structure should be assessed with respect to susceptibility to ice-induced vibrations.

6.1.3.4 The possibility of the occurrence of ice jamming, either locally within each leg (if truss structure), or globally underneath the structure in between the columns (or truss legs), should be established. The effects of ice jamming should be investigated and quantified.

6.1.4 SLOPED STRUCTURES

6.1.4.1 A sloped structure is categorized as being one of the following types:

- (i) a wide, upward sloping structure;
- (ii) a narrow, upward sloping structure;
- (iii) a wide, downward sloping structure;
- (iv) a narrow, downward sloping structure.

6.1.4.2 The relevant global interaction scenarios should consider limit states that involve overturning moment, base shear force and torsion moment (focussing on asymmetric or eccentric interactions).

6.1.4.3 For downward sloping structures in particular, the overturning moment involves both the horizontal and vertical components of the action, and so both must be considered. For upward sloping structures the components counteract.

6.1.4.4 For narrow sloping structures, ice induced vibrations should be investigated.

6.1.5 JACKETS AND JACK-UPS

6.1.5.1 The relevant global interaction scenarios should consider limit states that involve overturning moment, base shear force and torsion moment (focussing on asymmetric or eccentric interactions). The type of foundation need to be considered.

6.1.5.2 Local interaction scenarios should consider limit states that involve local bending and buckling of bracing members.

6.1.5.3 The possibility of the occurrence of ice jamming, either locally within each truss leg, or globally underneath the structure in between the truss legs, should be established. The effects of ice jamming should be investigated and quantified.

6.1.5.4 Susceptibility to ice-induced vibrations should be assessed. The assessment should consider also exposed secondary structural components (e.g. supported pipes carrying hydrocarbons in topside structure).

6.1.5.5 If the legs of jackets or jack-ups are modified by including cones to reduce the ice loading, the actual diameters of the cones in the waterline shall be used in the assessment of ice actions.

Table 6.1: Overview of relevant interaction scenarios for different fixed structure types.

Action	Interaction Scenario	Vertical Structures			Sloped structures	Jackets and jack-ups
		Single-leg	Multi-leg	Caisson		
Local actions	Crushing of first year level ice	x	x	x	x	X
	Crushing of multi-year ice or iceberg	x	N.A.	x	x	N.A.
Global actions	Crushing of first year level ice	x	x	x	N.A.	x
	Impact from multi-year ice or iceberg	x	N.A.	x	x	N.A.
	Ice ridge interaction	x	x	x	x	x
Other effects	Fatigue	x	x	N.A.	N.A.	x
	Ice induced vibrations	x	x	x	x	x
	Rubble accumulation and jamming	N.A.	x	x	x	x

7 SEA ICE ACTIONS ON FIXED STRUCTURES

7.1 GENERAL

7.1.1 LOCAL AND GLOBAL ACTIONS

7.1.1.1 Both local and global ice actions arising from interaction between ice and structure shall be considered during design of fixed Arctic offshore structures.

7.1.2 LIMITATIONS

7.1.2.1 The present section is only valid for fixed structures, and it provides guidance on estimating characteristic actions and nominal actions.

7.1.2.2 The present section covers only actions from first-year level ice and first year ice ridges.

7.1.2.3 Local actions from icebergs and multi-year ice ridges are considered in section 4.

7.1.2.4 The actions calculated by the methods presented herein are appropriate for fairly quasi-static interactions (as far as the structural dynamic response during the interaction is concerned); pronounced dynamic response due to cyclic failure of sea ice is considered in section 8.

7.1.3 GLOBAL CHARACTERISTIC ACTIONS

7.1.3.1 The global characteristic actions, associated with a specified return period, r (e.g. 100 years), and with a specified annual number of interaction events, n , is obtained as

$$f_r = f_{\text{nom}} \times \gamma_r(h_{\text{end}}, r, n), \quad (7.1)$$

where:

f_r is the characteristic action

f_{nom} is the nominal action

γ_r is a 'factor' scaling the nominal action into the characteristic action, where γ_r is a function of h_{end} , r and n .

7.1.3.2 The present section provides equations for establishing f_{nom} and γ_r for different interaction scenarios.

7.2 LOCAL ACTIONS

7.2.1 NOMINAL LOCAL PRESSURE FROM THIN LEVEL ICE

7.2.1.1 The nominal local pressure, p_L , depends on ice thickness h and can be obtained from:

$$p_L = 10.0 \text{ MPa, if } h \leq 0.35 \text{ m,} \quad (7.2)$$

$$p_L = 5.88 \times h^{-0.5} \text{ MPa, if } 0.35 \text{ m} < h \leq 2.5 \times a_d, \quad (7.3)$$

$$p_L = 3.72 \times a_d^{-0.5} \text{ MPa, if } 2.5 \times a_d \leq h, \quad (7.4)$$

where a_d is the vertical distance between two horizontal stiffening structural members (e.g. stringers) to which the plating is attached.

7.2.1.2 The appropriate area A over which the local pressure obtained from the previous section is to be applied is given by:

$$A = 0.4 \times w_d \times h, \text{ if } h \leq 2.5 \times a_d \leq 1.5 \text{ m,} \quad (7.5)$$

$$A = w_d \times a_d, \text{ if } 2.5 \times a_d \leq h \leq 1.5 \text{ m,} \quad (7.6)$$

where w_d is the horizontal distance between to vertical stiffening structural members (e.g. frames) to which the plating is attached.

7.2.1.3 Eqs. (7.2) to (7.6) are not valid for $h > 1.5$ m. In that case use Eq. (4.2) (section 4.2.2, page 11).

7.2.1.4 The scaling factor γ_r given herein is not applicable for local ice actions from thin ice. This is due to the insufficient quality of available data and insufficiently documented basis for the different equations available for local ice actions. The nominal local pressure from thin ice obtained herein (or from ISO 19906) should be considered as nominal, and no particular return period should be attached to them, until supporting detailed probabilistic analyses of the data can be provided.

7.3 GLOBAL LEVEL ICE ACTIONS ON VERTICAL STRUCTURES

7.3.1 INTRODUCTION

7.3.1.1 The present approach is recommended for estimating nominal and characteristic global level ice actions against a vertical fixed structure.

7.3.1.2 The equations given below are valid for vertical structures which have an aspect ratio (ratio of width, w , to ice thickness, h) greater than 10 and which interact with level ice the average end-of-season thickness of which is between 0.4 m and 1.2 m.

7.3.1.3 The global action should be applied in the waterline (but note that tidal changes should be considered).

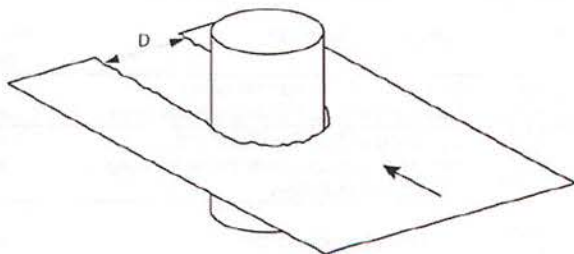


Figure 7.1: Incoming level ice against a vertical cylindrical structure.

7.3.2 REQUIRED INPUT VARIABLES

7.3.2.1 The required *structural* input variables are:

- the width w at the water level.

7.3.2.2 The required *environmental* input variables are:

- the average end-of-season sheet ice thickness, h_{end}
- the cumulative freezing degree-days, C_{FDD}
- the annual length of level ice passing the site, L_{tot}

7.3.2.3 In the case where the equations below are used to estimate the contribution to the global *ice ridge* action from the consolidated layer, which has thickness h_c , the thickness h_{end} appearing in the equations should be replaced by h_c .

7.3.3 THE NOMINAL GLOBAL LEVEL ICE ACTION

7.3.3.1 The nominal global level ice action, f_{nom} , applied to the structure in the waterline, is given by:

$$f_{\text{nom}} = C_R \times w^{0.84} \times \begin{cases} h_{\text{end}}^{0.65+0.2 \cdot h} & , h_{\text{end}} < 1 \text{ m} \\ h_{\text{end}}^{0.55} & , h_{\text{end}} \geq 1 \text{ m} \end{cases} \quad (7.7)$$

where C_R is a strength parameter determined by Eq. (7.8).

7.3.3.2 The strength parameter C_R is determined by:

$$C_R = 0.656 \times \left(\frac{\sigma_{c,\text{index}}}{\sigma_{c,\text{index,ref}}} \right) \quad (7.8)$$

where:

$\sigma_{c,\text{index}}$ is the compressive strength index, in MPa, as given in Section 7.3.4.

$\sigma_{c,\text{index,ref}}$ is the reference compressive strength index, taken as is 2.3 MPa.

7.3.3.3 Full scale field experience from the Baltic suggests that for narrow structures with a low aspect ratio, $w/h < 2$, Eq. (7.7) underestimates the action. For such structures, the nominal global level ice action should be estimated by using the following action:

$$f_{\text{nom}} = C_R \times w \times h_{\text{end}} \times \exp\left(-\frac{1}{3} \frac{w}{h_{\text{end}}}\right) \times \sqrt{1 + 5 \frac{h_{\text{end}}}{w}} \quad (7.9)$$

7.3.4 THE STRENGTH INDEX

7.3.4.1 The strength index, $\sigma_{c,\text{index}}$, appearing in Eq.(7.8), depends on the ice conditions at the location. The index can be determined either directly by Eq. (7.10) below, or, if more detailed ice information is available, from the expression for uniaxial compressive strength as given in Section 3.4.5.

7.3.4.2 A nominal value of the strength index, $\sigma_{c,\text{index}}$, can be obtained from:

$$\sigma_{c,\text{index}} = A_c \times \log_{10}(C_{\text{FDD}}) - B_c \quad (7.10)$$

where A_c and B_c are constants to be taken from Table 7.1.

Table 7.1: Values of A_c and B_c required in Eq. (7.10).

C_{FDD} range	A_c	B_c
250 – 500°C-days	1.78	3.35
500 – 2,000°C-days	2.24	4.59
2,000 – 5,000°C-days	1.69	2.75
5,000 – 8,000°C-days	1.86	3.39

7.3.5 THE CHARACTERISTIC GLOBAL LEVEL ICE ACTION

7.3.5.1 The following equations for the characteristic global level ice action against a vertical structure are considered valid only in cases where the end-of-season ice thickness, h_{end} , is in the range from 0.4 m to 1.2 m.

7.3.5.2 The equations given below have been formulated such that the results obtained from them approximate the results of a large set of fully probabilistic analyses. However, the approximations are only satisfactory over the given range of thickness. In the case where any parameter or input variable is outside the given range of applicability of the equations, it is recommended that a full probabilistic analysis is performed with site-specific descriptions of the input variables, in order to correctly estimate the required characteristic action.

7.3.5.3 By the present method, the characteristic global level ice action f_r is obtained through scaling the nominal action f_{nom} by the factor $\gamma_r(r, n)$, as expressed by Eq. (7.1), and as found in Section 0, via

$$\gamma_r(h_{\text{end}}, r, n) = 10^m \quad (7.11)$$

where $m = m(h_{\text{end}}, r, n)$ is determined from

$$m = A_0 + A_1 z + A_2 z^2 + Y_0 + Y_1 x + Y_2 x^2 \quad (7.12)$$

where:

$x = x(h_{\text{end}})$ is a variable dependent on the ice thickness, as given by Eq. (7.13);

$z = z(r, n)$ is a variable dependent on return period, r , and the annual number of interaction events, n , as given by Eq. (7.14);

$A_j = A_j(h_{\text{end}})$ are constants determined from Eq. (7.15);

Y_j are constants tabulated in Table 7.2.

The variables $x = x(h_{\text{end}})$ and $z = z(r, n)$ required in Eq.(7.12) are determined from:

$$x(h_{\text{end}}) = \ln(h_{\text{end}} - 0.25), \quad (7.13)$$

$$z(r, n) = \log_{10} \{ \log_{10} r + \log_{10} n \}, \quad (7.14)$$

where n is the number of annual interaction events, determined as described in Section 7.3.6. The factors A_0 , A_1 and A_2 , as appearing in Eq.(7.12), are obtained from:

$$\begin{aligned} A_0 &= B_0 + B_1 h_{\text{end}} + B_2 h_{\text{end}}^2, \\ A_1 &= C_0 + C_1 h_{\text{end}} + C_2 h_{\text{end}}^2, \\ A_2 &= E_0 + E_1 h_{\text{end}} + E_2 h_{\text{end}}^2, \end{aligned} \quad (7.15)$$

where B_j , C_j and E_j are constants, tabulated in Table 7.2.

Table 7.2: Values of B_i , C_i , E_i and Y_i

j	B_i	C_i	E_i	Y_i
0	-1.99980	1.41890	0.03760	0.87187
1	1.61200	-1.25260	-0.08450	-0.48524
2	-0.51670	0.41090	0.06090	0.03214

7.3.6 THE ANNUAL NUMBER OF IMPACTS n

7.3.6.1 The annual number of impacts, n , can be estimated from the 'amount', expressed in length, of level ice passing the location annually, L_{tot} , and the constant reference length for one crushing event, to be taken as $L_{\text{event}} = 90$ m. The estimate of the annual number of impacts is then simply the ratio of L_{tot} to L_{event} ,

$$n = \left(\frac{L_{\text{tot}}}{L_{\text{event}}} \right). \quad (7.16)$$

7.3.7 GLOBAL ACTION ON VERTICAL MULTI-LEG STRUCTURES

7.3.7.1 The global action from ice interacting with a vertical *multi-leg* structure is dependent on:

- the distance, L , between the individual columns (or truss legs);
- the width, w , of each column (or truss leg);
- the ice drift direction, α (see Figure 7.2).

7.3.7.2 Depending on the structural configuration, the columns (or truss legs) might be fully or partially sheltered from incoming ice. The effects of sheltering, which generally reduces the total action, should be taken into account. The equations given below approximate the effect of sheltering.

7.3.7.3 The total global action is the sum of individual load contributions from interaction between the ice and each column (or truss leg), but it is not a simple sum because temporal maxima in the action time series do not

occur at the same time. As the distance between each column (or truss leg) increases, the correlation between the individual time series decreases, and so the peak actions against the different columns (or truss legs) will not occur simultaneously. Hence, the total global action is smaller than the product of the number of columns (or truss legs) and the action against a single column (or truss leg) due to *non-simultaneous failure*.

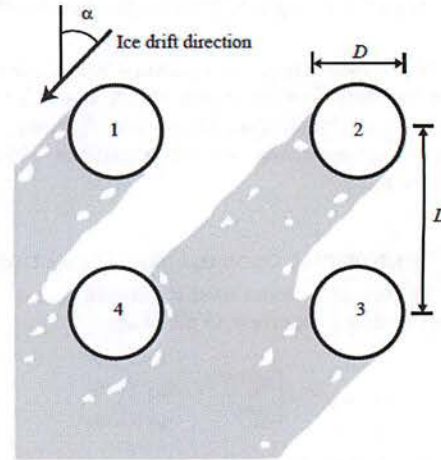


Figure 7.2: Four legged structure seen from above with ice drift towards the lower left hand corner.

7.3.7.4 The global action on a multi-leg structure f_{multi} can be scaled from the nominal action on a single-leg f_{nom} (as determined in section 0) by the factor K_{sn} which includes the effect of sheltering (section 7.3.7.2) and non-simultaneous failure (7.3.7.3),

$$f_{\text{multi}} = f_{\text{nom}} \times K_{sn}, \quad (7.17)$$

where K_{sn} is obtained from the equation given next, Eq. (7.18). Note that the effects of ice jamming are not included in K_{sn} appearing in these equations. No guidance on this is provided in the present document.

7.3.7.5 The factor K_{sn} can for a four legged structure be obtained from

$$K_{sn} = \begin{cases} 2.15 + 0.19(L/D - 2) & \text{if } 2 \leq L/D < 6, \\ 2.91 + 0.025(L/D - 6) & \text{if } 6 \leq L/D < 10. \end{cases} \quad (7.18)$$

7.4 GLOBAL LEVEL ICE ACTIONS ON PLANAR SLOPING STRUCTURES

7.4.1 INTRODUCTION

7.4.1.1 The present approach is recommended for estimating nominal and characteristic global level ice actions against a *planar sloping* fixed structure.

7.4.1.2 The present approach is in conformance with ISO 19906 A.8.2.4.4.3 and is based on Croasdale's equations as given therein.

7.4.1.3 In order to simplify the practical application of the methodology, and to provide insight into the relative contributions from the different action sources (e.g. rubble pile-up weight, breaking of level ice, ride-up of broken ice pieces), the equations presented herein are given in a different form than that of the equations presented in ISO 19906.

7.4.1.4 The equations for determining nominal actions on planar sloping structures are valid for both upward and downward breaking structures, while the equations for characteristic actions have been developed only for upward breaking structures.

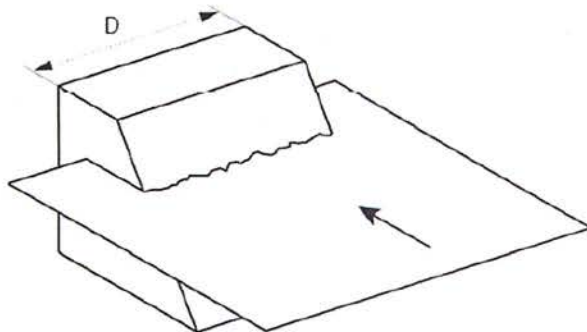


Figure 7.3: Incoming level ice failing against a planar sloping structure.

7.4.2 REQUIRED INPUT VARIABLES

7.4.2.1 The required *structural* input variables are:

- the width w at the water level
- the effective slope angle α , measured against the horizontal.

7.4.2.2 The required *environmental* input variables are:

- the sheet ice thickness h
- the rubble pile height H_r (see 7.4.2.6)
- the ice bulk density ρ_i
- the ice-structure friction coefficient μ
- the ice-ice friction coefficient μ_i
- the flexural strength σ_f

- the angle of repose θ_r (see Sect. 3.6.3)
- the rubble cohesion c
- the internal friction angle ϕ of the rubble.

7.4.2.3 When calculating characteristic actions using the methodology presented herein, *nominal values* of the environmental input variables, as given in section 3, should be used. This produces a nominal action, and the characteristic action is obtained by scaling the nominal action, as described herein.

7.4.2.4 In the case of a downward breaking structure, the sea water density ρ_w is also required. Unless specified otherwise, the nominal value of ρ_w may be taken as 1028 kg/m^3 .

7.4.2.5 In the case of a downward breaking structure, the ice bulk density ρ_i is to be replaced by the term $(\rho_w - \rho_i)$, whenever ρ_i appears in the equations.

7.4.2.6 The empirical relationship for the rubble pile height H_r as a function of surrounding level ice thickness h , as given by Eq. (3.18), can be used to estimate the rubble pile height. Special attention should be given to the structural configuration. In the case of a wide sloping structure ($w > 50 \text{ m}$), the rubble pile height might exceed the predicted value by Eq. (3.18).

7.4.3 THE CHARACTERISTIC GLOBAL LEVEL ICE ACTION

7.4.3.1 The equations given herein, for obtaining the characteristic global level ice action on a planar sloping structure, are considered valid over the following ranges of input variables:

$$10 \text{ m} \leq w \leq 100 \text{ m},$$

$$40^\circ \leq \alpha \leq 60^\circ,$$

$$0.4 \text{ m} \leq h_{\text{end}} \leq 1.0 \text{ m}.$$

7.4.3.2 Over the ranges of input variables specified above, the results of the equations offered herein are *approximations* to the results of a fully probabilistic analysis over the given ranges.

7.4.3.3 In the case where any input variable is outside the given associated range of applicability, a full probabilistic analysis is advised in order to obtain the characteristic actions more accurately.

7.4.3.4 The characteristic global level ice action is obtained by scaling the nominal action, obtained either from Sect. 7.4.4 (in the case of horizontal action) or from Sect. 7.4.5 (in the case of vertical action), according to:

$$f_r = f_{\text{nom}} \times 10^m, \quad (7.19)$$

where:

f_{nom} is the nominal action, as obtained either from Eqs. (7.23)-(7.25) for the horizontal action or

from Eqs. (7.26)-(7.28) for the vertical action;

m is obtained from

$$m = A_0 + A_1 z + A_2 z^2, \quad (7.20)$$

where:

A_j are constants obtained from Eq. (7.22) below;

z is a variable dependent on return period, r , and on the annual number of interaction events, n , as given by

$$z = \log_{10} \{ \log_{10} r + \log_{10} n \}, \quad (7.21)$$

where n must be provided to the designer, similarly as given in Sect. 7.3.6 for crushing events.

7.4.3.5 The factors A_0 , A_1 and A_2 , appearing in Eq. (7.20), are obtained from:

$$\begin{aligned} A_0 &= B_0 + B_1 \alpha + B_2 \alpha^2 + \dots \\ &\quad B_3 w + B_4 w^2 + B_5 \alpha w + B_6 h_{\text{end}} + B_7 h_{\text{end}}^2, \\ A_1 &= C_0 + C_1 \alpha + C_2 \alpha^2 + \dots \\ &\quad C_3 w + C_4 w^2 + C_5 \alpha w + C_6 h_{\text{end}} + C_7 h_{\text{end}}^2, \\ A_2 &= E_0 + E_1 \alpha + E_2 \alpha^2 + \dots \\ &\quad E_3 w + E_4 w^2 + E_5 \alpha w + E_6 h_{\text{end}} + E_7 h_{\text{end}}^2, \end{aligned} \quad (7.22)$$

where B_j , C_j and E_j are constants listed in Table 7.3 for horizontal actions and in Table 7.4 for vertical actions.

Table 7.3: Listed values of B_j , C_j and E_j for horizontal action.

j	B_j	C_j	E_j
0	5.40788×10^{-1}	1.38051	2.61936×10^{-1}
1	-1.21656×10^{-2}	-2.89311×10^{-2}	-1.25558×10^{-2}
2	1.10278×10^{-4}	3.44924×10^{-4}	1.91792×10^{-4}
3	9.70305×10^{-4}	-3.65380×10^{-3}	-2.96525×10^{-4}
4	-5.93629×10^{-6}	1.57593×10^{-5}	9.57174×10^{-6}
5	-1.34480×10^{-6}	2.33695×10^{-5}	-2.16855×10^{-5}
6	-4.23932×10^{-1}	-3.24006×10^{-1}	3.19969×10^{-1}
7	2.48477×10^{-1}	1.37281×10^{-1}	-2.41775×10^{-1}

Table 7.4: Listed values of B_j , C_j and E_j for vertical action.

j	B_j	C_j	E_j
0	2.37584×10^{-1}	4.55453×10^{-1}	3.38370×10^{-1}
1	-4.46606×10^{-3}	1.09656×10^{-2}	-3.92547×10^{-3}
2	4.19039×10^{-5}	-8.08837×10^{-5}	4.33761×10^{-5}
3	1.35250×10^{-3}	-2.32158×10^{-3}	-1.85530×10^{-3}
4	-9.00551×10^{-6}	2.53201×10^{-5}	1.18165×10^{-5}
5	-6.33349×10^{-7}	-2.88102×10^{-5}	-1.48282×10^{-6}
6	-1.78417×10^{-1}	-2.79129×10^{-1}	-1.81339×10^{-1}
7	1.08824×10^{-1}	5.45916×10^{-2}	8.22079×10^{-2}

7.4.4 THE NOMINAL HORIZONTAL ICE ACTION

7.4.4.1 The nominal horizontal component of the global ice action experienced by the structure is denoted as F_H and is given by:

$$F_H = f_{\text{comp}} \times (H_P + H_B + H_R + H_T + H_L), \quad (7.23)$$

where:

f_{comp} is the ice sheet compression factor (Sect. 7.4.6);

H_P is the horizontal component required to push the ice sheet through the ice rubble (Sect. 7.4.9.2);

H_B is the horizontal component of the ice sheet breaking action (Sect. 7.4.8);

H_R is the horizontal component required to push the broken ice sheet up the slope through the ice rubble (Sect. 7.4.12);

H_T is the horizontal component required to rotate the slabs of ice at the top of the slope (Sect. 0);

H_L is the horizontal component required to lift the ice rubble on top of the advancing ice sheet prior to breaking it (Sect. 0).

7.4.4.2 The horizontal action components required in Eq. (7.23) are, in the following, all expressed in terms of a set of reference actions, combined with dimensionless factors. For example, the component H_B is expressed as the product of a reference weight W_B and two dimensionless factors, f_{BS} and f_{HB} : $H_B = W_B \times f_{BS} \times f_{HB}$. Formulae and tabulated values are given below for the required reference actions and dimensionless factors.

7.4.4.3 The required reference actions are denoted herein as W_B , W_{slab} , $W_{\text{sheet,slope}}$, $W_{\text{rubble,slope}}$, $W_{\text{rubble,front}}$ and R_{cohesive} . The reference actions denoted by W represent weights, and the reference action denoted by R represents resistance. The reference actions are defined and obtained as described in Section 7.4.7.

7.4.4.4 The horizontal action components required in Eq. (7.23) may be expressed, in terms of the set of reference actions, in the following matrix form:

$$\begin{Bmatrix} H_P \\ H_B \\ H_R \\ H_T \\ H_L \end{Bmatrix} = \mathbf{A}_{5\text{-by-6 matrix}} \begin{Bmatrix} W_{\text{rubble,front}} \\ W_B \\ W_{\text{sheet,slope}} \\ W_{\text{slab}} \\ W_{\text{rubble,slope}} \\ R_{\text{cohesive}} \end{Bmatrix}, \quad (7.24)$$

where the aforementioned dimensionless factors are contained in the 5-rows-by-6-columns matrix \mathbf{A} , given as

$$A = \dots \begin{bmatrix} \mu_i & 0 & 0 & 0 & 0 & 0 \\ 0 & (f_{HR} f_{HS}) & 0 & 0 & 0 & 0 \\ \mu_i (\mu_i + \mu) f_{HR, front} & 0 & f_{HR} & 0 & (\mu_i + \mu) f_{HR, slope} & 0 \\ 0 & 0 & 0 & f_{HT} & 0 & 0 \\ (f_{HR} f_{HT, \phi}) & 0 & 0 & 0 & 0 & f_{HS} \end{bmatrix} \quad (7.25)$$

Again, formulae and tabulated values are given below for the required reference actions, appearing in Eq. (7.24), and for the dimensionless factors, appearing in Eq. (7.25).

7.4.4.5 Specifically, the required dimensionless factors required in Eq. (7.25) and given herein are:

- f_{HB} , given by Eq. (7.42);
- f_{BS} , given by Eq. (7.43) with Eq. (7.44);
- $f_{HR, front}$, given by Eq. (7.51);
- $f_{HR, slope}$, given by Eq. (7.50);
- f_{HT} , given by Eq. (7.60);
- $f_{HT, \phi}$, given by Eq. (7.56) with Eq. (7.57).

The factors μ and μ_i , also appearing in Eq. (7.25), are friction coefficients, described below.

Guidance note:

The sum of the elements of the *first* column of A , multiplied by $W_{rubble, front}$ and then by the factor f_{comp} (see Sect. 7.4.6), is the total contribution to F_H from $W_{rubble, front}$.

The sum of the elements of the *second* column of A , multiplied by W_B and then by the factor f_{comp} (see Sect. 7.4.6), is the total contribution to F_H from W_B .

Etc.

This provides, for example in a spreadsheet, a quick but insightful overview of the relative contributions to F_H from the different action *sources* (e.g. front rubble, rubble on slope, level ice breaking, broken level ice sliding up the slope, etc). In some cases this insight may be more useful in a design context than the insight provided by the original equations which give the relative contributions to F_H from the different horizontal action components, H_P , H_B , etc.

---e-n-d---o-f---G-u-i-d-a-n-c-e---n-o-t-e---

7.4.5 THE NOMINAL VERTICAL ICE ACTION

7.4.5.1 The nominal vertical component of the global ice action experienced by the structure is denoted as F_V and given by:

$$F_V = f_{comp} \times (V_P + V_B + V_R + V_T + V_L), \quad (7.26)$$

where:

- f_{comp} is the ice sheet compression factor (Sect. 7.4.6);
- V_P is the *vertical* component required to *push* the ice sheet *through the ice rubble* (Sect. 7.4.11);
- V_B is the vertical component of the ice sheet breaking action (Sect. 7.4.9);
- V_R is the vertical component required to push the broken ice sheet *up the slope* through the ice rubble (Sect. 7.4.13);
- V_T is the vertical component required to *rotate* the slabs of ice at the top of the slope (Sect. 7.4.17);
- V_L is the vertical component required to *lift* the ice rubble on top of the advancing ice sheet prior to breaking it (Sect. 7.4.15).

7.4.5.2 The action components V_B , V_P , V_R , V_L and V_T required in Eq. (7.26) are all expressed in terms of a set of reference actions combined with dimensionless factors. For example, the component V_B is expressed as the product of a reference weight W_B and one dimensionless factor, f_{BS} : $V_B = W_B \times f_{BS}$. Formulae and tabulated values are given below for the required reference actions and dimensionless factors.

7.4.5.3 The required reference actions are denoted herein as W_B , W_{slab} , $W_{sheet, slope}$, $W_{rubble, slope}$, $W_{rubble, front}$ and $R_{cohesive}$. The reference actions denoted by a W represent weights, and the reference action denoted by R represents resistance. The reference actions are defined and obtained as described in Section 7.4.7.

7.4.5.4 The vertical action components required in Eq. (7.26) may be expressed, in terms the set of reference actions, in the following matrix form:

$$\begin{Bmatrix} V_P \\ V_B \\ V_R \\ V_T \\ V_L \end{Bmatrix} = \mathbf{B}_{5\text{-by-}6\text{ matrix}} \begin{Bmatrix} W_{rubble, front} \\ W_B \\ W_{sheet, slope} \\ W_{slab} \\ W_{rubble, slope} \\ R_{cohesive} \end{Bmatrix}, \quad (7.27)$$

where the aforementioned dimensionless factors are contained in the 5-rows-by-6-columns matrix \mathbf{B} , given as

$$\mathbf{B} = \dots \begin{bmatrix} \mu_i f_{VP} & 0 & 0 & 0 & 0 & 0 \\ 0 & f_{BS} & 0 & 0 & 0 & 0 \\ \mu_i (\mu_i + \mu) f_{VR,front} & 0 & 1 & 0 & (\mu_i + \mu) f_{VR,slope} & 0 \\ 0 & 0 & 0 & f_{VT} & 0 & 0 \\ f_{HL,\phi} & 0 & 0 & 0 & 0 & 1 \end{bmatrix} \quad (7.28)$$

Again, formulae and tabulated values are given below for the required reference actions, appearing in Eq. (7.27), and for the dimensionless factors, appearing in Eq. (7.28).

7.4.5.5 Specifically, the required dimensionless factors required in Eq. (7.28) and given herein are:

- f_{VP} , given by Eq. (7.48);
- f_{BS} , given by Eq. (7.43) with Eq. (7.44);
- $f_{VR,front}$, given by Eq. (7.54);
- $f_{VR,slope}$, given by Eq. (7.53);
- f_{VT} , given by Eq. (7.62);
- $f_{HL,\phi}$, given by Eq. (7.56) with Eq. (7.57).

The factors μ and μ_i , also appearing in Eq. (7.28), are friction coefficients, described below.

Guidance note:

The sum of the elements of the first column of \mathbf{B} , multiplied by $W_{rubble,front}$ and then by the factor f_{comp} (see Sect. 7.4.6), is the total contribution to F_V from $W_{rubble,front}$.

The sum of the elements of the second column of \mathbf{B} , multiplied by W_B and then by the factor f_{comp} (see Sect. 7.4.6), is the total contribution to F_V from W_B .

This provides, for example in a spreadsheet, a quick but insightful overview of the relative contributions to F_V from the different action sources (e.g. front rubble, rubble on slope, level ice breaking, broken level ice sliding up the slope, etc). In some cases this insight may be more useful in a design context than the insight provided by the original equations which give the relative contributions to F_V from the different horizontal action components, V_P , V_B , etc.

---e-n-d---o-f---G-u-i-d-a-n-c-e---n-o-t-e---

7.4.6 THE ICE SHEET COMPRESSION FACTOR

7.4.6.1 The ice sheet compression factor f_{comp} , required in Eqs. (7.23) and (7.26), is a dimensionless factor which takes into account approximately the change in bending moment capacity (and thus in the apparent flexural strength) due to the compressive forces in the ice sheet.

7.4.6.2 f_{comp} is a function of slope angle α , ice-structure friction coefficient μ , ice sheet thickness h , ice sheet elastic modulus E , and sea water density ρ_w , and f_{comp} is given by

$$f_{comp} = \frac{1}{1 - g_{comp} \times \left(\frac{\rho_w h}{E} \right)^{\frac{1}{4}}} \quad (7.29)$$

7.4.6.3 The factor g_{comp} , required in Eq. (7.29), is a function of the slope angle α and the ice-structure friction coefficient μ , and is given by:

$$g_{comp} = 1.20 \times \left(\frac{\tan \alpha + \mu}{1 - \mu \tan \alpha} \right) \quad (7.30)$$

7.4.7 THE REFERENCE ACTIONS

7.4.7.1 W_B is a reference weight associated with the ice sheet breaking action, and it is defined as the weight of a sheet of ice of thickness h , surface area w^2 and density ρ_i . W_B is given by:

$$W_B = 9.81 \times \rho_i w^2 h \quad (7.31)$$

7.4.7.2 $W_{sheet,slope}$ is a reference weight defined as the weight of the broken ice sheet pushed upwards along the slope of the structure. The ice sheet has density ρ_i , thickness h , width w and length $H_r/\sin(\alpha)$. $W_{sheet,slope}$ is given by:

$$W_{sheet,slope} = \rho_i w h H_r \times f_{sheet,slope} \quad (7.32)$$

7.4.7.3 $f_{sheet,slope}$, appearing in Eq. (7.32), depends on slope angle α and is obtained from:

$$f_{sheet,slope} = \frac{9.81}{\sin \alpha} \quad (7.33)$$

7.4.7.4 $W_{rubble,slope}$ is a reference weight, defined as the weight of the portion of the rubble located on the portion of the slope of the structure visible above the mean water level. It is a function of ice density ρ_i , rubble porosity e , effective ride-up height H_r , width w and a rubble angle of repose θ , measured against the horizontal,

$$W_{\text{rubble,slope}} = (1-e)\rho_i w H_r^2 \times f_{\text{rubble,slope}} \quad (7.34)$$

7.4.7.5 The factor $f_{\text{rubble,slope}}$, appearing in Eq. (7.34), is a function of the slope angle α and the angle of repose θ_r ; $f_{\text{rubble,slope}}$ is obtained from:

$$f_{\text{rubble,slope}} = \frac{9.81}{2} \times \frac{1}{\tan \alpha} \times \left(1 - \frac{\tan \theta_r}{\tan \alpha}\right) \quad (7.35)$$

7.4.7.6 $W_{\text{rubble,front}}$ is a reference weight, defined as the weight of the portion of the rubble located *above* the incoming ice sheet and *in front of* the portion of the slope of the structure visible above the mean water level. The rubble has density ρ_i , rubble porosity e , effective height H_r , width w and a rubble angle of repose θ_r measured against the horizontal. $W_{\text{rubble,front}}$ is given by:

$$W_{\text{rubble,front}} = (1-e)\rho_i w H_r^2 \times f_{\text{rubble,front}} \quad (7.36)$$

7.4.7.7 $f_{\text{rubble,front}}$, appearing in Eq. (7.36), is a function of the slope angle α and the angle of repose θ_r . $f_{\text{rubble,front}}$ can be obtained from:

$$f_{\text{rubble,front}} = \frac{9.81}{2} \times \frac{1}{\tan \theta_r} \times \left(1 - \frac{\tan \theta_r}{\tan \alpha}\right)^2 \quad (7.37)$$

7.4.7.8 R_{cohesive} is a reference action, representing cohesive resistance over the vertical plane through the rubble in front of the slope of the structure. It is defined in terms of the rubble cohesion c , rubble height H_r , slope angle α and the angle of repose θ_r . R_{cohesive} is given by:

$$R_{\text{cohesive}} = c w H_r \times f_{\text{cohesive}} \quad (7.38)$$

7.4.7.9 The factor f_{cohesive} , appearing in Eq. (7.38), is a function of the slope angle α and the angle of repose θ_r ; f_{cohesive} is obtained from:

$$f_{\text{cohesive}} = \left(1 - \frac{\tan \theta_r}{\tan \alpha}\right) \quad (7.39)$$

7.4.7.10 W_{slab} is a reference weight, defined as the weight of a large slab of thickness h , length $3h$, width w and density ρ_i . W_{slab} is given by:

$$W_{\text{slab}} = 29.4 \times \rho_i w h^2 \quad (7.40)$$

7.4.8 THE H_B COMPONENT

7.4.8.1 The action component H_B required in Eq. (7.23) is given by:

$$H_B = (W_B \times f_{BS}) \times f_{HB} \quad (7.41)$$

7.4.8.2 The reference weight W_B is defined in Sect. 7.4.7.1 and obtained from Eq. (7.31).

7.4.8.3 The factor f_{HB} , also required in the matrix **A** in Eqs. (7.24) and (7.25), is a function of slope angle α and ice-structure friction coefficient μ ; f_{HB} is obtained from:

$$f_{HB} = \frac{(\tan \alpha + \mu)}{(1 - \mu \times \tan \alpha)} \quad (7.42)$$

7.4.8.4 The factor f_{BS} , also required in the matrix **A** in Eqs. (7.24) and (7.25), is a function of structural width w , ice sheet thickness h , ice sheet flexural strength σ_f , ice sheet elastic modulus E , ice density ρ_i , and the sea water density ρ_w . f_{BS} is given by:

$$f_{BS} = S^2 \times \left\{ 0.23 + 0.30 \times \left(\frac{w}{h}\right) \times \left(\frac{\rho_w h}{E}\right)^{\frac{1}{4}} \right\} \quad (7.43)$$

7.4.8.5 f_{BS} is expressed in terms of a dimensionless strength parameter S , which depends on structural width w , ice sheet thickness h , ice sheet flexural strength σ_f and ice density, and S is obtained from:

$$S = 0.6386 \times \frac{1}{w} \times \sqrt{\frac{\sigma_f h}{\rho_i}} \quad (7.44)$$

7.4.9 THE V_B COMPONENT

7.4.9.1 The action component V_B required in Eq. (7.26) is given by

$$V_B = W_B \times f_{BS} \quad (7.45)$$

7.4.9.2 The expression for V_B is identical to the bracketed term in Eq. (7.41), and the reference weight W_B is given by Eq. (7.31), while f_{BS} is obtained from Eqs. (7.43) and (7.44).

7.4.10 THE H_P COMPONENT

7.4.10.1 Given the ice-ice friction coefficient μ_i , also required in the matrix **A** in Eqs. (7.24) and (7.25), the action component H_P required in Eq. (7.23) is given by

$$H_P = \mu_i \times W_{\text{rubble,front}} \quad (7.46)$$

7.4.10.2 The reference weight $W_{\text{rubble,front}}$ is defined in Sect. 7.4.7.6 and obtained from Eq. (7.36).

7.4.11 THE V_P COMPONENT

7.4.11.1 Given the ice-ice friction coefficient μ_i , the action component V_P required in Eq. (7.26) is given by

$$V_P = (\mu_i \times W_{\text{rubble,front}}) \times f_{VP} \quad (7.47)$$

7.4.11.2 The bracketed term is identical to H_P in Eq. (7.46).

7.4.11.3 The reference weight $W_{\text{rubble,front}}$ is defined in Sect. 7.4.7.6 and obtained from Eq. (7.36).

7.4.11.4 The factor f_{VP} is a function of slope angle α and ice-structure friction coefficient μ . f_{VP} can be obtained from

$$f_{VP} = \frac{(1 - \mu \times \tan \alpha)}{(\tan \alpha + \mu)} \quad (7.48)$$

7.4.12 THE H_R COMPONENT

7.4.12.1 Given the ice-structure friction coefficient μ and the ice-ice friction coefficient μ_i , both required in the matrix **A** in Eqs. (7.24) and (7.25), the action component H_R in Eq. (7.23) is given by

$$H_R = f_{HB} \times W_{\text{sheet,slope}} + \dots \\ (\mu_i + \mu) \times f_{HR,slope} \times W_{\text{rubble,slope}} + \dots \\ \mu_i (\mu_i + \mu) \times f_{HR,front} \times W_{\text{rubble,front}} \quad (7.49)$$

where:

$W_{\text{sheet,slope}}$ is the reference weight defined in Sect. 7.4.7.2 and obtained from Eq. (7.32);

$W_{\text{rubble,slope}}$ is the reference weight defined in Sect. 7.4.7.4 and obtained from Eq. (7.34);

$W_{\text{rubble,front}}$ is the reference weight defined in Sect. 7.4.7.6 and obtained from Eq. (7.36);

f_{HB} is as described in Section 7.4.8.3, Eq. (7.42).

7.4.12.2 The factor $f_{HR,slope}$ in Eq. (7.49), also required in the matrix **A** in Eqs. (7.24) and (7.25), is a function of slope angle α and ice-structure friction coefficient μ ; $f_{HR,slope}$ is obtained from:

$$f_{HR,slope} = \frac{1}{1 - \mu \times \tan \alpha} \quad (7.50)$$

7.4.12.3 The factor $f_{HR,front}$ in Eq. (7.49), also required in the matrix **A** in Eqs. (7.24) and (7.25), is a function of slope angle α and ice-structure friction coefficient μ ; $f_{HR,front}$ is obtained from:

$$f_{HR,front} = \frac{\tan \alpha}{1 - \mu \times \tan \alpha} \quad (7.51)$$

7.4.13 THE V_R COMPONENT

7.4.13.1 Given the ice-structure friction coefficient μ and the ice-ice friction coefficient μ_i , the action component V_R required in Eq. (7.26) is given by

$$V_R = W_{\text{sheet,slope}} + (\mu_i + \mu) \times f_{VR,slope} \times W_{\text{rubble,slope}} + \dots \\ \mu_i (\mu_i + \mu) \times f_{VR,front} \times W_{\text{rubble,front}} \quad (7.52)$$

where:

$W_{\text{sheet,slope}}$ is the reference weight defined in Sect. 7.4.7.2 and obtained from Eq. (7.32);

$W_{\text{rubble,slope}}$ is the reference weight defined in Sect. 7.4.7.4 and obtained from Eq. (7.34);

$W_{\text{rubble,front}}$ is the reference weight defined in Sect. 7.4.7.6 and obtained from Eq. (7.36).

7.4.13.2 The factor $f_{VR,slope}$ in Eq. (7.52) is a function of slope angle α and ice-structure friction coefficient μ ; $f_{VR,slope}$ is obtained from

$$f_{VR,slope} = \frac{1}{\tan \alpha} \times \frac{1}{\left(1 + \frac{\mu}{\tan \alpha}\right)} \quad (7.53)$$

7.4.13.3 The factor $f_{VR,front}$ in Eq. (7.52) is a function of slope angle α and ice-structure friction coefficient μ ; $f_{VR,front}$ is obtained from

$$f_{VR,front} = \frac{1}{\left(1 + \frac{\mu}{\tan \alpha}\right)} \quad (7.54)$$

7.4.14 THE H_L COMPONENT

7.4.14.1 The action component H_L in Eq. (7.23) is given by

$$H_L = f_{HB} \times (f_{HL,\phi} \times W_{\text{rubble,front}} + R_{\text{cohesive}}) \quad (7.55)$$

where:

R_{cohesive} is the reference action defined in Sect. 7.4.7.8 and obtained from Eq. (7.38);

$W_{\text{rubble,front}}$ is the reference weight defined in Sect. 7.4.7.6 and obtained from Eq. (7.36);

f_{HB} is obtained from Eq. (7.42).

7.4.14.2 The factor $f_{HL,\phi}$ in Eq. (7.55), and also required in the matrix **A** in Eqs. (7.24) and (7.25), is a function of rubble angle of repose θ_r and rubble internal friction coefficient μ_ϕ ; it is given by



$$f_{HL,\phi} = 1 + \mu_{\phi} \times \tan \theta_r. \quad (7.56)$$

7.4.14.3 The rubble internal friction coefficient μ_{ϕ} in Eq. (7.56) is related to the rubble internal friction angle ϕ via

$$\mu_{\phi} = \tan \phi. \quad (7.57)$$

7.4.14.4 The factor f_{HL} in Eq. (7.55) is identical to the factor f_{HB} given in 7.4.8.3, Eq. (7.42).

7.4.15 THE V_L COMPONENT

7.4.15.1 The action component V_L required in Eq. (7.26) is given by

$$V_L = f_{HL,\phi} \times W_{\text{rubble,front}} + R_{\text{cohesive}}. \quad (7.58)$$

where:

R_{cohesive} is the reference action defined in Sect. 7.4.7.8 and obtained from Eq. (7.38);

$W_{\text{rubble,front}}$ is the reference weight defined in Sect. 7.4.7.6 and obtained from Eq. (7.36);

$f_{HL,\phi}$ is the factor is defined in Sect. 0 and obtained from Eqs. (7.56) and (7.57).

7.4.15.2 The expression for V_L is identical to the bracketed term in Eq. (7.55) for the action component H_L .

7.4.16 THE H_T COMPONENT

7.4.16.1 The action component H_T in Eq. (7.23) is given by

$$H_T = W_{\text{slab}} \times f_{HT}. \quad (7.59)$$

7.4.16.2 W_{slab} is defined in Sect. 7.4.7.10 and obtained from Eq. (7.40).

7.4.16.3 The factor f_{HT} , also required in the matrix **A** in Eqs. (7.24) and (7.25), is a function of slope angle α and ice-structure friction coefficient μ , f_{HT} is obtained from:

$$f_{HT} = \frac{1}{2 \times (\tan \alpha - \mu)}. \quad (7.60)$$

7.4.17 THE V_T COMPONENT

7.4.17.1 The action component V_T required in Eq. (7.26) is given by

$$V_T = W_{\text{slab}} \times f_{VT}. \quad (7.61)$$

7.4.17.2 W_{slab} is defined in Sect. 7.4.7.10 and obtained from Eq. (7.40).

7.4.17.3 The factor f_{VT} is a function of slope angle α and ice-structure friction coefficient μ , f_{VT} is obtained from:

$$f_{VT} = \frac{(1 - \mu \times \tan \alpha)}{2 \times (\tan^2 \alpha - \mu^2)}. \quad (7.62)$$

7.5 GLOBAL LEVEL ICE ACTIONS ON CONICAL STRUCTURES

7.5.1 INTRODUCTION

7.5.1.1 The present approach is recommended for estimating nominal and characteristic global level ice actions against a *conical* fixed structure.

7.5.1.2 The present approach is in conformance with ISO 19906 A.8.2.4.4.2 and is based on Ralston's equations as given therein.

7.5.1.3 In order to simplify the practical application of the methodology, and to provide insight into the relative contributions from the different action sources (e.g. rubble pile-up weight, breaking of level ice, ride-up of broken ice pieces), the equations presented herein are given in a different form than that of the equations presented in ISO 19906.

7.5.1.4 The equations for determining nominal actions on conical structures are valid for both upward and downward breaking cones, while the equations for characteristic actions have been developed only for upward breaking cones.

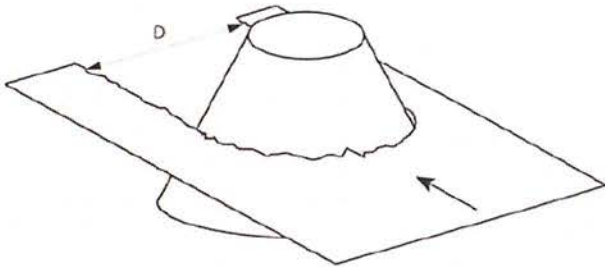


Figure 7.4: Incoming level ice failing against a conical structure.

Guidance note:

Users of ISO 19906 should be advised that equations (A.8-25) and (A.8-26) given therein, which are valid in the case of a simple *two-dimensional* interaction, are *not* applicable to the horizontal and vertical ice action components obtained from Ralston's equations, since they have been obtained from a plastic limit analysis which takes into account the *three-dimensional* interaction process.

---e-n-d-o-f---G-u-i-d-a-n-c-e---n-o-t-e---

7.5.2 REQUIRED INPUT VARIABLES

7.5.2.1 The required *structural* input variables are:

- the width w at the water level
- the width w_T at the top of the cone
- the slope angle α , measured against the horizontal.

7.5.2.2 The required *environmental* input variables are:

- the sheet ice thickness h
- the effective ride-up thickness $h_r \geq h$
- the ice bulk density ρ_i
- the ice-structure friction coefficient μ
- the flexural strength σ_f

7.5.2.3 When calculating characteristic actions using the methodology presented herein, nominal values of the environmental input variables, as given in section 3, should be used. This produces a nominal action, and the characteristic action is obtained by scaling the nominal action, as described herein.

7.5.2.4 In the case of a downward breaking cone, the sea water density ρ_w is also required. Unless specified otherwise, the nominal value of ρ_w may be taken as 1028 kg/m^3 .

7.5.2.5 In the case of a downward breaking structure, the ice bulk density ρ_i is to be replaced by the term $(\rho_w - \rho_i)$, whenever ρ_i appears in the equations.

7.5.3 THE CHARACTERISTIC GLOBAL LEVEL ICE ACTION

7.5.3.1 The equations for characteristic global level ice action on conical structures are considered valid for the following range of input variables:

$$4.0 \text{ m} \leq w \leq 16.0 \text{ m},$$

$$0.4 \leq q_T \leq 0.6, \quad \text{where } q_T = w_T/w$$

$$40^\circ \leq \alpha \leq 60^\circ,$$

$$0.4 \text{ m} \leq h_{\text{end}} \leq 1.0 \text{ m}.$$

7.5.3.2 Over the ranges of input variables specified above, the results of the equations offered herein are *approximations* to the results of a fully probabilistic analysis over the given ranges.

7.5.3.3 In the case where any input variable is outside the given associated range of applicability, a full probabilistic analysis is advised in order to obtain the characteristic actions more accurately.

7.5.3.4 The characteristic global level ice action is found by scaling the nominal action, obtained either from Sect. 7.4.4 (in the case of horizontal action) or from Sect. 7.4.5 (in the case of vertical action), according to:

$$f_r = f_{\text{nom}} \times 10^m \quad (7.63)$$

where:

f_{nom} is the nominal action, as determined either from Eq. (7.67) for the horizontal action or

from Eq. (7.68) for the vertical action; see also Eqs. (7.69) and (7.70);

m is obtained from

$$m = A_0 + A_1 z + A_2 z^2, \quad (7.64)$$

where:

A_j are constants obtained from Eq. (7.66);

z is a variable dependent on return period, r , and the annual number of interaction events, n , as given by:

$$z = \log_{10} \{ \log_{10} r + \log_{10} n \}, \quad (7.65)$$

where n must be provided to the designer in this case (see Sect. 7.3.6 for crushing events).

7.5.3.5 The factors A_0 , A_1 and A_2 , appearing in Eq. (7.64) are obtained from:

$$\begin{aligned} A_0 &= B_0 + B_1 w + B_2 w^2 + \dots \\ &\quad B_3 \alpha + B_4 h_{\text{end}} + B_5 w h_{\text{end}} + B_6 \alpha h_{\text{end}}, \\ A_1 &= C_0 + C_1 D + C_2 w^2 + \dots \\ &\quad C_3 \alpha + C_4 h_{\text{end}} + C_5 w h_{\text{end}} + C_6 \alpha h_{\text{end}}, \\ A_2 &= E_0 + E_1 w + E_2 w^2 + \dots \\ &\quad E_3 \alpha + E_4 h_{\text{end}} + E_5 w h_{\text{end}} + E_6 \alpha h_{\text{end}}, \end{aligned} \quad (7.66)$$

where B_j , C_j and E_j are constants listed in Table 7.5 for horizontal actions and in Table 7.6 for vertical actions.

Table 7.5: Listed values of B_j , C_j and E_j for horizontal action.

j	B_j	C_j	E_j
0	-3.02993×10^{-2}	2.83389×10^{-1}	1.50160
1	1.61873×10^{-2}	-1.42080×10^{-1}	5.65375×10^{-2}
2	-3.32980×10^{-4}	4.12674×10^{-3}	-3.01633×10^{-3}
3	-3.51547×10^{-3}	2.81836×10^{-2}	-2.33858×10^{-2}
4	5.75443×10^{-2}	1.17417	-2.20405
5	-1.15136×10^{-2}	3.32351×10^{-2}	1.55350×10^{-2}
6	4.30722×10^{-3}	-3.46225×10^{-2}	3.71408×10^{-2}

Table 7.6: Listed values of B_j , C_j and E_j for vertical action.

j	B_j	C_j	E_j
0	-2.15703×10^{-1}	1.69912	1.09419×10^{-1}
1	1.80451×10^{-2}	-1.53345×10^{-1}	6.74327×10^{-2}
2	-1.43479×10^{-4}	2.13249×10^{-3}	-1.26939×10^{-3}
3	-9.16591×10^{-4}	5.18560×10^{-3}	-6.03260×10^{-4}
4	3.00029×10^{-1}	-7.92604×10^{-1}	-2.68724×10^{-2}
5	-1.87330×10^{-2}	9.04126×10^{-2}	-3.85835×10^{-2}
6	1.09411×10^{-3}	-4.60470×10^{-3}	1.02032×10^{-3}

7.5.4 THE NOMINAL HORIZONTAL ICE ACTION

7.5.4.1 The total horizontal component of the nominal global ice action experienced by the structure is denoted as F_H and is given by:

$$F_H = W_{\text{ref}} \times \tan \alpha \times (f_{HB,\mu} \times f_B + f_{HR,\mu} \times f_R), \quad (7.67)$$

where:

W_{ref} is the reference weight as given by Eq. (7.71);

α is the prescribed slope angle;

f_R is the ride-up factor (Sect. 7.5.8);

$f_{B,\sigma}$ is the breaking strength factor (Sect. 7.5.9);

$f_{HR,\mu}$ is the horizontal ride-up friction factor (Sect. 7.5.12);

$f_{HB,\mu}$ is the horizontal breaking friction factor (Sect. 7.5.10).

7.5.5 THE TOTAL VERTICAL ICE ACTION

7.5.5.1 The total vertical component of the nominal ice action is denoted as F_V and is given by

$$F_V = 1.273 \times W_{\text{ref}} \times (f_{VB,\mu} \times f_B + f_{VR,\mu} \times f_R), \quad (7.68)$$

where:

W_{ref} is the reference weight as given by Eq. (7.71);

α is the prescribed slope angle;

f_R is the ride-up factor (Sect. 7.5.8);

$f_{B,\sigma}$ is the breaking strength factor (Sect. 7.5.9);

$f_{VR,\mu}$ is the effective vertical ride-up friction factor (Sect. 7.5.13);

$f_{VB,\mu}$ is the vertical breaking friction factor (Sect. 7.5.11).

7.5.6 THE ICE ACTIONS: NO FRICTION

7.5.6.1 The horizontal and vertical components of the nominal ice action, as found above, may be expressed in matrix form,

$$\begin{Bmatrix} F_H \\ F_V \end{Bmatrix} = W_{\text{ref}} \begin{bmatrix} \tan \alpha & 0 \\ 0 & 1.273 \end{bmatrix} \begin{bmatrix} f_{HB,\mu} & f_{HR,\mu} \\ f_{VB,\mu} & f_{VR,\mu} \end{bmatrix} \begin{Bmatrix} f_B \\ f_R \end{Bmatrix}. \quad (7.69)$$

The reference weight is common to both components; the first matrix on the right hand side highlights the strong dependence of F_H on α , and the second matrix includes all friction-dependent behaviour. In the idealized case of no friction, $\mu = 0$, the second matrix reduces to

$$\begin{bmatrix} f_{HB,\mu} & f_{HR,\mu} \\ f_{VB,\mu} & f_{VR,\mu} \end{bmatrix} = \begin{bmatrix} 1 & 1 \\ 1 & \left(1 + \left(\frac{r}{s} - 1\right) \cos^2 \alpha\right) \end{bmatrix}. \quad (7.70)$$

7.5.7 THE REFERENCE WEIGHT

7.5.7.1 W_{ref} is a reference weight, simply defined as the weight of a circular plate of sheet ice of density ρ_i , diameter w and thickness h . W_{ref} is given by

$$W_{ref} = 7.705 \times \rho_i w^2 h. \quad (7.71)$$

7.5.8 THE RIDE-UP FACTOR, F_R

7.5.8.1 The ride-up factor f_R is the product of two factors: (i) the ride-up slope factor $f_{R,\alpha}$ and (ii) the ride-up thickness factor, $f_{R,h}$.

$$f_R = f_{R,h} f_{R,\alpha}. \quad (7.72)$$

7.5.8.2 The ride-up slope factor $f_{R,\alpha}$ is a function of the slope angle α and the diameters w and w_r , where the latter is defined by either Eq. (7.87) or Eq. (7.88).

7.5.8.3 The diameters w_r and w combine into a single dimensionless parameter, the diameter ratio $q_R = w_r/w$, and $f_{R,\alpha}$ can be expressed as a function of α and q_R only:

$$f_{R,\alpha} = \left(\frac{1 - q_R^2}{\pi \times \cos \alpha} \right). \quad (7.73)$$

7.5.8.4 The ride-up thickness factor, $f_{R,h}$, is simply the ratio of the effective ride-up thickness, h_r , to the level ice thickness, h ,

$$f_{R,h} = \frac{h_r}{h}. \quad (7.74)$$

7.5.8.5 The effective ride-up thickness is described in Sect. 7.5.14 and obtained as described therein.

7.5.9 THE BREAKING STRENGTH FACTOR, F_B

7.5.9.1 The breaking strength factor f_B is a function of the level ice thickness h , the bulk ice density ρ_i , the flexural strength σ_f and the structural width w .

7.5.9.2 The variables on which f_B depends all combine into a single dimensionless strength S , and f_B can be expressed as a function of S only. The dimensionless strength S is obtained from:

$$S = 0.6386 \times \frac{1}{w} \sqrt{\frac{\sigma_f h}{\rho_i}}. \quad (7.75)$$

7.5.9.3 The dimensionless strength parameter S defined here is identical to $1/\sqrt{G}$, where G is the corresponding parameter used in ISO 19906 (A.8-35).

7.5.9.4 Depending on the magnitude of S , f_B can be approximated by one of the following three asymptotically correct equations:

$$S < 0.78 \Rightarrow \dots \quad (7.76)$$

$$f_{B,\sigma} = 0.368 \times S + 0.323 \times S^2 + 0.0830 \times S^3,$$

$$0.78 \leq S \leq 1.7 \Rightarrow \dots \quad (7.77)$$

$$f_{B,\sigma} = 0.177 + 0.569 \times S^2,$$

$$1.7 < S \Rightarrow \dots \quad (7.78)$$

$$f_{B,\sigma} = 0.352 + 0.510 \times S^2.$$

7.5.9.5 The form of the original function approximated by the three equations given above is similar to that of Eq. (A.8-35) in ISO 19906.

7.5.10 THE HORIZONTAL BREAKING FRICTION FACTOR, $f_{HB,\mu}$

7.5.10.1 The horizontal breaking friction factor $f_{HB,\mu}$ is a function of the slope angle α and the friction coefficient μ . The behaviour of $f_{HB,\mu}$ is shown in Figure 7.5 and are listed in Table 7.7.

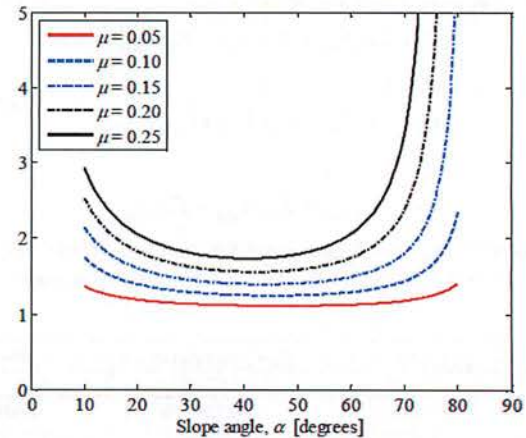


Figure 7.5: The horizontal breaking friction factor, $f_{HB,\mu}$.

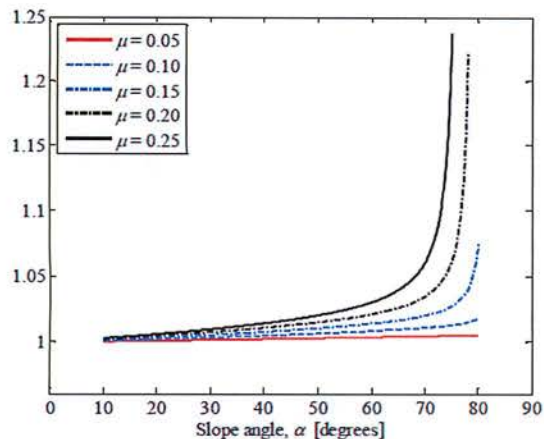
Table 7.7: Tabulated values of $f_{HB,\mu}$.

Slope angle, α [degrees]	Friction coefficient, μ [dim.less]					
	0.05	0.10	0.15	0.20	0.25	0.30
10	1.373	1.752	2.137	2.527	2.924	3.327
20	1.197	1.401	1.611	1.828	2.053	2.285
30	1.144	1.296	1.456	1.626	1.804	1.994
35	1.132	1.272	1.422	1.582	1.754	1.940
40	1.124	1.259	1.404	1.563	1.736	1.926
45	1.121	1.254	1.401	1.565	1.747	1.951
50	1.122	1.258	1.413	1.589	1.791	2.026
55	1.127	1.272	1.442	1.643	1.883	2.175
60	1.137	1.300	1.498	1.744	2.058	2.470
65	1.155	1.350	1.601	1.940	2.420	3.151
70	1.187	1.443	1.810	2.384	3.410	5.762
75	1.251	1.647	2.361	4.039	12.66	N.A.

7.5.11 THE VERTICAL BREAKING FRICTION

FACTOR, $f_{VB,\mu}$

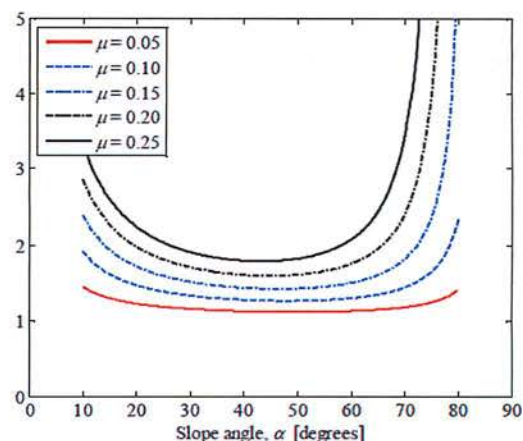
7.5.11.1 The vertical breaking friction factor $f_{VB,\mu}$ is a function of the slope angle α and the friction coefficient μ . The behaviour of $f_{VB,\mu}$ is shown in Figure 7.6 and listed in Table 7.8.

Figure 7.6: The vertical breaking friction factor, $f_{VB,\mu}$.

7.5.12 THE HORIZONTAL RIDE-UP FRICTION

FACTOR, $f_{HR,\mu}$

7.5.12.1 The horizontal ride-up friction factor $f_{HR,\mu}$ is a function of the slope angle α and the friction coefficient μ . The behaviour of $f_{HR,\mu}$ is shown in Figure 7.7 and listed in Table 7.9.

Figure 7.7: The horizontal ride-up friction factor, $f_{HR,\mu}$.Table 7.8: Tabulated values of $f_{VB,\mu}$.

Slope angle, α [degrees]	Friction coefficient, μ [dim. less]					
	0.05	0.10	0.15	0.20	0.25	0.30
10	1.001	1.001	1.002	1.002	1.003	1.003
20	1.001	1.002	1.004	1.005	1.006	1.007
30	1.002	1.004	1.006	1.008	1.010	1.012
35	1.002	1.004	1.007	1.009	1.012	1.015
40	1.002	1.005	1.008	1.011	1.014	1.018
45	1.003	1.006	1.009	1.013	1.017	1.022
50	1.003	1.007	1.011	1.015	1.020	1.027
55	1.004	1.008	1.012	1.018	1.025	1.033
60	1.004	1.009	1.014	1.021	1.030	1.042
65	1.004	1.010	1.017	1.026	1.040	1.060
70	1.005	1.011	1.020	1.035	1.061	1.120
75	1.005	1.013	1.028	1.062	1.238	N.A.

Table 7.9: Tabulated values of $f_{HR,\mu}$.

Slope angle, α [degrees]	Friction coefficient, μ [dim. less]					
	0.05	0.10	0.15	0.20	0.25	0.30
10	1.456	1.917	2.383	2.855	3.333	3.817
20	1.235	1.476	1.723	1.977	2.237	2.505
30	1.166	1.339	1.519	1.709	1.907	2.116
35	1.148	1.305	1.470	1.646	1.833	2.032
40	1.137	1.284	1.441	1.611	1.795	1.995
45	1.131	1.273	1.429	1.600	1.790	2.002
50	1.129	1.272	1.433	1.615	1.822	2.061
55	1.132	1.282	1.456	1.661	1.904	2.198
60	1.140	1.307	1.508	1.756	2.071	2.483
65	1.157	1.354	1.607	1.947	2.426	3.156
70	1.189	1.445	1.813	2.387	3.411	5.756
75	1.252	1.648	2.362	4.038	12.65	N.A.

7.5.13 THE EFFECTIVE VERTICAL RIDE-UP FRICTION FACTOR, $F_{VR,\mu}$

7.5.13.1 Here, the term 'effective' is used, since the factor represents other effects in addition to friction; the term is simply used for simplicity and convenience, so that the action equations may be written in the form of Eq. (7.69) and (7.70).

7.5.13.2 $f_{VR,\mu}$ is a function of the slope angle α and the friction coefficient μ . The behaviour of $f_{VR,\mu}$ is shown in Figure 7.8 and listed in Table 7.10.

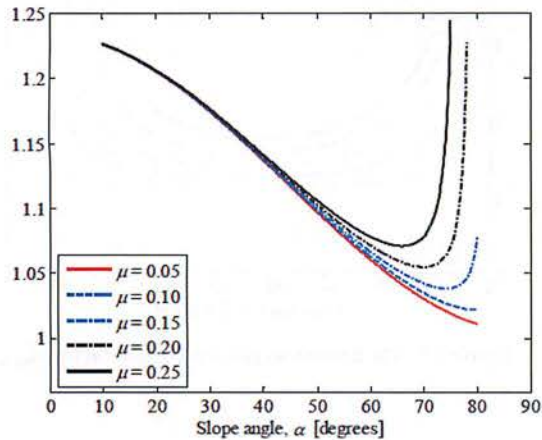


Figure 7.8: The effective vertical ride-up friction factor, $f_{VR,\mu}$.

Table 7.10: Tabulated values of $f_{VR,\mu}$.

	Friction coefficient, μ [dim.less]					
	0.05	0.10	0.15	0.20	0.25	0.30
10	1.227	1.227	1.227	1.227	1.227	1.227
20	1.206	1.207	1.207	1.207	1.207	1.207
30	1.176	1.176	1.176	1.177	1.178	1.178
35	1.157	1.158	1.158	1.159	1.160	1.161
40	1.138	1.139	1.139	1.141	1.142	1.144
45	1.118	1.119	1.120	1.122	1.124	1.127
50	1.098	1.099	1.101	1.104	1.107	1.111
55	1.078	1.080	1.083	1.086	1.091	1.097
60	1.060	1.063	1.067	1.071	1.078	1.088
65	1.044	1.047	1.053	1.060	1.071	1.090
70	1.030	1.035	1.042	1.055	1.079	1.136
75	1.019	1.026	1.038	1.071	1.245	N.A.

7.5.14 THE EFFECTIVE RIDE-UP THICKNESS h_r

7.5.14.1 h_r is the *effective* ride-up thickness, the purpose of which is to take into account rubble accumulation over the conical face of the structure.

7.5.14.2 If rubble accumulation can be neglected, the effective ride-up thickness is taken as being identical to the sheet ice thickness, and hence $h_r = h$.

7.5.14.3 If rubble accumulation cannot be neglected, the effective ride-up thickness may be estimated from the equation given below, which is based on rubble volume considerations. From these, the effective ride-up thickness is obtained as the equivalent thickness of level ice covering the front conical surface. The equivalent level ice imagined to cover the conical surface is assigned a volume identical to the estimated rubble volume.

7.5.14.4 The effective ride-up thickness h_r may be estimated from either:

$$\text{if } H_r < H, \\ \text{then } h_r = \left(\frac{w + w_r}{2} \right) \left(\frac{\sin \alpha}{2} \right) \times \dots \\ \left(\sqrt[3]{ \left(1 + \frac{8V_{ice}}{\pi H_r \left(\frac{w + w_r}{2} \right)^2} \right) - 1 } \right); \quad (7.79)$$

or

$$\text{if } H_r \geq H, \\ \text{then } h_r = \left(\frac{w + w_T}{2} \right) \left(\frac{\sin \alpha}{2} \right) \times \dots \\ \left(\sqrt[3]{ \left(1 + \frac{8V_{ice}}{\pi H \left(\frac{w + w_T}{2} \right)^2} \right) - 1 } \right); \quad (7.80)$$

where:

- H is the height of the conical section;
- H_r is the nominal rubble pile height (Sect. 7.5.14.5);
- α is the prescribed slope angle;
- w is the waterline diameter of the conical section;
- w_T is the diameter of the top end of the conical section;
- w_r is the rubble pile width at the top of the rubble pile (Sect. 7.5.14.12), when this is below w_T ;
- V_{ice} is the estimated total volume of ice, V_{ice} , in the rubble pile in front of the cone (Sect. 7.5.14.8).

7.5.14.5 Eqs. (7.79) and (7.80) require the *nominal* rubble pile height, H_r . This can be estimated from Eq. (3.18).

7.5.14.6 In the case where the nominal rubble pile height, H_r , exceeds the height of the cone, H , an *effective* rubble pile height, $H_{r,eff}$, needs to be estimated in order to account for geometry effects, under the assumption that the rubble pile will change its shape when its height reaches the vertical cylindrical section of the structure above the conical section. The relevant equation for $H_{r,eff}$ is given in Sect. 7.5.14.11.

7.5.14.7 Eqs. (7.79) and (7.80) require also the rubble pile width at the top of the rubble pile, w_r , an equation for which is given in Sect. 7.5.14.12.

7.5.14.8 Eqs. (7.79) and (7.80) require also the volume of sea ice in the rubble pile, V_{ice} :

$$V_{ice} = V_{r,eff} (1 - e), \quad (7.81)$$

where:

e is the effective porosity of the ice rubble (which, unless a specific value is given, may be estimated as suggested in Sect. 3.6.4);

$V_{r,eff}$ is the effective volume of the rubble pile (see below).

7.5.14.9 The effective volume of the rubble pile, $V_{r,eff}$, can be estimated from:

$$\begin{aligned} &\text{if } H_r < H, \\ &\text{then } V_{r,eff} = V_{rubble+cone} + \dots \\ &\quad - \frac{\pi}{24} (w^2 + w w_r + w_r^2) H_r, \end{aligned} \quad (7.82)$$

or

$$\begin{aligned} &\text{if } H_r \geq H, \\ &\text{then } V_{r,eff} = V_{rubble+cone} + \dots \\ &\quad - \frac{\pi}{24} (w^2 + w w_T + w_T^2) H + \dots \\ &\quad - \frac{\pi w_T^2}{8} (H_{r,eff} - H), \end{aligned} \quad (7.83)$$

where:

H is the height of the conical section;

H_r is the nominal rubble pile height (Sect. 7.5.14.5);

$H_{r,eff}$ is the *effective* rubble pile height (Sect. 7.5.14.11), required in case $H_r \geq H$;

w is the waterline diameter of the conical section;

w_T is the diameter of the top end of the conical section;

w_r is the rubble pile width at the top of the rubble pile (Sect. 7.5.14.12) when this is below w_T ;

$V_{rubble+cone}$ is the total volume of both the rubble pile and the structure (see below).

7.5.14.10 The total volume of both the rubble pile and the structure, $V_{rubble+cone}$, can be estimated from:

$$\begin{aligned} &\text{if } H_r < H, \\ &\text{then } V_{rubble+cone} = \dots \\ &\quad \frac{H_r}{2} \left(\frac{w + w_r}{2} \right) \left(w_r + \frac{H_r}{\tan \theta_r} \right), \end{aligned} \quad (7.84)$$

or

$$\begin{aligned} &\text{if } H_r \geq H, \\ &\text{then } V_{rubble+cone} = \dots \\ &\quad \frac{H_{r,eff}}{2} \left(\frac{w + w_T}{2} \right) \left(w_T + \frac{H_{r,eff}}{\tan \theta_r} \right), \end{aligned} \quad (7.85)$$

where:

H is the height of the conical section;

H_r is the nominal rubble pile height (Sect. 7.5.14.5);

$H_{r,eff}$ is the *effective* rubble pile height (Sect. 7.5.14.11), required in case $H_r \geq H$;

w is the waterline diameter of the conical section;

w_T is the diameter of the top end of the conical section;

w_r is the rubble pile width at the top of the rubble pile (Sect. 7.5.14.12) when this is below w_T ;

θ_r is the nominal angle of rubble repose (see Sect. 3.6.3).

7.5.14.11 In the case where the nominal rubble height, H_r , exceeds the height of the cone, H , the *effective* rubble pile height, $H_{r,eff}$, can be estimated as follows¹:

$$\begin{aligned} &\text{if } H_r \geq H, \\ &\text{then } H_{r,eff} = \dots \\ &\quad H_r \left(1 - \frac{\tan \theta_r}{\tan \alpha} \right) + \tan \theta_r \left(\frac{w - w_T}{2} \right), \end{aligned} \quad (7.86)$$

where:

w is the waterline diameter of the conical section;

w_T is the diameter of the top end of the conical section;

α is the conical slope angle;

θ_r is the nominal angle of rubble repose (see Sect. 3.6.3).

7.5.14.12 In the case where the nominal rubble height, H_r , is *less than* the height of the cone, H , the rubble

¹ *Note:* Possible improvements in Eq. (7.86) have been identified after the completion of this work; thus, the equation may appear in a different form in future documentation and publication.

pile width at the top of the rubble pile, w_r , can be estimated as:

$$\text{if } H_r < H, \text{ then } w_r = w - \frac{2H_r}{\tan \alpha}, \quad (7.87)$$

otherwise

$$\text{if } H_r \geq H, \text{ then } w_r = w_T, \quad (7.88)$$

where:

- H is the height of the conical section;
- H_r is the nominal rubble pile height;
- α is the prescribed slope angle;
- w is the waterline diameter of the conical section;
- w_T is the diameter of the top end of the conical section.

7.5.14.13 As basis for the equations given above, the assumed shape of the pile of the rubble in front of the cone is shown in Figure 7.9 below.

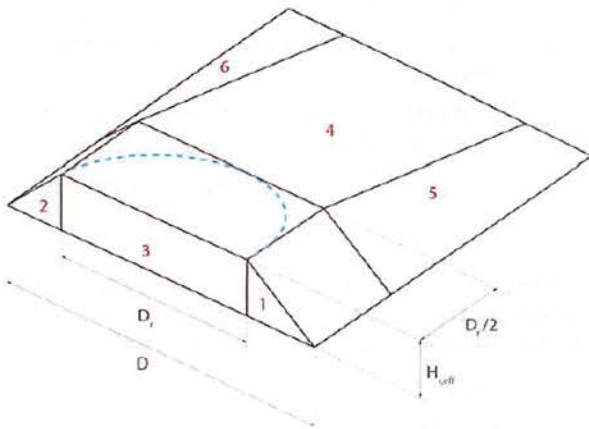


Figure 7.9: The assumed shape of the rubble pile in front of the cone; the circumference of the diameter of the cone at the top of the rubble pile is indicated by the dashed curve.

7.6 FIRST-YEAR ICE RIDGE ACTIONS

7.6.1 INTRODUCTION

7.6.1.1 Ice ridges represent, in most geographical areas where icebergs and multiyear ice do not exist, the dominating source of ice loads. The interaction between a structure and an ice ridge thus represents the most severe interaction scenario.

7.6.1.2 Action components from the consolidated layer and from the ridge keel shall be combined by simple addition, as shown in Eq. (7.89), in order to estimate the total action from an ice ridge,

$$F_R = F_c + F_k \quad (7.89)$$

7.6.1.3 When calculating the nominal action component from the *consolidated* layer, the consolidated layer thickness should be used instead of the level ice thickness.

7.6.1.4 Unless other information exists, the consolidated layer thickness can be assumed to be 1.5 times the end of the season level ice thickness, h_{end} (as specified in 3.3.2.2). See Table 7.11 for references to sections herein relevant for ridge keel action calculations.

Table 7.11: Sections needed for ridge action calculation.

Structure type	Consolidated layer	Keel
Vertical structures	Section 7.3	Section 7.7
Wide sloping structures	Section 7.4	Section 7.8
Narrow conical structures	Section 7.5	Section 7.9

7.6.1.5 The vertical action contribution from the ice ridge keel on sloping structures is not considered herein.

7.7 GLOBAL ICE RIDGE ACTIONS ON VERTICAL STRUCTURES

7.7.1 INTRODUCTION

7.7.1.1 The present approach is recommended for estimating nominal and characteristic global ice ridge actions against a *vertical* fixed structure.

7.7.1.2 For calculation of the nominal action component of the consolidated layer see Sect. 7.3.

7.7.2 REQUIRED INPUT VARIABLES

7.7.2.1 The required *structural* input variable is:

- the width w at the water level

7.7.2.2 The required *environmental* input variables are:

- the keel draught H_k
- the consolidated layer thickness h_c
- the angle of internal friction ϕ of the keel rubble.

7.7.2.3 Recommended *nominal* values of the following input variables can be found in Sect. 3:

- the apparent cohesion c of the keel rubble
- the ice bulk density ρ_i
- the sea water density ρ_w
- the keel porosity e

7.7.2.4 When calculating characteristic actions, nominal values, as given in section 3, of the environmental input variables should be used.

7.7.2.5 The *effective* keel depth, h_k , used to determine the keel action (taking into account surcharge effects), can be estimated from:

$$h_k = 1.1 \times (H_k - h_c). \quad (7.90)$$

7.7.3 THE NOMINAL KEEL ACTION

7.7.3.1 The vertical component of the keel action can be taken as zero.

7.7.3.2 The horizontal component of the keel action is denoted $F_{k,H}$ and is given by:

$$F_{k,H} = \mu_\phi h_k w \left(\frac{h_k \mu_\phi \gamma_e}{2} + 2c \right) \left(1 + \frac{h_k}{6w} \right), \quad (7.91)$$

where:

μ_ϕ is the passive pressure coefficient as given by Eq. (7.92).

γ_e is the effective buoyancy of the keel as given by Eq. (7.93).

and the remaining input variables are as defined in Sect. 7.7.2.

7.7.3.3 The passive pressure coefficient, μ_ϕ , is a function of the angle of internal friction ϕ and is given by

$$\mu_\phi = \tan \left(45^\circ + \frac{\phi}{2} \right). \quad (7.92)$$

7.7.3.4 The effective buoyancy of the keel, γ_e , is given by:

$$\gamma_e = 9.81(1-e)(\rho_w - \rho_i). \quad (7.93)$$

7.7.4 THE CHARACTERISTIC GLOBAL ICE RIDGE ACTION ON VERTICAL STRUCTURES

7.7.4.1 The equations given herein, for obtaining the characteristic global ice ridge action against a vertical structure, are considered valid over the following ranges of input variables:

$$4 \text{ m} \leq w \leq 16 \text{ m},$$

$$0.4 \text{ m} \leq h_{\text{end}} \leq 1.2 \text{ m},$$

$$9.4 \sqrt{h_{\text{end}}} \leq H_{k,\text{end}} \leq 18.7 \sqrt{h_{\text{end}}}.$$

7.7.4.2 Over the ranges of input variables specified above, the results of the equations offered herein are *approximations* to the results of a fully probabilistic analysis over the given ranges.

7.7.4.3 In the case where any input variable is outside the given associated range of applicability, a full probabilistic analysis is advised in order to obtain the characteristic actions more accurately.

7.7.4.4 Following Eq. (7.89), the total *nominal* ice ridge action f_{nom} is obtained as the sum of the nominal action contributions from: (i) the consolidated layer (using the recommendations from Sect. 7.3); and (ii) the keel (Sect. 7.7.3 above).

7.7.4.5 The *characteristic* global ice ridge action, f_r , is obtained by scaling the total nominal ice ridge action, f_{nom} , according to:

$$f_r = f_{\text{nom}} \times 10^m, \quad (7.94)$$

where m is obtained from

$$m = A_0 + A_1 z + A_2 z^2, \quad (7.95)$$

where:

A_j are constants obtained from Eq. (7.97) below;

z is a variable dependent on return period, r , and on the annual number of interaction events, n , as given by:

$$z = \log_{10} \{ \log_{10} r + \log_{10} n \}, \quad (7.96)$$

where n is the number of annual interaction events as given by Section 7.3.6.

7.7.4.6 The factors A_0 , A_1 and A_2 appearing in Eq. (7.96) are obtained from:

$$\left. \begin{aligned} A_0 &= B_0 + B_1 h_{\text{end}} + B_2 h_{\text{end}}^2 + \dots \\ &\quad B_3 w + B_4 w^2 + B_5 H_{k,\text{end}} + B_6 H_{k,\text{end}}^2, \\ A_1 &= C_0 + C_1 h_{\text{end}} + C_2 h_{\text{end}}^2 + \dots \\ &\quad C_3 w + C_4 w^2 + C_5 H_{k,\text{end}} + C_6 H_{k,\text{end}}^2, \\ A_2 &= E_0 + E_1 h_{\text{end}} + E_2 h_{\text{end}}^2 + \dots \\ &\quad E_3 w + E_4 w^2 + E_5 H_{k,\text{end}} + E_6 H_{k,\text{end}}^2. \end{aligned} \right\} (7.97)$$

where B_j , C_j and E_j are constants listed in Table 7.12 below.

Table 7.12: Listed values of B_j , C_j and E_j

j	B_j	C_j	E_j
0	4.0282×10^{-1}	6.8291×10^{-1}	7.5499×10^{-2}
1	-3.0780×10^{-1}	-2.5584×10^{-1}	-2.1882×10^{-1}
2	7.8359×10^{-2}	5.4791×10^{-2}	1.3440×10^{-1}
3	-3.5452×10^{-3}	-9.0501×10^{-3}	-3.5798×10^{-3}
4	1.0677×10^{-4}	2.9139×10^{-4}	1.2459×10^{-4}
5	-2.0192×10^{-2}	1.2855×10^{-2}	3.2225×10^{-2}
6	8.1371×10^{-4}	-8.1977×10^{-5}	-8.5604×10^{-4}

7.8 GLOBAL ICE RIDGE ACTIONS ON PLANAR SLOPING STRUCTURES

7.8.1 INTRODUCTION

7.8.1.1 The present approach is recommended for estimating nominal and characteristic global keel action components against a *planar sloping* fixed structure.

7.8.1.2 The validity of the present approach is limited to scenarios involving interaction with *first year* ice ridges.

7.8.1.3 The validity of the equations presented below is limited to upward and downward breaking structures with constant width below the waterline.

7.8.1.4 The assumed failure mode may not be realistic in cases of small slope angles, and the equations presented below may overestimate the keel action components.

7.8.1.5 For estimating the nominal action component from the consolidated layer, see Sect. 7.4.

7.8.2 REQUIRED INPUT VARIABLES

7.8.2.1 The required *structural* input variables are:

- the width w at the water level
- the slope angle α , measured against the horizontal

7.8.2.2 The required *environmental* input variables are:

- the ice-structure friction coefficient μ
- the variables listed in Sects. 7.7.2.2 and 7.7.2.3.

7.8.2.3 When calculating characteristic actions, nominal values, as given in section 3, of the environmental input variables should be used.

7.8.3 THE NOMINAL HORIZONTAL KEEL ACTION

7.8.3.1 The nominal horizontal component of the keel action is obtained as recommended in Sect. 7.7.3.

7.8.4 THE CHARACTERISTIC GLOBAL ICE RIDGE ACTION ON PLANAR SLOPING STRUCTURES

7.8.4.1 The equations given herein, for obtaining the characteristic global ice ridge action against a planar sloping structure, are considered valid over the following ranges of input variables:

$$10 \text{ m} \leq w \leq 100 \text{ m},$$

$$40^\circ \leq \alpha \leq 60^\circ,$$

$$0.4 \text{ m} \leq h_{\text{end}} \leq 1.0 \text{ m},$$

$$9.4 \sqrt{h_{\text{end}}} \leq H_{k,\text{end}} \leq 18.7 \sqrt{h_{\text{end}}}.$$

7.8.4.2 Over the ranges of input variables specified above, the results of the equations offered herein are *approximations* to the results of a fully probabilistic analysis over the given ranges.

7.8.4.3 In the case where any input variable is outside the given associated range of applicability, a full probabilistic analysis is advised in order to obtain the characteristic actions more accurately.

7.8.4.4 Following Eq. (7.89), the total *nominal* ice ridge action f_{nom} is obtained as the sum of the nominal action contributions from: (i) the consolidated layer (using the recommendations from Sect. 7.3); and (ii) the keel (Sects. 7.8.3.1 and 7.7.3).

7.8.4.5 The *characteristic* global ice ridge action, f_r , is obtained by scaling the total nominal ice ridge action, f_{nom} , according to:

$$f_r = f_{\text{nom}} \times 10^m, \quad (7.98)$$

where m is obtained from

$$m = A_0 + A_1 z + A_2 z^2, \quad (7.99)$$

where:

A_j are constants obtained from either Eq. (7.101) or Eq. (7.102) below;

z is a variable dependent on return period, r , and the annual number of interaction events, n , as given by:

$$z = \log_{10} \{ \log_{10} r + \log_{10} n \}, \quad (7.100)$$

where n is the number of annual interaction events which need to be given to the designer in this case.

7.8.4.6 The factors A_0 , A_1 and A_2 appearing in Eq. (7.99) are obtained, in the case of vertical action, from:

$$\begin{aligned} A_0 &= B_0 + B_1 \alpha + B_2 w + \dots \\ &\quad B_3 w^2 + B_4 \alpha w + B_5 h_{\text{end}} + B_6 h_{\text{end}}^2, \\ A_1 &= C_0 + C_1 \alpha + C_2 w + \dots \\ &\quad C_3 w^2 + C_4 \alpha w + C_5 h_{\text{end}} + C_6 h_{\text{end}}^2, \\ A_2 &= E_0 + E_1 \alpha + E_2 w + \dots \\ &\quad E_3 w^2 + E_4 \alpha w + E_5 h_{\text{end}} + E_6 h_{\text{end}}^2, \end{aligned} \quad (7.101)$$

where B_j , C_j and E_j are constants listed in Table 7.14 below.

7.8.4.7 The factors A_0 , A_1 and A_2 appearing in Eq. (7.99) are obtained, in the case of horizontal action, from:

$$\left. \begin{aligned} A_0 &= B_0 + B_1 \alpha + B_2 w + B_3 w^2 + \dots \\ &\quad B_4 h_{\text{end}} + B_5 H_{k,\text{end}} + B_6 H_{k,\text{end}}^2 + \dots \\ &\quad B_7 H_{k,\text{end}} h_{\text{end}} \\ A_1 &= C_0 + C_1 \alpha + C_2 w + C_3 w^2 + \dots \\ &\quad C_4 h_{\text{end}} + C_5 H_{k,\text{end}} + C_6 H_{k,\text{end}}^2 + \dots \\ &\quad C_7 H_{k,\text{end}} h_{\text{end}} \\ A_2 &= E_0 + E_1 \alpha + E_2 w + E_3 w^2 + \dots \\ &\quad E_4 h_{\text{end}} + E_5 H_{k,\text{end}} + E_6 H_{k,\text{end}}^2 + \dots \\ &\quad E_7 H_{k,\text{end}} h_{\text{end}} \end{aligned} \right\} (7.102)$$

where B_j , C_j and E_j are constants listed in Table 7.13.

Table 7.13: Values of B_j , C_j and E_j for horizontal action.

j	B_j	C_j	E_j
0	1.16048×10^{-1}	5.58639×10^{-1}	3.91905×10^{-1}
1	-5.81265×10^{-4}	-4.29735×10^{-4}	-5.64971×10^{-4}
2	-9.48700×10^{-4}	-4.53437×10^{-3}	1.12179×10^{-3}
3	5.77574×10^{-6}	2.76189×10^{-5}	-8.30433×10^{-6}
4	-4.39881×10^{-2}	1.04182×10^{-1}	-1.67006×10^{-1}
5	5.50602×10^{-3}	-1.33821×10^{-3}	2.23565×10^{-2}
6	3.75835×10^{-5}	1.44690×10^{-3}	-1.35240×10^{-3}
7	-2.65392×10^{-3}	-2.89530×10^{-2}	1.91905×10^{-2}

Table 7.14: Values of B_j , C_j and E_j for vertical action.

j	B_j	C_j	E_j
0	1.01617×10^{-1}	5.48272×10^{-1}	6.11938×10^{-1}
1	-2.86873×10^{-4}	4.06803×10^{-3}	2.38024×10^{-4}
2	4.78568×10^{-4}	-4.98838×10^{-3}	-1.04056×10^{-3}
3	-2.60788×10^{-6}	5.16909×10^{-5}	-5.13162×10^{-6}
4	-4.02064×10^{-8}	-5.16413×10^{-5}	1.72561×10^{-5}
5	-3.84276×10^{-2}	2.27399×10^{-1}	-8.83134×10^{-1}
6	3.50455×10^{-2}	-2.29101×10^{-1}	4.55798×10^{-1}

7.9 GLOBAL ICE RIDGE ACTIONS ON CONICAL STRUCTURES

7.9.1 INTRODUCTION

7.9.1.1 The present approach is recommended for estimating nominal and characteristic global keel action components against a *conical sloping* fixed structure.

7.9.1.2 The validity of the present approach is limited to scenarios involving interaction with *first year* ice ridges.

7.9.1.3 The validity of the equations presented below is limited to upward breaking conical structures.

7.9.1.4 The assumed failure mode may not be realistic in cases of small slope angles, and the equations presented below may overestimate the keel action components.

7.9.1.5 For estimating the nominal action component from the consolidated layer, see Sect. 7.5.

7.9.2 REQUIRED INPUT VARIABLES

7.9.2.1 The required *structural* input variables are:

- the diameter w at the water level
- the slope angle α , measured against the horizontal

7.9.2.2 The required *environmental* input variables are:

- the consolidated layer thickness h_c
- the ice-structure friction coefficient μ
- the variables listed in 7.7.2.2 and 7.7.2.3.

7.9.2.3 When calculating characteristic actions, nominal values, as given in section 3, of the environmental input variables should be used.

7.9.3 THE NOMINAL HORIZONTAL KEEL ACTION

7.9.3.1 The nominal horizontal component of the keel action is obtained as recommended in Sect. 7.7.3.

7.9.3.2 To account for the increasing diameter below the waterline, the actual diameter used in the equations should be a little higher than the structural diameter w . It is here recommended to use an *effective* diameter, given by:

$$w_e = w + \frac{2}{\tan(\alpha)} \left(h_c + \frac{h_k}{3} \right), \quad (7.103)$$

where the variables are as already defined (Sect. 7.9.2).

7.9.4 THE CHARACTERISTIC GLOBAL ICE RIDGE ACTION ON CONICAL STRUCTURES

7.9.4.1 The equations given herein, for obtaining the characteristic global ice ridge action against a conical structure, are considered valid over the following ranges of input variables:

$$4 \text{ m} \leq w \leq 16 \text{ m},$$

$$0.4 \leq q_T \leq 0.6,$$

$$0.4 \text{ m} \leq h_{\text{end}} \leq 1.2 \text{ m},$$

$$40^\circ \leq \alpha \leq 60^\circ,$$

$$9.4 \sqrt{h_{\text{end}}} \leq H_{k,\text{end}} \leq 18.7 \sqrt{h_{\text{end}}}.$$

7.9.4.2 Over the ranges of input variables specified above, the results of the equations offered herein are *approximations* to the results of a fully probabilistic analysis over the given ranges.

7.9.4.3 In the case where any input variable is outside the given associated range of applicability, a full probabilistic analysis is advised in order to obtain the characteristic actions more accurately.

7.9.4.4 Following Eq. (7.89), the total nominal ice ridge action f_{nom} is obtained as the sum of the nominal action contributions from: (i) the consolidated layer (using the recommendations from Sect. 7.5); and (ii) the keel (Sect. 7.7.3 above).

7.9.4.5 The characteristic global ice ridge action, f_r , is obtained by scaling the total nominal ice ridge action, f_{nom} , according to:

$$f_r = f_{nom} \times 10^m, \quad (7.104)$$

where m is obtained from

$$m = A_0 + A_1 z + A_2 z^2, \quad (7.105)$$

where:

A_j are constants obtained from either Eq. (7.97) or Eq. (7.108) below;

z is a variable dependent on return period, r , and on the annual number of interaction events, n , as given by:

$$z = \log_{10} \{ \log_{10} r + \log_{10} n \}, \quad (7.106)$$

where n is the number of annual interaction events which need to be given to the designer in this case.

7.9.4.6 The factors A_0 , A_1 and A_2 appearing in Eq. (7.105) are obtained, *in the case of horizontal actions*, as:

$$\left. \begin{aligned} A_0 &= B_0 + B_1 \alpha^2 + B_2 w + B_3 w^2 + \dots \\ &\quad B_4 h_{end} + B_5 h_{end}^2 + B_6 H_{k,end} + \dots \\ &\quad B_7 H_{k,end}^2 + B_8 H_{k,end} \alpha \\ A_1 &= C_0 + C_1 \alpha^2 + C_2 w + C_3 w^2 + \dots \\ &\quad C_4 h_{end} + C_5 h_{end}^2 + C_6 H_{k,end} + \dots \\ &\quad C_7 H_{k,end}^2 + C_8 H_{k,end} \alpha \\ A_2 &= E_0 + E_1 \alpha^2 + E_2 w + E_3 w^2 + \dots \\ &\quad E_4 h_{end} + E_5 h_{end}^2 + E_6 H_{k,end} + \dots \\ &\quad E_7 H_{k,end}^2 + E_8 H_{k,end} \alpha \end{aligned} \right\} \quad (7.107)$$

where B_j , C_j , and E_j are constants listed in Table 7.15 below.

7.9.4.7 A_0 , A_1 and A_2 appearing in Eq. (7.105) are obtained, *in the case of vertical actions*, as:

$$\left. \begin{aligned} A_0 &= B_0 + B_1 w + B_2 w^2 + \dots \\ &\quad B_3 \alpha + B_4 h_{end} + B_5 h_{end} w + B_6 h_{end} \alpha, \\ A_1 &= C_0 + C_1 w + C_2 w^2 + \dots \\ &\quad C_3 \alpha + C_4 h_{end} + C_5 h_{end} w + C_6 h_{end} \alpha, \\ A_2 &= E_0 + E_1 w + E_2 w^2 + \dots \\ &\quad E_3 \alpha + E_4 h_{end} + E_5 h_{end} w + E_6 h_{end} \alpha, \end{aligned} \right\} \quad (7.108)$$

where B_j , C_j and E_j are constants listed in Table 7.16 below.

Table 7.15: Listed values of B_j , C_j and E_j for horizontal action.

j	B_j	C_j	E_j
0	1.0913×10^{-1}	6.4443×10^{-1}	3.9651×10^{-1}
1	-6.2116×10^{-6}	3.0257×10^{-5}	-4.4835×10^{-5}
2	-4.5573×10^{-3}	-1.2194×10^{-2}	1.6271×10^{-3}
3	1.0430×10^{-4}	3.4513×10^{-4}	-1.5338×10^{-4}
4	-3.3434×10^{-1}	-1.8569×10^{-1}	1.0085×10^{-1}
5	1.6945×10^{-1}	5.4454×10^{-2}	-1.1796×10^{-1}
6	2.1313×10^{-2}	3.5491×10^{-2}	-8.8061×10^{-3}
7	-4.9338×10^{-4}	-3.8094×10^{-4}	1.0681×10^{-4}
8	-3.9350×10^{-5}	-3.4725×10^{-4}	2.2629×10^{-4}

Table 7.16: Listed values of B_j , C_j and E_j for vertical action.

j	B_j	C_j	E_j
0	-1.5596×10^{-1}	1.4986	5.5230×10^{-1}
1	4.0375×10^{-3}	-8.7563×10^{-2}	2.5186×10^{-2}
2	-7.9827×10^{-5}	1.8805×10^{-3}	-1.6749×10^{-3}
3	-4.4318×10^{-4}	2.1239×10^{-3}	2.6501×10^{-3}
4	2.8473×10^{-1}	-3.5000×10^{-1}	-6.2749×10^{-1}
5	-4.0956×10^{-3}	2.7984×10^{-2}	1.7777×10^{-2}
6	4.4526×10^{-4}	-1.0040×10^{-3}	-2.8956×10^{-3}

7.10 REFERENCES

ISO 19906:2010(E), *Petroleum and natural gas industries — Arctic offshore structures*, International Organization for Standardization, Switzerland.

8 ICE INDUCED DYNAMIC STRUCTURAL RESPONSE

8.1 GENERAL

8.1.1 ISO 19906

8.1.1.1 ISO 19906 prescribes that dynamic actions shall be considered, both locally and globally, especially in cases of interaction with first year or multiyear *level ice*.

8.1.2 FULL SCALE EXPERIENCE

8.1.2.1 The cyclic failure of ice and resulting dynamic structural response have been observed on a wide variety of fixed structures, such as lighthouses, bridge piers, jackets, caissons and multi-leg structures, in both Arctic and sub-Arctic areas.

8.1.2.2 Full scale experience suggests that any structure that can be considered relatively narrow or relatively flexible is potentially vulnerable to ice induced dynamic response.

8.1.3 DEFINITION AND IMPORTANCE

8.1.3.1 The term Ice-Induced Vibrations (IIV) and ice induced response is here used for any vibration caused by interaction with ice, including frequency lock-in but not excluding other types of vibration, such as the response associated with intermittent or continuous crushing.

8.1.3.2 Particular attention should be given to narrow structures, flexible structures, structures with vertical faces exposed to ice action and structures with high topside weight.

8.1.3.3 Analyses of ice induced dynamic response is required to assess: (i) vibrations, in especially topside structures; (ii) fatigue damage; and (iii) soil degradation.

8.2 ICE INDUCED DYNAMIC RESPONSE OF VERTICAL STRUCTURES

8.2.1 DIFFERENT TYPES OF VIBRATIONS

8.2.1.1 Ice induced dynamic structural response of vertical structures is here classified into three categories:

- (i) intermittent crushing at low ice velocities (Sect. 8.2.1.2); (ii) frequency lock-in at intermediate ice velocities (Sect. 8.2.1.3); and (iii) continuous crushing at high ice velocities (Sect. 8.2.1.4).

8.2.1.2 *Intermittent crushing* occurs under very low ice velocities, and the period between successive ice action peaks is much longer (20 times or more) than the dominant period of structural vibration. For the purpose of calculating actions and action effects, intermittent crushing can be considered to be quasi-static.

8.2.1.3 *Frequency lock-in* can occur under a specific interval of ice drift velocities, and is characterized by periodically fluctuating ice actions, with the ice action

frequency being 'locked' on the frequency of structural vibration, which is very close to one of the natural frequencies of the structure.

8.2.1.4 *Continuous crushing* occurs under high ice drift velocities (typically larger than 0.1 m/s), during which both the ice action and structural vibration may be characterized as stochastic processes. Normally the magnitude of the stochastic ice action and the structural vibration are significantly lower than those associated with frequency lock-in, mainly due to the low and brittle failure strength of ice and due to the non-simultaneous failure along the ice-structure interface. Nevertheless, continuous crushing may cause accumulated damage to relatively compliant structures, whose fatigue life should therefore be assessed.

8.2.2 SUSCEPTIBILITY TO FREQUENCY LOCK-IN

8.2.2.1 Based on full-scale data from several sites, it is generally considered that structures with a fundamental natural frequency lower than 5 Hz should be considered as vulnerable to ice-induced frequency lock-in.

8.2.2.2 In general, susceptibility to frequency lock-in depends on structural characteristics such as mass distribution, stiffness distribution, natural frequencies and damping, and on ice parameters such as ice thickness, ice drift velocity, etc.

8.2.2.3 Frequency lock-in is a physically complex process, involving cyclic failure of the ice edge and interaction between ice and structure, and a general complete criterion for the onset of frequency lock-in has not yet been developed.

8.2.2.4 An empirical criterion, by which susceptibility of frequency lock-in is assessed, is given in ISO 19906 (Eq. A.8-69 therein). This is based on the idea that frequency lock-in is avoided if the modal damping is higher than the 'negative damping' associated with the energy fed into the structure by the dynamic ice action. The structure is *not* considered to be susceptible to frequency lock-in if the following criterion is satisfied:

$$\xi_n \geq \frac{\phi_{nc}^2}{4\pi f_n M_n} h\theta, \quad (8.1)$$

where:

- h is the ice thickness, in metres;
- θ is an empirical coefficient, to be taken as $\theta = 40 \times 10^6 \text{ kg/m/s}$;

(Note: There are uncertainties regarding the value of this coefficient).

- f_n is the natural frequency, in Hz, of the n -th mode of vibration;

- M_n is the modal mass associated with the mode of vibration, and if mass normalization is used the modal mass equals unity (see Sect. 8.2.2.5);

ζ_n is the modal damping of the n -th mode of vibration as a fraction of critical damping;

ϕ_{ic} is the value of the mode shape at the ice action application point; usually the mode shapes are mass normalized, in which case the modal mass M_n is unity; the mode shape can be scaled in any alternative way, provided the modal mass is determined accordingly (see below).

8.2.2.5 The modal mass is expressed as:

$$M_n = \int m(z)\phi_n^2(z)dz, \quad (8.2)$$

where:

$\phi_n(z)$ is the n -th mode shape, in which z is the spatial coordinate along the structure elevation, measured from the seabed;

$m(z)$ is the mass distribution along the structure elevation.

Note that the mode shapes can be scaled in any consistent way considered convenient: if mass normalization is used, the mode shape is scaled such that $M_n = 1$ for all mode shapes; another approach is to scale the mode shape such that the maximum displacement in the mode shape has unit value, in which case each mode shape generally has a different modal mass different from unity.

Guidance note:

Example of susceptibility to frequency lock-in on the Norströmgrund lighthouse is found in Appendix A.1.1.

---e-n-d-o-f-G-u-i-d-a-n-c-e---n-o-t-e---

8.2.3 DYNAMIC RESPONSE UNDER FREQUENCY LOCK-IN

8.2.3.1 The dynamic ice action associated with the frequency lock-in scenario is a *periodic* action, whose time series is close to being either harmonic or triangular. A general saw-tooth loading function (Figure.A.8-23 in ISO 19906) can be used to determine the structural response. The ice action time series is shown in Figure 8.1, and the variables indicated therein are explained below (Sect. 8.2.3.2).

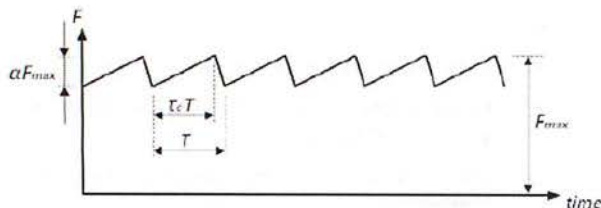


Figure 8.1: Ice action time series for assessing structural response under frequency lock-in.

8.2.3.2 The variables indicated in Figure 8.1 are as follows:

F_{max} is the peak value in the ice action time series;

this peak is treated herein as independent of time;

T is the period of the ice action time series; normally it is equal to the lowest or second natural frequency of the structure, depending on which mode of vibration is considered relevant;

αF_{max} is the range in which the ice action time series fluctuates; typical values of α (which depends on ice characteristics and ice-structure interaction characteristics) are in the range from 0.1 to 0.5, based on full scale observations;

τ_c is the ratio of the duration of positive rate of change in the ice action to the period T ; typical values of τ_c (which depends on ice characteristics and ice-structure interaction characteristics) are in the range from 0.5 to 0.9, based on full scale observations.

8.2.3.3 F_{max} can be determined using methods described in Section 7 (either characteristic action or nominal action).

8.2.3.4 Maximizing α will maximize the dynamic response, and so α can be conservatively taken to be 0.5.

8.2.3.5 Unless a structure-specific and site-specific value is given, τ_c can be assigned a nominal value of 0.7.

8.2.3.6 Once the ice action time series has been constructed based on Figure 8.1 and the variables given below, the time series can be applied to a computational model (e.g. a finite element model) of the structure, from which structural response can be estimated.

8.2.3.7 To obtain an *initial* estimate of the structural response under saw tooth excitation, a simple analytical single degree of freedom (SDoF) model can be used (for example, the SDof version of the MDoF model given below). The method can be used to explore sensitivity to the input variables which influence the dynamic structural response under general saw tooth excitation.

8.2.3.8 If the structure is discretized as a multi-degrees-of-freedom (MDoF) system, whose natural frequencies mode shapes can be obtained from finite element analysis, then the vector of the amplitudes of the dynamic components of the structural displacement, \mathbf{q}_{max} , can be approximated as:

$$\mathbf{q}_{max} \approx (\alpha F_{max}) \left(\frac{T_m^2}{A_r \zeta_m \pi^4} \right) (\mathbf{v}_{m,p}) \mathbf{v}_m, \quad (8.3)$$

where αF_{max} is as defined in Sect. 8.2.3.2, and where:

T_m is the m -th natural period, which is the same as the ice action period T in Figure 8.1;

ζ_m is the modal damping ratio of the m -th mode;

\mathbf{v}_m is the m -th mass-normalized mode shape, represented as a vector;

$\mathbf{v}_{m,p}$ is the m -th mass-normalized mode shape at the point of ice loading on the structure; i.e. it is

the p -th entry of the vector v_m , corresponding to the response at the point of ice loading (i.e. the p -th coordinate in the vector v_m);

A_τ is a dimensionless factor dependent on τ_c and obtained from Table 8.1.

Ratio τ_c	Factor A_τ	Factor B_τ
0.5	2	1
0.7	2.08	1.04
0.9	2.32	1.16

8.2.3.9 The vector of the amplitudes of the velocity components is:

$$\dot{q}_{\max} = (\alpha F_{\max}) \left(\frac{T_m}{B_\tau \zeta_m \pi^2} \right) (v_{m,p}) v_m, \quad (8.4)$$

where B_τ is a dimensionless factor dependent on τ_c and obtained from Table 8.1, and the other variables are as described in Sect. 8.2.3.8 above.

Guidance note:

An example of estimating frequency lock-in response of Norströmsgrund lighthouse based on the procedure above is found in Appendix A.1.2.

---e-n-d---o-f---G-u-i-d-a-n-c-e---n-o-t-e---

8.2.4 CONTINUOUS CRUSHING

8.2.4.1 The ice action and structural response under continuous crushing can both be considered as wide-band stochastic processes, mainly due to the brittle and non-simultaneous failure of the ice edge along the face of the structure.

8.2.4.2 A typical stochastic ice action time series is shown in Figure 8.2; this particular time series has been obtained from actual *in situ* load panel measurements from a real structure.

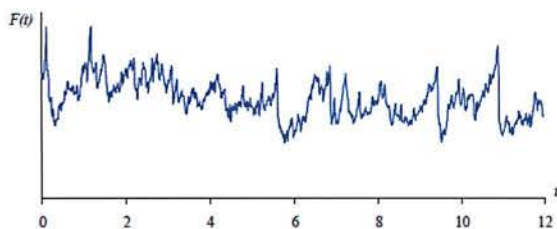


Figure 8.2: Typical stochastic ice action time series during continuous crushing.

8.2.4.3 The dynamic structural response under continuous crushing may be determined by applying a particular type of ice action time series, as described below, to a computation model of the structure (e.g. a finite element model).

8.2.4.4 The type of time series described below is a realization of a random time series that is to be generated from a specified *frequency spectrum*.

8.2.4.5 The continuous crushing frequency spectrum specified below is a simple but generic model based on full scale local ice load measurements (by panel data) from the MDP-1 jacket in the Bohai Bay and from the Norströmsgrund lighthouse in the Bay of Bothnia.

8.2.4.6 The basis for the model presented herein is limited and its range of applicability has not been verified through comparisons with full scale measurements from other structures, so the model should only be used for *preliminary assessments*.

8.2.4.7 The constructed frequency spectrum captures the non-simultaneous failure of ice during continuous crushing. The (auto-)spectral density of the ice action $S(f)$, expressed as a function of the frequency f , is given by:

$$S(f) = \frac{\tilde{S}(\tilde{f}) h \sigma_F^2}{v}, \quad (8.5)$$

where:

f is frequency;

\tilde{f} is a dimensionless frequency, specified in Sect. 8.2.4.8 below;

$S(f)$ is the required spectral density of the local ice load, to be determined;

$\tilde{S}(\tilde{f})$ is the specified generic spectral density in dimensionless form, as given in Sect. 8.2.4.15;

v is the drift velocity of the ice;

h is the ice thickness;

σ_F is the standard deviation in the ice action time series, as given in Sect. 8.2.4.14.

8.2.4.8 The dimensionless frequency \tilde{f} is given by:

$$\tilde{f} = \frac{f h}{v}. \quad (8.6)$$

8.2.4.9 The time series obtained from the spectral density is to be applied over a small segment of the computational model of the structure, as described below. Several time series realizations will then be applied over that part of the structure against which the crushing ice is interacting, and the global action is then the sum of these individual time series.

8.2.4.10 For a given structure, the entire structure width should be divided into local segments of *two metres width* (a recommended characteristic width). In the case where this is not possible (e.g. end segments), treat the last remaining local segment as an individual segment of whatever remaining length there is: for example, if the

structure width is 5 m, then the widths of local segments are 2 m, 2 m and 1 m.

8.2.4.11 For each local segment, calculate: (i) the peak ice action value; (ii) the mean value; and (iii) the standard deviation; all using Eqs. (8.7) - (8.9).

8.2.4.12 The peak ice action F_{\max} for each local segment is obtained as

$$F_{\max} = A_k \times \left(\frac{w_s}{w_0} \right)^{-0.1} \times w_s \times h^{0.5}, \quad (8.7)$$

where:

A_k is an empirical constant equal to 1.7 MPa m^{1/2};

w_s is the width of the considered segment;

w_0 is a reference width equal to 1.2 m.

8.2.4.13 The mean ice action F_{mean} on each segment can be estimated from:

$$F_{\text{mean}} = 0.4 F_{\max}. \quad (8.8)$$

8.2.4.14 The standard deviation σ_F in the ice action time series, about the mean F_{mean} , on each segment can be obtained as:

$$\sigma_F = 0.3 F_{\text{mean}}. \quad (8.9)$$

8.2.4.15 The ice action $F_s(t)$ on one segment can be determined by the sum of N harmonic components by:

$$F_s(t) = F_{\text{mean}} + \sum_{i=1}^N A_i \sin(2\pi i \Delta f t + \theta_i), \quad (8.10)$$

where:

F_{mean} is the mean ice action obtained above (Sect. 8.2.4.13);

A_i is the amplitude of the i -th harmonic component, as obtained in Sect. 8.2.4.19 below;

Δf is the frequency resolution in the underlying spectral density, as obtained in Sect. 8.2.4.16 below;

θ_i is the realization of the random phase of the i -th harmonic component, taken to be uniformly distributed in the interval from 0 to 2π ,

N is the number of harmonic components to be included, as obtained in Sect. 8.2.4.17.

8.2.4.16 The frequency resolution Δf is obtained from

$$\Delta f = \frac{1}{T_{\text{simulation}}}, \quad (8.11)$$

where $T_{\text{simulation}}$ is the desired duration of the entire ice action time series.

8.2.4.17 Given the spectral resolution Δf , the number N of harmonic components to be included is limited by the largest frequency f_{\max} required in the time series,

$$N = \frac{f_{\max}}{\Delta f}, \quad (8.12)$$

where f_{\max} depends on the dynamic characteristics of the structure (i.e. on natural frequencies and modal damping): f_{\max} needs to be sufficiently large such that it includes the range of relevant natural frequencies of the structure which may be excited by the ice crushing actions.

8.2.4.18 As a result of the method by which the spectral model has been developed, there is an upper bound to f_{\max} above which the model is not valid,

$$f_{\max} \leq \frac{15v}{h}. \quad (8.13)$$

As an alternative to determining N from Eq. (8.12), which requires a consideration of the structural dynamic characteristics, N may be determined from

$$N = \frac{15v}{h\Delta f}, \quad (8.14)$$

which is the *largest* number of frequency components supported by the spectral model. Here, N may appear to be large; however, computational efforts are reduced by using the efficient Fast Fourier Transform (FFT) algorithm (available in standard mathematical software packages) for generating the time series via inverse FFT.

8.2.4.19 For each frequency component in the original spectrum, $S_i = S(f_i) = S(i\Delta f)$, the harmonic amplitude A_i of the i -th component at frequency $f_i = i\Delta f$ is obtained from:

$$A_i = \sqrt{2 S_i \Delta f}. \quad (8.15)$$

8.2.4.20 In Eq. (8.15), the spectral density S_i at f_i is obtained from Eq. (8.5), which then requires the dimensionless spectral density \tilde{S}_i at the i -th frequency f_i ; this is obtained from

$$\tilde{S}_i = 0.27 \left(\frac{f_i h}{v} + 0.25 \right)^{-1.9} \quad i = 1, 2, \dots, N. \quad (8.16)$$

This is the specified spectral model referred to above (Sect. 8.2.4.4).

8.2.4.21 The sampling frequency, i.e. the temporal resolution in the obtained ice action time series, need only be large enough to capture correctly the dynamic response of the structure. For the present model, the temporal resolution is limited by

$$\frac{h}{30v} \leq \Delta t, \quad (8.17)$$

so although Δt could in general be arbitrarily small, it can in the present case not be smaller than $h / (30v)$.

8.2.4.22 The procedure described above should be repeated for all segments, where the resulting ice action on the structure is the sum of individual ice actions on all segments.

8.2.4.23 As an example, Figure 8.3 shows a simulated time series (bottom part of figure), obtained from the procedure described above, compared with a measured time series (top part of figure).

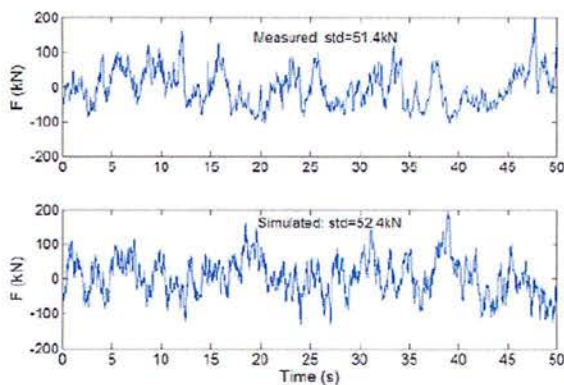


Figure 8.3: Ice action time series for a narrow conical structure.

8.3 ICE INDUCED DYNAMIC RESPONSE OF NARROW CONICAL STRUCTURES

8.3.1 DYNAMIC ICE ACTION TIME SERIES FOR A NARROW CONICAL STRUCTURE

8.3.1.1 The dynamic structural response of a narrow conical structure, against which the ice fails in flexure, may be determined by applying a particular type of ice action time series, as described below, to a computational model of the structure (e.g. a finite element model).

8.3.1.2 The general dynamic ice action time series relevant for a narrow conical structure is illustrated in Figure 8.4. This particular form of time series is based on field data from the JZ20-2 MUQ platform in the Bohai Sea, and *deviates* from the time series proposed in ISO 19906.

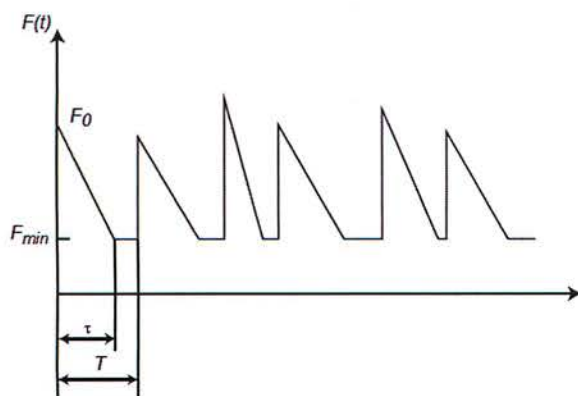


Figure 8.4: Ice action time series; narrow conical structure.

8.3.1.3 The variables identified in Figure 8.4 are:

F_0 is the local peak in the ice action time series, $F(t)$;

F_{\min} is the minimum value of $F(t)$; see Sect. 8.3.2.2;

τ is the duration of the unloading phase;

T is the random period between two peaks.

8.3.2 PARAMETERS IN THE ICE ACTION TIME SERIES

8.3.2.1 For the simulation of total length $T_{\text{simulation}}$, a set of random realizations of F_0 shall be generated, based on: (i) the assumption that F_0 is a Gaussian random variable (an assumption which is based on full scale measurements from the Bohai Sea); (ii) the assumption that $F_{0,\text{mean}}$ is as given in Sect. 8.3.2.3; (iii) the assumption that $F_{0,\text{max}}$ is as given in Sect. 8.3.2.2.

8.3.2.2 The maximum value of the peaks, $F_{0,\text{max}}$, in the total duration of simulation $T_{\text{simulation}}$, shall be estimated using the instruction in section 7.5.3, by setting $F_{0,\text{max}} = f_r$, as obtained therein.

8.3.2.3 The coefficient of variation (CoV) of F_0 can be taken as 0.4, and the mean of F_0 , i.e. $F_{0,\text{mean}}$, may be determined as:

$$F_{0,\text{mean}} = 0.56 \times F_{0,\text{max}} \quad (8.18)$$

8.3.2.4 The minimum value F_{\min} depends largely on: (i) the degree to which the ice failure is simultaneous; (ii) the ice clearing mechanism; (iii) the diameter of the cone; (iv) the presence of snow. The following empirical equation can be used to conservatively estimate F_{\min} :

$$F_{\min} = \begin{cases} 0 & \text{if } D \leq 4 \text{ m,} \\ 0.075 \times (w-4) \times F_{0,\text{max}} & \text{if } 4 \text{ m} < D < 10 \text{ m,} \\ 0.45 \times F_{0,\text{max}} & \text{if } D \geq 10 \text{ m.} \end{cases} \quad (8.19)$$

8.3.2.5 The ratio τ/T can vary between 0.3 and 1.0. A value of 0.3 is recommended for areas similar to the Bohai Sea. In lack of more detailed information, the analysis shall be repeated for several different values of the ratio τ/T and the most unfavourable value shall be chosen.

8.3.2.6 In principle, the period T may be estimated as $T = L_b/v$, where L_b is the (random) breaking length of ice sheet and v is the (possibly random) ice sheet drift velocity.

8.3.2.7 In practice, the period T can be expressed in terms of a nominal ice thickness h as $T = k h / v$, with k being a random quantity typically varying between 3 and 10. It is here recommended to sample T from a Gaussian distribution, with $k_{\text{mean}} = 7$ and a CoV of 0.5.

8.3.2.8 From the information above (F_{\min} from Sect. 8.3.2.4; a set of values of F_0 from Sects. 8.3.2.1 to 8.3.2.3; a set of values of T from Sect. 8.3.2.7; and a suitable ratio τ/T from Sect. 8.3.2.5) an ice action time series as that shown in Figure 8.4 can be generated.

8.4 FATIGUE

8.4.1 INTRODUCTION

8.4.1.1 Cyclic ice action may contribute to fatigue damage of structures. Fatigue damage can be analyzed using S-N curves (see e.g. DNV-RP-C203, '*Fatigue design of offshore steel structures*'). Methods based on fracture mechanics can also be used and are especially recommended for critical components where failure can be expected to lead to 'high-risk' consequences.

8.4.1.2 All the significant stress ranges which contribute to fatigue damage should be considered. A conservative method is suggested here that does not underestimate the stress range or number of occurrences.

8.4.1.3 In order to perform a fatigue analysis it is assumed that the following information is available:

- Relative frequency distribution of level ice thickness h , classed into, say, five classes (or more, depending on the amount of data available);
- Relative frequency distribution of ice velocity v , classed into, say, five classes (or more, depending on the amount of data available);
- Average annual amount of level ice passing the site, L_{tot} ;
- Relative frequency distribution of ridge keel depth classed into, say, five classes (or more, depending on the amount of data available).

8.4.2 NUMBER OF OCCURRENCES

8.4.2.1 The following describes a simple step-by-step approach for obtaining the number of occurrences required for the fatigue analysis.

8.4.2.2 The relative frequency distribution of ice velocity v and ice thickness h can each be represented by relative number counts in five (or more, depending on the amount of data available) equally large bins (or classes). Assuming that the distributions are independent, the joint relative frequency of each combination of ice velocity and ice thickness can be found from a resulting 5-by-5 matrix, where each element is the product of the associated relative frequencies of the ice velocity and ice thickness. For example (for *illustration* only):

		relative freq. of h		
		0.333	0.500	0.167
relative freq. of v	0.250	0.083	0.125	0.042
	0.500	0.167	0.250	0.083
	0.250	0.083	0.125	0.042
		Joint freq. of h and v		

8.4.2.3 The total duration of ice exposure, T_{tot} , can be estimated from

$$T_{tot} = L_{tot} / v_{average} \quad (8.20)$$

where $v_{average}$ is the average ice drift velocity, which is available from the ice velocity relative frequency data.

8.4.2.4 The duration of *each* combination of velocity and thickness is then obtained by multiplying T_{tot} by each of the probabilities (or relative frequencies) in the joint frequency table (Sect. 8.4.2.2). This results in a new table of interaction durations for each combination of velocity and thickness. These will be used to compute the number of interactions associated with each combination (see below).

8.4.2.5 In the case of sloping structures, a mean ice action peak-to-peak period \bar{T} can be defined, in terms of ice velocity v and breaking length L_b ,

$$\bar{T} = L_b / v. \quad (8.21)$$

8.4.2.6 For the present purpose, the breaking length L_b may be conservatively taken as $L_b = 3 \times h$, in order to deliberately overestimate the amount of occurrences.

8.4.2.7 The number of occurrences for each combination of ice velocity and ice thickness is now found by dividing the interaction duration for each combination with the average peak-to-peak ice action period associated with that particular combination.

8.4.2.8 In the case of vertical structures, the fatigue damage contribution from continuous crushing is relatively minor and is covered by overestimating the fatigue damage caused by intermittent crushing and frequency lock-in scenarios. These scenarios are easier to handle since in these cases the structures typically respond harmonically at a single response period (typically the fundamental natural period). In this case, the peak-to-peak period \bar{T} required in Sect. 8.4.2.7 is taken to be equal to the fundamental natural period.

8.4.2.9 If the random vibration caused by continuous crushing is significant and cannot be neglected, spectral models have to be applied in order to estimate the relevant fatigue damage.

8.4.2.10 The number of ridge interactions is given from the average annual distribution of ridge keels passing the site.

8.4.3 STRESS RANGE

8.4.3.1 For each combination of ice thickness and ice velocity, an ice loading scenario (intermittent crushing, frequency lock-in or continuous crushing) has to be chosen. Here a conservative approach is proposed where all the ice velocities higher than 0.3 m/s cause continuous crushing, and the velocities below 0.3 m/s cause intermittent crushing or frequency lock-in.



8.4.3.2 The ice actions obtained for intermittent crushing and frequency lock-in independent of ice velocity, and it is supposed that 10% of the scenarios are frequency lock-in under all the ice thicknesses, while the remaining 90% are intermittent crushing. This classification may be changed according to specific site conditions.

8.4.3.3 The predicted ice action is applied to the finite element model of the structure, in order to detect the location with highest fluctuating stress. The calculated stress is multiplied by a stress concentration factor, which yields the desired stress hot spot stress level.

Guidance note:

An example on fatigue estimation according to the procedure given above is found in Appendix A.1.4.

---e-n-d---o-f---G-u-i-d-a-n-c-e---n-o-t-e---

8.5 REFERENCES

Kärnä, T., 2006, 'How to use saw-tooth force function to model self-excited vibration', Technical Report No. Karna-6-2006, Version 1.0.

Kärnä, T., 2008, 'Modelling Ice Induced Vibrations of Vertical Structures', Technical Report No. Karna-16-2008.

DNV-RP-C203, *Fatigue design of offshore steel structures*. Recommended Practice.

ISO 19906:2010(E), *Petroleum and natural gas industries — Arctic offshore structures*, International Organization for Standardization, Switzerland.

9 FLOATING STRUCTURES IN ICE

9.1 GENERAL

9.1.1 ACTION EFFECTS VERSUS ACTIONS

9.1.1.1 For a floating structure in ice, the environmental actions experienced by the structure include those associated with ice failure. The ice actions depend primarily on:

- the properties and characteristics of the ice environment and of the ice features;
- the configuration of the structure, and on the ice-structure interaction process.

9.1.1.2 For floating structures the interaction process is particularly important, because the ice actions are implicitly and non-linearly dependent on the structural response (i.e. the ice action depends on the structural configuration, which again depends on the ice action, etc; also).

9.1.1.3 In the present guideline, the IFORM contour approach is adopted as an approach for estimating *characteristic action effects* on floating structures in ice. The IFORM contour approach is widely used in design of structures in waves (DNV-RP-C205).

9.1.2 LOCAL ACTIONS

9.1.2.1 Refer to Sect. 4 for local actions from icebergs and multi-year ice ridges.

9.1.2.2 Rules from any Recognized Class Society (RCS) may apply and may be relevant for ice strengthening of floating structures. Such rules are mostly applicable to ship-shaped units and usually cover strengthening of the hull only.

9.1.3 LIMITATIONS OF PRESENT GUIDELINES

9.1.3.1 The present section is only valid for floating structures.

9.1.3.2 The present section covers only action effects from first-year ice ridges. General guidance on estimating characteristic action effects is given.

9.1.3.3 The effects of operational measures such as ice management and disconnection are not included in the present considerations.

9.1.3.4 The action effects estimated by the methods presented in the present section can be considered quasi-static as applied in structural design. Any dynamic effect should be taken into account when estimating the characteristic action effect.

9.1.4 CHARACTERISTIC ACTION EFFECTS

9.1.4.1 By the present approach, the characteristic action effect is generally obtained from a three step procedure. The procedure is outlined in Figure 9.1. The three steps are:

1. Determine a set of environmental states represented by H_k and h_c , by using IFORM contour formulations (see Sect. 9.1.4.2).
2. Estimate the maximum action effect in each state (see Sect. 9.1.4.3).
3. Multiply the maximum action effect (obtained from the most severe environmental state) by a scaling factor to estimate the *characteristic action effect* (see Sect. 9.1.4.4).

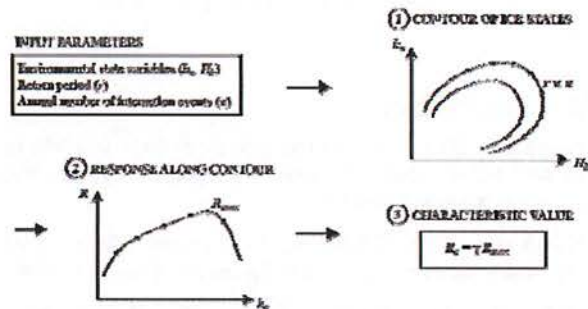


Figure 9.1: A stepwise procedure for estimating characteristic action effects.

9.1.4.2 The IFORM contours are specific to each interaction scenario. In this guideline, only generic but *simplified* IFORM contours are given for the ice ridge interaction scenario.

9.1.4.3 The action effect in a given environmental state should be determined from a validated numerical response model. The response model should capture: (i) the linear and non-linear hydrostatic stiffness characteristics of the floating structure; (ii) any important non-linear interaction effect between the structure and the ice; (iii) non-linear characteristics of the stationkeeping system. The response model need to incorporate sufficient details to capture the required action effect.

9.1.4.4 The generic scaling factor given in Sect. 10.1.3.1 has been obtained from a full probabilistic analysis for a particular system. For other strongly nonlinear systems the relevant factor will be different, and a fully probabilistic analysis of the action effect is recommended for each system.

9.2 REFERENCES

DNV-RP-C205, *Environmental conditions and environmental loads*, Recommended Practice. October 2010.



10 ICE ACTION EFFECTS IN FLOATING STRUCTURES

10.1 ICE RIDGE INTERACTION

10.1.1 INTRODUCTION

10.1.1.1 The present approach is recommended for estimating characteristic action effects from interaction between *first year ice ridges and floating structures*.

10.1.2 REQUIRED INPUT VARIABLES

10.1.2.1 The required *design* input variables are:

- the return period, r
- the annual number of ice ridge interactions, n .

10.1.2.2 The required *environmental* input variables are:

- the consolidated layer thickness, h_c
- the ice ridge keel draught, H_k .

10.1.3 SCALING FACTOR

10.1.3.1 Based on the results of a fully probabilistic analysis of a spar structure interacting with first year ice ridges, the scaling factor for this interaction scenario should be no less than 2.0.

10.1.3.2 The scaling factor given in the previous section has not been verified by any full scale data, due to the lack of availability of such data.

10.1.4 IFORM CONTOUR FORMULATION FOR ICE RIDGE INTERACTION

10.1.4.1 The IFORM contour formulation relevant for ice ridge interaction involves *two* key environmental input variables: the consolidated layer thickness, h_c , and the ice ridge keel draught, H_k . Calculated coordinates for both variables define the contour.

10.1.4.2 The simplified contour formulation given herein is valid for an environment characterized by an end-of-season level ice thickness of 1.0 m and an average keel draught 12.5 m.

10.1.4.3 Similar formulations as that given herein can be made available for other environments, upon request.

10.1.4.4 The consolidated layer h_c coordinate in the design contour is given by Eq. (10.5).

10.1.4.5 The keel draught H_k coordinate in the design contour, conditional on the consolidated layer coordinate, is given by Eq. (10.9).

10.1.4.6 In the following, the equations are expressed in terms of standard MS Microsoft Excel (©Microsoft Corporation) function names, for ease of application.

10.1.4.7 The required exceedance probability P_{ex} is given by:

$$P_{ex} = \frac{1}{r n} \quad (10.1)$$

10.1.4.8 The radius R of the IFORM circle in the u -space associated with the prescribed exceedance probability P_{ex} is determined from:

$$R = -\text{NORM.INV}(P_{ex}; 0; 1), \quad (10.2)$$

where NORM.INV denotes the inverse of the normal cumulative distribution function, in this case the standard normal distribution (with zero mean and unit variance).

10.1.4.9 A u -space vector coordinate u_1 is determined as:

$$u_1 = R \cos \theta, \quad (10.3)$$

where θ is discretized, here ranging from 2.5 to 5 (measured in radians). A different range might be more appropriate for a different environment.

10.1.4.10 The probability value F_1 is then, for all resulting values of u_1 from Eq. (10.3), given by:

$$F_1 = \text{NORM.DIST}(u_1; 0; 1; 1), \quad (10.4)$$

where NORM.DIST denotes the normal distribution, in this case the standard normal distribution (with zero mean and unit variance).

10.1.4.11 The coordinate of h_c in the design contour is then given by:

$$h_c = 6 - \left(\frac{1}{a_3} \right) \times \left\{ \text{GAMMA.INV}(F_1; a_1; 1) \right\}^{\left(\frac{1}{a_2} \right)}, \quad (10.5)$$

where:

GAMMA.INV denotes the inverse of the gamma cumulative distribution function;

a_1, a_2, a_3 , are distribution parameters, in the gamma distribution, as given below.

$$\left. \begin{aligned} a_1 &= 13.5539 \\ a_2 &= 2.3034 \\ a_3 &= 0.6054 \end{aligned} \right\} \quad (10.6)$$

10.1.4.12 The u -space vector coordinate u_2 is the determined from:

$$u_2 = R \sin \theta, \quad (10.7)$$

where θ is discretized, here ranging from 2.5 to 5 (measured in radians). A different range might be more appropriate for a different environment.

10.1.4.13 The probability value F_2 is then, for all resulting values of u_2 from Eq. (10.7), given by:

$$F_2 = \text{NORM.DIST}(u_2, 0, 1, 1). \quad (10.8)$$

10.1.4.14 The coordinate of H_k in the design contour is then given by:

$$H_k = 50 - \left(\frac{1}{b_3}\right) \times \left\{ \text{GAMMA.INV}(F_2; b_1; 1) \right\}^{\left(\frac{1}{b_2}\right)}, \quad (10.9)$$

where:

$b_1, b_2, b_3,$ are distribution parameters, conditional on each value of h_c , as calculated from Eq. (10.5); these distribution parameters are calculated from

$$\left. \begin{aligned} b_1 &= \exp \left\{ \frac{2.1133 \times h_c + 5.8537}{10} \right\} \\ b_2 &= \frac{100}{(1.39 \times h_c + 5.69)} \\ b_3 &= \frac{1}{50 - (3.3 \times h_c + 9.2)} \end{aligned} \right\}. \quad (10.10)$$

10.1.4.15 Figure 10.1 shows the resulting IFORM contour from the given simplified formulation in the case of $P_{ex} = 10^{-5}$.

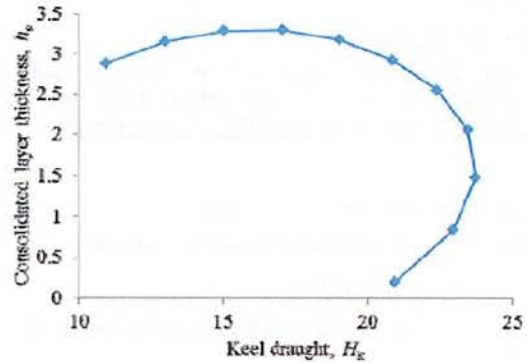


Figure 10.1: The IFORM contour for the given simplified contour formulation for $P_{ex} = 10^{-5}$.

APPENDIX A

A APPLICATION EXAMPLES

A.1 ICE INDUCED DYNAMIC STRUCTURAL RESPONSE

A.1.1 SUSCEPTIBILITY TO FREQUENCY LOCK-IN

An example considering the fundamental mode of vibration of the lighthouse Norströmsgrund is given here.

The displacement-normalized fundamental mode shape, and nodal masses along the elevation, are given in Table A.1 (as given by Kämä, 2008), and it can be seen that the displacement-normalized modal amplitude at the ice action point (at the elevation 14.18 m) is 0.22.

Elevation x (m)	Mode shape displacement normalized	Nodal mass (kg)
0.00	0.00	2,051,853
3.50	0.05	1,555,677
7.00	0.10	688,260
11.75	0.17	309,250
14.18	0.22	0
16.50	0.26	212,100
19.65	0.32	100,566
22.80	0.39	59,521
25.85	0.47	55,417
28.95	0.56	52,146
31.50	0.64	26,405
34.30	0.73	21,217
37.10	0.82	22,788
39.55	0.91	22,321
42.30	1.00	22,321

The following input variables for Eq. (8.1) are given (Kämä, 2008):

$$\begin{aligned}\phi_{ic} &= 0.22, & f_1 &= 2.4 \text{ Hz}, \\ M_1 &= 1.65 \times 10^5 \text{ kg}, & \theta &= 40 \times 10^6 \text{ kg/m/s}, \\ h &= 0.22 \text{ m and } 0.7 \text{ m}.\end{aligned}$$

Based on this input, the right hand side of Eq. (8.1) is calculated to be 0.088 and 0.28 for 0.22 m and 0.7 m ice thickness, respectively.

The maximum damping ratio of the fundamental mode is reported as being around 0.04, which means that the condition of Eq. (8.1) is *not fulfilled* for the two selected values of ice thickness.

This means that the result of Eq. (8.1) implies that *ice induced vibrations should be expected to occur, which is also confirmed by field experience*.

A.1.2 DYNAMIC RESPONSE OF THE NORSTRÖMSGRUND LIGHTHOUSE

The fundamental mass-normalized mode shape v_m is listed in Table A.2, and $v_{m,p} = 5.5 \times 10^{-4}$ at the ice loading point, as required in Eqs. (8.3) and (8.4).

Table A.2: The fundamental mass-normalized mode shape of the Norströmsgrund lighthouse.

Elevation (m)	Mass-normalized mode shape
0	0
3.50	1.2×10^{-4}
7.00	2.5×10^{-4}
11.75	4.2×10^{-4}
14.18	5.5×10^{-4}
16.50	6.5×10^{-4}
19.65	8.0×10^{-4}
22.80	9.7×10^{-4}
25.85	1.2×10^{-3}
28.95	1.4×10^{-3}
31.50	1.6×10^{-3}
34.30	1.8×10^{-3}
37.10	2.0×10^{-3}
39.55	2.3×10^{-3}
42.30	2.5×10^{-3}

Other required input for Eqs. (8.3) and (8.4):

$$\begin{aligned}\text{Damping ratio: } \zeta_m &= 0.04, \\ \text{Saw tooth period coefficient: } \tau_c &= 0.9, \\ \text{Period: } T_1 &= 1 / f_1 = 0.431.\end{aligned}$$

According to ISO 19906, when, the maximum structure velocity at the point of application of the ice loading is about 1.4 times the highest ice velocity at which frequency lock-in can take place. Then, an equation is given, Eq. (A.8-71) in ISO 19906), which relates the highest ice velocity during lock-in with the natural frequency of the structure, which, when combined with the previous statements, amount to:

$$\dot{q}_{\max, \text{ ice level}} = 1.4 \times \gamma_v f_n, \quad (\text{A.1})$$

in which $\gamma_v = 0.06$, and f_n is the n -th natural frequency, and where the equation is only considered to be valid for $f_n < 5$ Hz. The remainder of the present case study is based on the assumption that Eq. (A.1) is valid; however, DNV has since learned from Prof. Määttänen (personal communication) that this equation is based on a misunderstanding during the development of ISO 19906 and that, specifically, the equation (Eq. (A.8-71) in ISO 19906) that relates the ice velocity during lock-in with natural frequency is incorrect and should not have been included in ISO 19906. The ice velocity during lock-in remains as an input variable, and so the equation is

$$\dot{q}_{\max, \text{ ice level}} = 1.4 v_{\text{ice, during lock-in}} \quad (\text{A.2})$$

Nevertheless, the remainder of this case study proceeds as if Eq. (A.1) were true, in order to demonstrate the methodology given herein, which does *not* depend on Eq. (A.1) being true.

Now, substituting all the given parameters above into Eq. (A.1), it follows from Eq. (8.3) that:

$$\alpha f_{\max} = 2.16 \times 10^6 N. \quad (\text{A.3})$$

Considering the ice condition in the Gulf of Bothnia, the maximum ice action f_{\max} is calculated as the characteristic ice action with a 100 year return period, as described in section 7, and the following inputs are used:

- Structure width, $w = 7.2$ m
- End-of-season level ice thickness, $h_{\text{end}} = 0.9$ m
- Annual average freezing degree days,
 $C_{\text{FDD}} = 1200$ °C-days
- Nominal ice crushing strength,
 $\sigma_{\text{c,nom}} = 2.32$ MPa
- Number of annual average interaction events,
 $n = 1.11 \times 10^{-4}$
- Return period (in years), $r = 100$.

This results in $f_{\max} = 10$ MN, so that $\alpha = 0.216$, which falls in the range (0.1 - 0.5) recommended by ISO 19906.

Now, it should be noted that a couple of parameters influence the ratio α and subsequent estimation of structural response using Eqs. (8.3) and (8.4). Particularly, higher damping ratios correlate positively with higher values of α , as listed in Table A.3.

Table A.3: Effect of damping ratio on the ice action ratio α .

Damping ratio	Factor α
2%	0.108
3%	0.162
4%	0.216
5%	0.270

It has to be noticed that the effect shown in Table A.3 does not mean that increasing damping ratios *cause* increasing ratios α . In fact, it is expected that if the structure has higher damping, a larger amplitude of the dynamic component of the ice action is required, and thus a larger value of α , to cause frequency lock-in and achieve the same structural vibration level. The suggested range $\alpha = 0.1 - 0.5$ is mainly based on dynamic ice action measurement, and any ratio α in the range is likely to occur. If the structure is given, then increasing the ratio α will cause higher structural vibration. From another point of view, if the structure is designed with higher damping ratio, it becomes more difficult to trigger ice induced frequency lock-in since a higher ice ratio α is required.

However, there must be a limitation on this ratio, which means that the dynamic ice action is not able to fluctuate too much, and thus $\alpha_{\max} = 0.5$ is an estimated upper bound.

Using the load factor $\alpha = 0.216$ and substituting all the parameters and the mass normalized mode shape into Eq. (8.3), the amplitude of the dynamic displacement of the structure is obtained as listed in the table below.

Table A.4: Initially estimated amplitude of dynamic structural displacement of Norströmsgrund lighthouse

Elevation (m)	Displacement amplitude (cm)
0	0
3.50	0.29
7.00	0.61
11.75	1.03
14.18	1.34
16.50	1.59
19.65	1.95
22.80	2.37
25.85	2.93
28.95	3.42
31.50	3.91
34.30	4.39
37.10	4.88
39.55	5.62
42.30	6.10

A.1.3 CANTILEVER BEAM APPROXIMATION

The present example considers the case where the structure is sufficiently simple to be represented as a cantilever beam. In this case, the mode shape required in Eqs. (8.3) and (8.4) can be obtained analytically.

The formula for calculating the fundamental mass-normalized mode shape of a cantilever beam is given by:

$$\psi_1(x) = A \times \{ \cos(k_1 x) - \cosh(k_1 x) \} + \dots \\ B \times \{ \sin(k_1 x) - \sinh(k_1 x) \}, \quad (\text{A.4})$$

where:

$$A = -\frac{1}{\sqrt{\mu L}} \frac{\{ \cos(k_1 L) + \cosh(k_1 L) \}}{\sin(k_1 L) \sinh(k_1 L)}, \\ B = -\frac{1}{\sqrt{\mu L}} \frac{\{ \sin(k_1 L) - \sinh(k_1 L) \}}{\sin(k_1 L) \sinh(k_1 L)}, \quad (\text{A.5})$$

where:

- μ is the mass per unit length;
- L is the total length of the cantilever beam;
- k_1 is the fundamental wave number, where $k_1 L = 1.875$ is a constant dimensionless number;
- x is the spatial coordinate along the beam.

The Norströmsgrund lighthouse may be simplified as a cantilever beam with hollow pipe cross section. The following input variables are appropriate:

- Total height of the structure: $L = 42.3$ m
- First order natural frequency: $f_1 = 2.32$ Hz
- Density of the concrete: $\rho = 2,400$ kg/m³
- Young's modulus of the concrete: $E = 50$ GPa.

With $L = 42.3$ m and $k_1 L = 1.875$, $k_1 = 0.0443$.

Assuming that the outer and inner diameters of the cantilever beam are $D_0 = 5$ and $D_1 = 4.15$, which satisfies the following equation for the fundamental wavenumber,

$$(k_1 L)^4 = \mu \frac{(2\pi f_1)^2}{EI} L^4 \quad (\text{A.6})$$

in which I is the 2nd moment of area of the cross section, the mass per unit length is obtained as:

$$\mu = \rho \frac{\pi(D_0^2 - D_1^2)}{4} = 14,660 \quad (\text{A.7})$$

With the mass per unit length and wave number k_1 obtained above, the mode shape is calculated as listed in Table A.5; in particular, the value of the mass-normalized mode shape at the ice loading point (elevation: 14.18 m) is 4.2×10^{-4} .

Table A.5: The fundamental mode shape calculated using analytical cantilever beam model and the FE model.

Elevation x (m)	Mode shape by cantilever model		Mode shape by finite element model	
	Normalized by mass	Normalized to 1.0 at top level	Normalized by mass	Normalized to 1.0 at top level
0	0	0	0	0
3.50	2.9×10^{-5}	0.01	1.2×10^{-4}	0.05
7.00	1.1×10^{-4}	0.04	2.5×10^{-4}	0.10
11.75	3.0×10^{-4}	0.12	4.3×10^{-4}	0.17
14.18	4.2×10^{-4}	0.17	5.5×10^{-4}	0.22
16.50	5.6×10^{-4}	0.22	6.6×10^{-4}	0.26
19.65	7.6×10^{-4}	0.30	8.2×10^{-4}	0.32
22.80	9.8×10^{-4}	0.39	1.0×10^{-3}	0.39
25.85	1.2×10^{-3}	0.48	1.2×10^{-3}	0.47
28.95	1.4×10^{-3}	0.57	1.4×10^{-3}	0.56
31.50	1.7×10^{-3}	0.65	1.6×10^{-3}	0.64
34.30	1.9×10^{-3}	0.74	1.9×10^{-3}	0.73
37.10	2.1×10^{-3}	0.83	2.1×10^{-3}	0.82
39.55	2.3×10^{-3}	0.91	2.3×10^{-3}	0.91
42.30	2.5×10^{-3}	1.0	2.6×10^{-3}	1.0

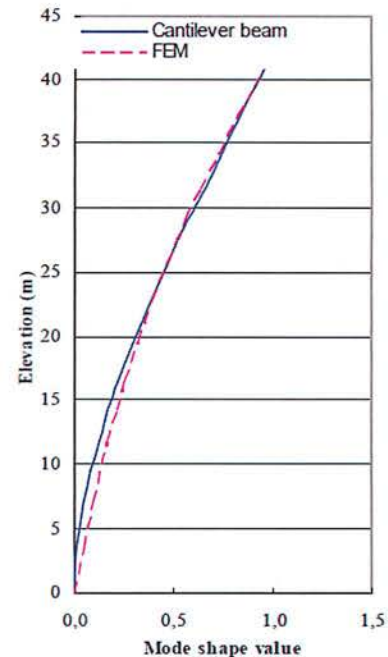


Figure A.1: Comparison between the mode shapes obtained from analytical cantilever beam model and from the FE model.

Accordingly, the amplitude of dynamic structural displacement (listed Table A.6) in of the cantilever beam can be estimated using Eqs. (8.3), as the same input parameters are given as follows:

$$\begin{aligned} \alpha f_{\max} &= 2.6 \times 10^6 \text{ N}, & \zeta_1 &= 0.04 \\ T_1 &= 1 / f_1 = 0.431, & \tau_c &= 0.9. \end{aligned}$$

Table A.6: Displacement amplitude calculated using cantilever beam model.

Elevation (m)	Displacement amplitude
0	0
3.50	0.05
7.00	0.21
11.75	0.56
14.18	0.78
16.50	1.04
19.65	1.42
22.80	1.83
25.85	2.24
28.95	2.61
31.50	3.17
34.30	3.54
37.10	3.91
39.55	4.29
42.30	4.66

A.1.4 EXAMPLE OF FATIGUE ESTIMATION

A simple example of estimating fatigue damage caused by dynamic ice actions is demonstrated as follows. In practice, more accurate statistics of ice conditions and detailed structural analysis are needed.

Assuming the distribution of ice thickness and ice velocity is known at a specific site, the joint probability for each combination of ice thickness and ice velocity is obtained, as listed in Table A.7. It should be noted here the summation of all the joint probabilities is 1.0. It is assumed here that the fatigue damage contribution caused by ice thickness less than 0.3 m can be neglected, which in practice needs to be checked in advance by calculating by FEA the hot-spot stress in the structure.

Table A.7: Joint probability of ice thickness and ice velocity.

Ice thickness range (m)	Average ice thickness (m)	Ice velocity range (m/s)			
		0.0-0.1	0.1-0.2	0.2-0.3	0.3-0.4
0.3-0.4	0.35	0.026	0.026	0.026	0.026
0.4-0.5	0.45	0.026	0.063	0.063	0.026
0.5-0.6	0.55	0.026	0.083	0.083	0.026
0.6-0.7	0.65	0.026	0.083	0.083	0.026
0.7-0.8	0.75	0.026	0.063	0.063	0.026
0.8-0.9	0.85	0.026	0.026	0.026	0.026

Assuming that the total annual accumulated length of ice passing the site is given (or estimated), for this example, as 500 km, and assuming the average ice velocity is 0.1 m/s, the average effective ice period is obtained as $5 \times 10^6 \text{ s} = 58 \text{ days}$.

The average effective ice period is distributed among the combinations of ice thickness and ice velocity, based on the probabilities listed in Table A.7, so that the effective ice period for each ice thickness-velocity combination is obtained, as listed in Table A.8.

Table A.8: The effective ice period for each combination of ice thickness and ice velocity (in seconds).

Ice thickness range (m)	Average ice thickness (m)	Ice velocity range (m/s)			
		0.0-0.1	0.1-0.2	0.2-0.3	0.3-0.4
0.3-0.4	0.35	1.3×10^5	1.3×10^5	1.3×10^5	1.3×10^5
0.4-0.5	0.45	1.3×10^5	3.13×10^5	3.13×10^5	1.3×10^5
0.5-0.6	0.55	1.3×10^5	4.17×10^5	4.17×10^5	1.3×10^5
0.6-0.7	0.65	1.3×10^5	4.17×10^5	4.17×10^5	1.3×10^5
0.7-0.8	0.75	1.3×10^5	3.13×10^5	3.13×10^5	1.3×10^5
0.8-0.9	0.85	1.3×10^5	1.3×10^5	1.3×10^5	1.3×10^5

For a vertical structure, the three ice loading scenarios must be analysed separately. According to the methodology demonstrated in the section about fatigue assessment, the ice velocity interval 0.3-0.4 m/s causes continuous crushing. In the present example it is assumed that the contribution from continuous crushing can be neglected, and only intermittent crushing and frequency lock-in scenario are considered. In these two scenarios, the vibration period is the fundamental natural period of the structure. Assuming, for this example, this natural period to be 0.4 s, the effective ice periods in Table A.8 can be transformed into number of occurrences by dividing the effective ice periods by 0.4 s. The results are shown and further simplified in Table A.9 and Table A.10.

Table A.9: The number of occurrences for each combination of ice thickness and ice velocity.

Ice thickness range (m)	Average ice thickness (m)	Ice velocity range (m/s)			
		0.0-0.1	0.1-0.2	0.2-0.3	0.3-0.4
0.3-0.4	0.35	3.25×10^5	3.25×10^5	3.25×10^5	3.25×10^5
0.4-0.5	0.45	3.25×10^5	7.83×10^5	7.83×10^5	3.25×10^5
0.5-0.6	0.55	3.25×10^5	10.4×10^5	10.4×10^5	3.25×10^5
0.6-0.7	0.65	3.25×10^5	10.4×10^5	10.4×10^5	3.25×10^5
0.7-0.8	0.75	3.25×10^5	7.83×10^5	7.83×10^5	3.25×10^5
0.8-0.9	0.85	3.25×10^5	3.25×10^5	3.25×10^5	3.25×10^5

Table A.10: The number of occurrences for intermittent crushing and frequency lock-in.

Ice thickness range (m)	Average ice thickness (m)	Ice velocity range (0-0.3 m/s)	
		Intermittent crushing	Frequency lock-in
0.3-0.4	0.35	8.78×10^5	9.75×10^4
0.4-0.5	0.45	1.70×10^6	1.89×10^5
0.5-0.6	0.55	2.16×10^6	2.41×10^5
0.6-0.7	0.65	2.16×10^6	2.41×10^5
0.7-0.8	0.75	1.70×10^6	1.89×10^5
0.8-0.9	0.85	8.78×10^5	9.75×10^4

It is assumed that 10% of the number of occurrences causes frequency lock-in for the velocity range 0-0.3 m/s. For each ice thickness-ice velocity combination, the average ice thickness is given as input to the dynamic ice action model, and then the predicted ice action is applied to a finite element model of the structure to obtain the corresponding hot spot stress.

Assuming the final stress levels are obtained as Table A.11, which in practice needs to be calculated with caution, the fatigue damage caused by annual ice passing can be estimated with the help of S-N curves and the values in Table A.10 and Table A.11.



Table A.11: The stress level for each combination of ice thickness and ice velocity (in MPa).

Average ice thickness (<i>m</i>)	Ice velocity range (0–0.3 m/s)	
	Intermittent crushing	Lock-in
0.35	100	120
0.45	120	130
0.55	130	140
0.65	140	150
0.75	150	160
0.85	160	170

-o0o-